Botrytis cinerea communicating across kingdoms: from LTR retrotransposons to extracellular vesicles.

Dissertation der Fakultät für Biologie der
Ludwig-Maximilians-Universität München.

Constance Tisserant (M. Sc.)

München, 2022

Diese Dissertation wurde angefertigt unter der Leitung von PD Dr. Arne Weiberg am Lehrstuhl für Genetik, Fakultät für Biologie der Ludwig-Maximilians-Universität München.

Erstgutachter:	PD Dr. Arne Weiberg
Zweitgutachter:	Prof. Dr. Silke Robatzek
Dissertation eingereicht am:	2022.04.20
Tag der mündlichen Prüfung:	2022.09.15

Eidesstattliche Erklärung

Ich versichere hiermit an Eides statt, dass die vorgelegte Dissertation von mir selbständig und ohne unerlaubte Hilfe angefertigt ist.

München, den 20.04.2022 Constance Tisserant

(Unterschrift)

Erklärung

Hiermit erkläre ich, *

☐ dass die Dissertation nicht ganz oder in wesentlichen Teilen einer anderen Prüfungskommission vorgelegt worden ist.

☐ dass ich mich anderweitig einer Doktorprüfung ohne Erfolg **nicht** unterzogen habe.

☐ ~~dass ich mich mit Erfolg der Doktorprüfung im Hauptfach ..... und in den Nebenfächern ..... bei der Fakultät für ..... der ..... (Hochschule/Universität) unterzogen habe.~~

☐ ~~dass ich ohne Erfolg versucht habe, eine Dissertation einzureichen oder mich der Doktorprüfung zu unterziehen.~~

München, den 20.04.2022 Constance Tisserant

(Unterschrift)

*) Nichtzutreffendes streichen

Table of Contents

List of publications

1. Bielska E., Birch P.R.J., Buck A.H., Abreu-Goodger C., Innes R.W., Jin H., Pfaffl M.W., Robatzek S., Regev-Rudzki N., **Tisserant C.**, Wang S., and Weiberg A. Highlights of the mini‐symposium on extracellular vesicles in inter‐organismal communication, held in Munich, Germany, August 2018. *J. Extracell. Vesicles* 8, 1590116 (**2019**).

2. **Tisserant C.**, and Weiberg A. Extracellular vesicles in plant host-microbe interaction**.** *Trillium Extracell Vesicles*, 1 (**2019**).

3. Kwon S., **Tisserant C.**, Tulinski M., Weiberg A. & Feldbrügge M. Inside-out: from endosomes to extracellular vesicles in fungal RNA transport. *Fungal Biol. Rev.* 34, 89–99 (**2020**).

4. Porquier A.*****, **Tisserant C.***, Salinas F., Glassl C., Wange L., Enard W., Hauser A., Hahn M., and Weiberg A. Retrotransposons as pathogenicity factors of the plant pathogenic fungus Botrytis cinerea. *Genome Biol.* 22, 225 (**2021**).
   ***** These authors contributed equally to this work.

Abbreviation Index

Ago/AGO	Argonaute coding gene/protein
A. thaliana	*Arabidopsis thaliana*
atago1-27	*A. thaliana ago1* mutant
atdcl1-7	*A. thaliana dcl1* mutant
*At*EVs	*A. thaliana* extracellular vesicles
*At*sRNAs	*A. thaliana* small RNAs
Avr gene	avirulence gene, effector-coding gene
B. cinerea	*Botrytis cinerea*
*Bc*EVs	*Botrytis cinerea* extracellular vesicles
bcdcl1-dcl2	*B. cinerea dcl1 dcl2* double mutant
*Bc*sRNAs	*B. cinerea* small RNAs
CD63	human tetraspanin protein
ckRNAi	cross-kingdom RNA interference
CSP	conventional secretion pathway
CWDEs	cell wall degrading enzymes
Dcl/DCL	Dicer-like coding gene and protein
DIRS	dictyostelium intermediate repeat sequence
DNA	desoxyribonucleic acid
dsRNA	double-stranded RNA
DUC	differential ultracentrifugation
Elf18	elongation factor 18 (PAMP)
ERV	endogenous retroviruses
ESCRT	endosomal sorting complex required for transport
ETI	effector-triggered immunity
EVs	extracellular vesicles
FDR	false discovery rate
Flg22	flagellin 22
hc-siRNAs	heterochromatic small interfering RNAs
HIGS	host-induced gene silencing
HR	hypersensitive response
Gag	coding gene for the Gag protein of retrotransposon
gDNA	genomic DNA
GXM	glucuronoxylomannan
ILVs	intraluminal vesicles
IN	integrase domain
ISEV	International Society for Extracellular Vesicles
LINE	long interspersed element
loess	locally weighted least squares regression
LTR	long terminal repeat
MAPK	mitogen-activated protein kinase
MIP	methylation induced premeiotically
miRNA	micro RNA
milRNA	miRNA-like RNA
MNase	Micrococcal nuclease
MSUD	meiotic silencing by unpaired DNA
MVs	microvesicles

MVB	multi vesicular body
nat-siRNAs	natural antisense small interfering RNAs
ncRNAs	non-coding RNAs
nm	nanometre
NB-LRR	nucleotide-binding and leucine rich repeat, also called NOD-like receptor or NLR
NGS	next generation sequencing
NTA	nanoparticle tracking analysis
OMVs	outer membrane vesicles
ORF	open reading frame
PAMPs	pathogen-associated molecular patterns
PCR	polymerase chain reaction
PEN1	Penetration 1 protein
pha-siRNA	phased secondary small interfering RNA
piRNAs	piwi-interacting RNAs
PLE	Penelope-like element
Pol	coding gene for the Pol protein of retrotransposons
pri-miRNA	primary miRNAs
PRRs	pattern recognition receptors
PTGS	post-transcriptional gene silencing
PTI	PAMP triggered immunity
qRT-PCR	quantitative reverse-transcription polymerase chain reaction
RBP	RNA-binding proteins
RDR	RNA dependant RNA polymerase
RIP	repeat-induced point mutation
RISC	RNA-induced silencing complex
RNA	ribonucleic acid
RNAi	RNA interference
RNAseq	RNA sequencing
rRNAs	ribosomal RNAs
ROS	reactive oxygenated species
RT	reverse transcription
RTase	reverse transcriptase domain
RT-PCR	reverse-transcription polymerase chain reaction
SEM	scanning electron microscopy
SIGS	spray-induced gene silencing
SINE	short interspersed element
siRNA	small interfering RNA
sn/snoRNAs	small nucleolar RNAs
sRNAs	small RNAs
sRNAseq	small RNA sequencing
ssRNA	single-stranded RNA
tasiRNAs	trans-acting siRNAs
TE	transposable element
TEM	transmission electron microscopy
TET	tetraspanin protein
TGS	transcriptional gene silencing
tRFs	tRNA-derived sRNAs and tRNA fragments
tRNAs	transfer RNAs
USP	unconventional secretion pathway
V(D)J	variability, diversity and joining
VLPs	virus-like particles
wt	wild-type
5mC	5-methylcytosine

Summary

Botrytis cinerea is a filamentous fungal pathogen able to infect more than 1400 plant species, causing the grey mould disease. For successful infection, *B. cinerea* small RNA effectors (*Bc*sRNAs) are transported from the fungal cells to the host plant cells where they hijack the host RNA interference (RNAi) pathway, a strategy called cross-kingdom RNAi (ckRNAi). Remarkably, the majority of *Bc*sRNA effectors are produced from long terminal repeat (LTR) retrotransposons.

The first part of this study focused on understanding the relationship between LTR retrotransposons and *B. cinerea* pathogenicity. By using a set of 6 different wild-type (wt) *B. cinerea* strains, we highlighted a positive relationship between the presence of LTR retrotransposons, the production of *Bc*sRNAs, and aggressiveness. It appeared that, in the wild, some *B. cinerea* strains only carried silenced LTR retrotransposon copies which were mutated by the fungal defence mechanism called repeat-induced point mutation (RIP). This led to the silencing of LTR retrotransposon expression, thus an inhibition of the production of *Bc*sRNA effectors, and therefore decreased aggressiveness. In addition, insertion of a LTR retrotransposon in a naturally occurring less aggressive strain resulted in the production of *Bc*sRNAs, enhanced aggressiveness and manipulation of the host transcriptome. Altogether, we identified for the first time LTR retrotransposons as pathogenicity factors for *B. cinerea*.

The second part of this study focused on investigating a possible means of transport for *Bc*sRNA effectors from *B. cinerea* cells to host plant cells. Extracellular vesicles (EVs) are secreted nanoparticles, containing various cargoes, which were shown to mediate cross-kingdom communications. However, *B. cinerea* EVs (*Bc*EVs) were never studied, and we hypothesised they could transport *Bc*sRNA effectors. After optimising a differential ultracentrifugation (DUC) protocol, *Bc*EVs were isolated and characterised by nanoparticle tracking analysis (NTA). Electron microscopy imaging showed their spherical shape while being released from *B. cinerea* hyphae. While nuclease protection assays suggested an intravesicular location of *Bc*sRNAs, small RNA sequencing (sRNAseq) analysis revealed a *Bc*sRNA depletion in *Bc*EVs compared to mycelium, suggesting another means of transport for *Bc*sRNAs. Interestingly, we found tRNA-derived sRNAs to be enriched in *Bc*EVs compared to mycelium, raising fascinating new possibilities about other RNA species involved in cross-kingdom communications.

Introduction

Botrytis cinerea, a devastating plant pathogen

Botrytis cinerea, a fungal plant pathogen, is the causative agent of the grey mould disease. Capable of infecting more than 1400 plant species, including prevalent agricultural crops (many vegetables, fruits, flowers and trees), *B. cinerea* causes worldwide agricultural yield losses of 10 to 100 billion dollars every year (Boddy, 2016). This filamentous fungus belonging to the phylum of Ascomycota displays visible infection sites on host plants, with symptoms varying from one host to another. Often recognisable by its grey and fluffy mycelium covering the infected tissue, it can also display a more soaked and watery appearance. Infection can occur pre- or post-harvest, on healthy or ripe tissues. *B. cinerea* is a necrotrophic pathogen, which means the infection eventually leads to the death of the attacked cells, with the pathogen feeding and growing thanks to their content in a saprophyte-like manner (Nakajima & Akutsu, 2014). Scientists agree on placing *B. cinerea* in the top 10 list of the most important plant pathogens, according to scientific and economic importance (Dean et al., 2012). Because of its considerable economic and agricultural impacts, *B. cinerea* gathers many interests and understanding its mechanisms of virulence is relevant for field and resource protection. Therefore, it is one of the most studied necrotrophic plant pathogens (Boddy, 2016). Despite its devastating impact in agriculture, *B. cinerea* is sought after by winemakers as one way of making sweet wine. In this situation, the infection is beneficial and called noble rot. One of *B. cinerea*'s symptoms is to decrease the water content in grape berries, thus increasing sugar levels, allowing the production of wines sweeter than usual. Reaching the right state of infection is extremely challenging as it greatly depends on climatic conditions such as humidity or temperature, making these wines rare and onerous.

Although approximately 35 *Botrytis* species are identified up to this day (Valero-Jiménez et al., 2019), the current work focuses on *Botrytis cinerea*. *B. cinerea* is the most extensively studied species within the genus and has a wider host range than other

Botrytis species which are mainly restricted to a single or a small number of host plant species (Staats, 2004).

B. cinerea life style & morphology

B. cinerea (Persoon: Fries) is the name of the anamorph stage (asexual stage) while the teleomorph stage (sexual stage) name is *Botryotinia fuckeliana* (Williamson et al., 2007). This second stage is rarer. Most of the time, *B. cinerea* reproduces asexually (Fig. 1). To this end, it produces macroconidia (commonly referred as spores) which are held by conidiophores arising from the mycelia, in a process called sporulation. When the macroconidia are released in the environment and find a support for growth (*i.e.* host plants) they germinate and generate new hyphae on which will develop primary appressoria (penetrating structures) for feeding (Romanazzi & Feliziani, 2014). *B. cinerea* hyphae are septate (*i.e.* divided in sections by internal cross-walls) and the cells are multinucleated (*i.e.* carrying several nuclei). In unfavourable conditions, *B. cinerea* survives by producing dormant structures called sclerotia, which are needed for sexual reproduction. In this later process, fruiting bodies called apothecia are formed by fertilisation of the sclerotia (maternal parent) by microconidia (paternal parent) (Rodenburg et al., 2018). Apothecia produce ascospores which germinate in mycelium. Asexual reproduction mainly takes place during summer when numerous hosts are present, making the propagation fast and easy; while sclerotia structures can undergo winter and will lead to sexual reproduction during spring (Williamson et al., 2007). Interestingly, light has an important role in *B. cinerea* reproduction, as conidia are developed in the light while sclerotia in the dark (Cohrs et al., 2016). In addition, it was shown that the fungus circadian clock impacts its efficiency to induce lesions on *Arabidopsis thaliana* leaves (Hevia et al., 2015), thus making light intensity a factor regulating life cycle and virulence (Schumacher, 2017).

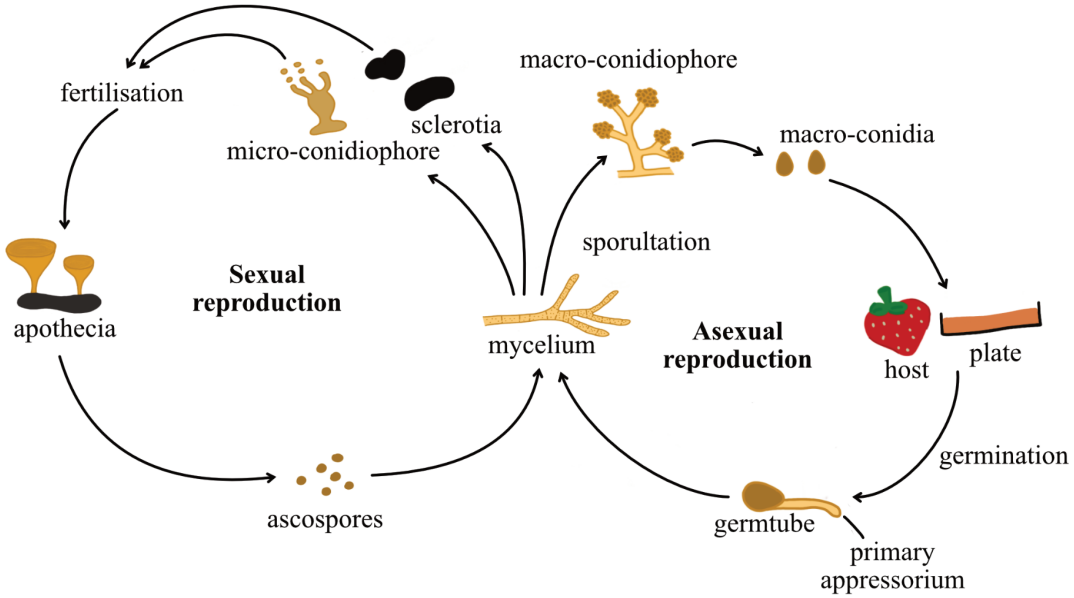

Figure 1: *B. cinerea* life cycle has two subcycles, the asexual reproduction cycle and the sexual reproduction cycle.

B. cinerea life cycle is divided in two, sexual and asexual reproduction. During sporulation, tree-like structures called conidiophores arise from the grey mycelium and contain the macroconidia (often miscalled spores or simply conidia). Macroconidia are small egg-shaped structures of 10 to 20 mm. In the wild, macroconidia are released in the environment, for example by the wind, and land on plant hosts (or plate with growth medium in the laboratory). The macroconidia attach and germinate, generating new hyphae, which first develop at the tip of the feeding structures called primary appressoria (Romanazzi & Feliziani, 2014), then *B. cinerea* mycelium grows. This completes the asexual reproduction. *B. cinerea* can survive in unfavourable conditions thanks to the formation of dormant structures called sclerotia. Sclerotia are dark and irregular with a discoid shape, and a size ranging from 1 to 10 mm. To achieve sexual reproduction, the sclerotia (maternal parent) are fertilised by the microconidia (paternal parent), resulting in the formation a fruiting bodies called apothecia (Rodenburg et al., 2018). Apothecia are yellowish and shaped like what we commonly call mushrooms. They can reach around 12 mm high. Apothecia produce ascospores which germinate in mycelium.

B. cinerea, a plant infection mastermind

B. cinerea is a necrotrophic fungus (*i.e.* the infection leads to host cell death) and possesses many tools for host infection, a process happening in several steps. At the very beginning, microconidia are dispersed by natural elements such as the wind and land on host plants where they attach if the conditions are favourable (such as high humidity). Germination is triggered and a germ tube is produced with an appressorium which penetrates the host surface. *B. cinerea* is an opportunistic pathogen and takes advantage of already present wounds or infection sites to penetrate the host. Nevertheless, without any pre-entry

site present, *B. cinerea* is well equipped to penetrate intact and healthy hosts. The first barrier layer that *B. cinerea* encounters is the plant cuticle (consisting of cutin), often covered by a layer of hydrophobic wax. Both might be degraded by a mixture of *B. cinerea*-secreted enzymes such as lipases and cutinases, although these mechanisms are still poorly understood (Kars & van Kan, 2007). The next obstacle to overcome is the plant cell wall, made of different types of polysaccharides and pectin. To this end, *B. cinerea* secretes a set of cell wall degrading enzymes (CWDEs) such as pectinases, cellulases and hemicellulases (Boddy, 2016).

Once the cell wall is damaged, the first cells *B. cinerea* attacks are the underlying epidermal cells. Host cells are killed prior to invasion by the hypha. For this, *B. cinerea* secretes numerous low molecular weight diffusible proteins and metabolites, including apoptosis-inducing compounds, triggering host cell death and allowing *B. cinerea* mycelium to then feed on it. The best-known phytotoxic metabolites are botrydial, botcinolide or oxalic acid. As another tool for successful infection, *B. cinerea* exploits the plant immune response linked to reactive oxygen species (ROS) by producing its own ROS and enhancing the plant apoptotic response called hypersensitive response (HR) (Kars & van Kan, 2007). The primary lesions are only a few millimetres wide and expand into spreading lesions; later, the necrotrophic plant tissues are covered by conidiating fungal mycelium.

This typical necrotrophic pattern of infection is questioned, however. It was suggested that during the earliest time of infection, *B. cinerea* displays a biotrophic stage, therefore making *B. cinerea* a hemibiotroph pathogen (Veloso & van Kan, 2018) needing the host plant to stay alive for successful establishment of the infection. Programmed cell death can be achieved in two ways: apoptosis or autophagy, which are considered as two mutually antagonistic mechanisms and both pathways are on a permanent equilibrium. The fungus *Sclerotinia slcerotiorum* suppresses autophagy and induces apoptosis in its plant hosts, and both mechanisms are crucial for successful infection (Veloso & van Kan, 2018). Similarly, *B. cinerea* germination on the plant would induce autophagy, however, a direct autophagic response from the plant would lead to resistance against *B. cinerea* and this was never reported. Indeed, death of the plant cell in which *B. cinerea* conidium has freshly germinated would lead to the abortion of the infection process as the mycelium could not develop further. If *B. cinerea* can suppress this early response, the mycelium can grow further on the plant, allowing the production of enough biomass to ensure a strong start to the infection.

Therefore, it seems *B. cinerea* has found a way to manipulate the plant's early immune response by first suppressing autophagy and then inducing apoptosis.

The idea of a hemibiotrophic lifestyle for *B. cinerea* is supported by observations of endophytic (*i.e.* symptomless) *B. cinerea* infections. Remarkably, in some cases *B. cinerea* lesions do not appear as quickly as said before. Infected strawberries (*Fragaria spp*.) are first invaded in their flowers where *B. cinerea* stays quiescent for several weeks until the fruit develops and is close to ripening (van Kan, 2005). Internally infected seeds of *Primula polyantha* lead to plants growing normally at first and showing systemic infections afterwards (Barnes & Shaw, 2003). In addition, *B. cinerea* hyphae were observed within roots and leaves in lettuce (*Lactuca sativa*) without showing any external lesions (Sowley et al., 2010).

B. cinerea is a multifaceted pathogen with a variety of infection patterns, from biotrophic to necrotrophic or even endophyte. Moreover, it can penetrate healthy or damaged plants, on any tissue or organ. For some plant species, the fungus can only be found on fruits or flowering parts, while in others it can affect various plant organs (van Kan et al., 2014). Altogether it shows how complex the infection processes and host-pathogen relations can be.

The plant immune system defending against pathogens

To defend themselves against the permanent threats of pathogens, plants have developed an efficient immune system. However, unlike animals, plants do not possess an adaptive immune system with mobile defender cells. Instead, plant immunity solely depends on cell-autonomous responses, comparable to the animal innate system. The common vision of the plant immune system is that it relies on two major branches, and is called the “zig-zag model” (Jones & Dangl, 2006).

The first branch of the response is initiated by the recognition of slowly-evolving pathogens, at the plant's external surface. Pathogens from various kingdoms, such as bacteria, fungi, nematodes or aphids, carry molecular elicitors called pathogen-associated molecular patterns (PAMPs). PAMPs are conserved among species of a microbial group, for example the flagellin of bacteria or cell wall components of fungi. PAMPs are recognised by plant transmembrane pattern recognition receptors (PRRs) (Zipfel & Felix, 2005). PRRs activation by PAMP recognition induces the first layer of immune response, the PAMP-triggered immunity (PTI) (Zipfel, 2014). The signalling cascade following PRRs stimulation triggers

early immune responses such as synthesis of reactive oxygenated species (ROS), a rapid increase of cytoplasmic Ca^{2+}, the activation of a MAP-kinase (MAPK) pathway and phytohormone signalling (Bigeard et al., 2015). This response provides a basal immunity and stops pathogens from further colonising the host. However, PTI is only effective against non-adapted pathogens (Jones & Dangl, 2006).

On the other hand, adapted pathogens or successful pathogens can overcome PTI with the help of secreted proteins, called effectors, which are important for virulence. Effectors are encoded by avirulence genes (Avr genes) (De Wit et al., 2009) and trigger the second layer of immunity called effector-triggered immunity (ETI), which acts inside the host cells, strongly and locally. ETI is activated by the specific recognition of effectors by nucleotide-binding and leucine-rich repeat (NB-LRR) proteins (also called NOD-like receptors or NLRs), leading to a strong immune response. NB-LRR proteins are encoded by resistance genes (Dangl & Jones, 2001). Successful ETI rapidly leads to similar responses to PTI (*e.g.* ROS production) but also triggers a hypersensitive cell death response (HR) of infected cells (Cui et al., 2015), preventing the pathogen from expanding further. This confers resistance against pathogens except necrotrophs, as they feed on dead cells, therefore profiting from apoptosis (Jones & Dangl, 2006). Pathogens and plants permanently co-evolve in an arms race to possess new effector proteins to bypass ETI response, and adapted NB-LRR proteins to trigger ETI (Anderson et al., 2010). At population levels, this pathogen-host coevolution is illustrated by high polymorphisms in resistance genes (*i.e.* NB-LRR-coding genes) (Stukenbrock & McDonald, 2009).

As previously mentioned, PTI and ETI are triggered by distinct mechanisms but can lead to similar downstream responses, and both pathways were considered as independent in the "zigzag" model. However, recent studies show interactions between both layers as activating ETI in the absence of PTI does not confer immunity (Ngou et al., 2021; Yuan, Jiang, et al., 2021). Hence, ETI can be seen as an amplification module depending on the previous PTI response (Yuan, Ngou, et al., 2021). This suggests that neither of them is sufficient for effective immunity and they should rather be considered as a whole because of their complex interplay.

As a consequence of their different attack strategies, the immune responses to biotrophs and necrotrophs have to differ. While biotrophs need to keep the host plant alive and do not survive the plant HR response, necrotrophs would profit from host cell death.

Thus, a fine-tuning of the immune response is necessary and mediated by three phytohormones: salicylic acid, jasmonic acid and ethylene. While salicylic acid-dependent signalling pathways would be involved against biotrophs, jasmonic acid-ethylene-dependent signalling pathways would be involved against necrotrophs (Glazebrook, 2005; McDowell & Dangl, 2000). However, some studies tend to show that jasmonic acid-dependent signalling pathways play a role in defence against the obligate biotroph powdery mildews (Antico et al., 2012), thus going against the previous suggestions. While the molecular mechanisms remain to be elucidated, it suggests a cross-talk between these three phytohormone-dependent pathways, and more complex pathways than initially thought.

Because of their central role in plant-pathogen interactions, protein effectors were extensively studied over the last decades. However, small RNAs (sRNAs) have been completely overlooked and ignored. Recently, studies have shown the role of sRNAs in plant-pathogen interactions as well and have identified them as a new class of effector, as they are the core of a process called cross-kingdom RNA interference (ckRNAi), which is explained in the following paragraph. In this doctoral thesis, the two main research axes focus around sRNA effectors from the plant pathogen *B. cinerea*.

Cross-kingdom RNA interference, *B. cinerea's* special weapon

B. cinerea complex infection processes, especially the balance between early biotrophic stage and later necrotrophic stage, support the use of cross-kingdom RNA interference (ckRNAi) as a pertinent strategy for infection. ckRNAi is a means of communication between two species of different kingdoms with sRNAs as messengers. It involves the exchange of sRNAs from one species to another, in order to hijack the RNA interference (RNAi) pathway and silence mRNA genes of the recipient species. In our study case, *B. cinerea* aims to silence host plant immunity related genes (Weiberg et al., 2013), hence finding a way to escape the plant's early immune response and ensuring a successful infection. This places sRNAs in the front scene during plant-*B. cinerea* interactions and brings out sRNAs as an important class of effectors (Weiberg & Jin, 2015), in a parallel to protein effectors.

General knowledge about small RNAs and RNA interference

ckRNAi and RNAi are mediated by a particular type of RNA: small RNAs. The majority of sRNAs are 20-to-24 nucleotide (nt) long, non-coding (nc), RNAs involved in the suppression of gene expression through sequence-specific transcriptional and post-transcriptional repression. RNAi is conserved in eukaryotic organisms (Bologna & Voinnet, 2014). sRNAs are involved in a variety of processes such as development, biotic and abiotic stress responses, RNA stability and processing. sRNAs can be divided into several subclasses depending on their biogenesis (Fig. 2). Micro RNAs (miRNAs) are typically 20 to 22 nt-long and originate from primary miRNAs (pri-miRNAs) containing a stem-loop structure (Carthew & Sontheimer, 2009). Small interfering RNAs (siRNAs) are typically 20-to-24 nt and derive from long double-stranded RNA precursors, with their production depending on RNA dependent RNA polymerases (RDRs). Both miRNAs and siRNAs are processed by RNase III-like endonuclease Dicer-like (DCL) proteins and other protein partners into short double-stranded RNAs (Bologna & Voinnet, 2014). In plants, several types of siRNAs exist: natural antisense small interfering RNAs (nat-siRNA), phased secondary small interfering RNAs (pha-siRNAs) and heterochromatic small interfering RNAs (hc-siRNAs). In mammals only, a third class exists: piwi-interacting RNAs (piRNAs), which are processed in a Dicer-independent manner. They protect the germline against invasive elements such as transposons (Wilson & Doudna, 2013). Similarly, filamentous fungi have developed genome defence mechanisms against transposons based on RNAi, such as quelling in *Neurospora crassa* (Li et al., 2010; Torres-Martínez & Ruiz-Vázquez, 2017). Like siRNAs, they are produced from a long RNA precursor thanks to RDRs.

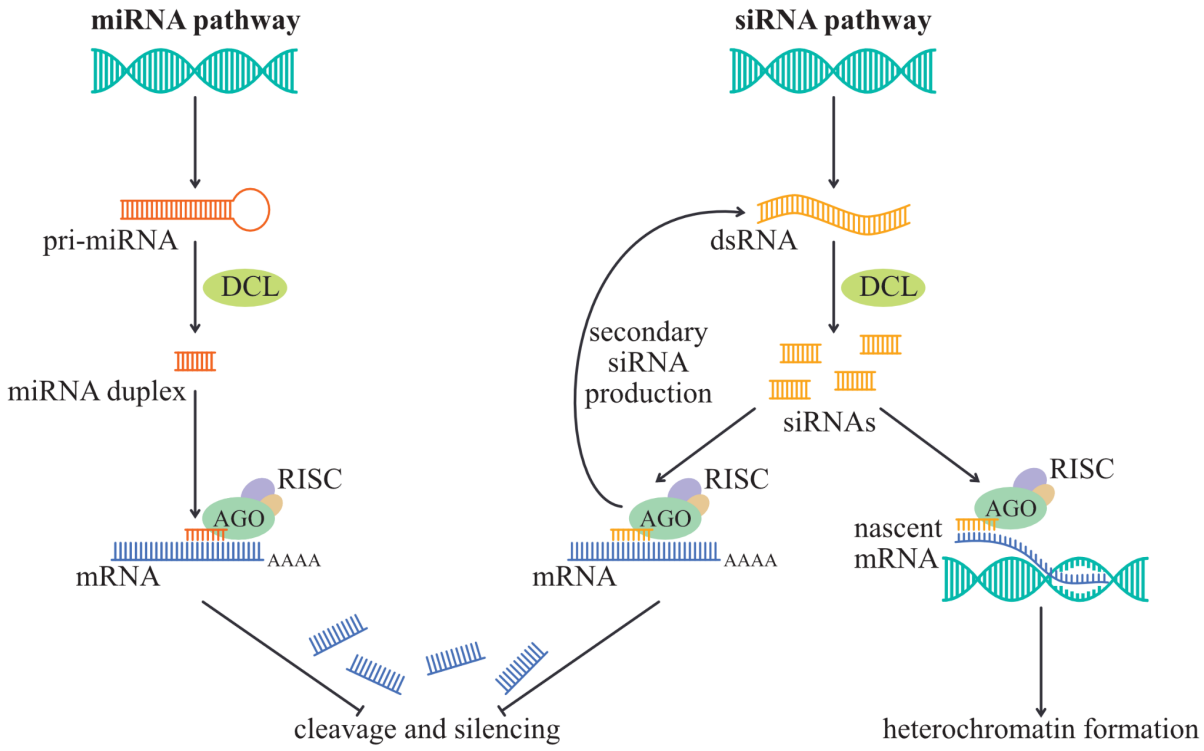

Figure 2: Simplified overview of the RNA interference pathway.
Micro RNAs are processed from primary microRNA (pri-miRNAs), characterised by a hairpin structure. pri-miRNAs are encoded in the genome. Small interfering RNAs are processed from double-stranded RNAs (dsRNAs) which are themselves expressed from the genome (or, alternatively, invasive nucleic acids such as viruses). Both types of precursors are cleaved into double–stranded smaller fragments by RNase III-like endonuclease Dicer-like (DCL) proteins, then exported into the cytoplasm where guide strands associate with AGO proteins and form RISC complexes which to target and silence target mRNAs. mRNA targeting by RISC can trigger the production of secondary siRNAs to enhance the silencing. In plants, RISC can target nascent transcripts and trigger the recruitment of DNA methyltransferases which methylate DNA and induce heterochromatin formation to silence the gene expression.

Once exported into the cytoplasm, the guide strand of small RNAs associates with Argonaute (AGO) proteins of the RNA-induced silencing complex (RISC) to target and silence genes in a sequence-specific manner. In most eukaryotes, except insects and mammals, association with RISC and mRNA targeting can also trigger the biogenesis of secondary siRNAs, produced by RDRs, in order to strengthen the silencing (Chen et al., 2010; Manavella et al., 2012).

For example, *A. thaliana* genome encodes for ten AGO proteins, which selectively load sRNAs depending on their length and 5' nucleotides (Bologna & Voinnet, 2014). This either leads to the cleavage of the mRNA target (post-transcriptional gene silencing, PTGS) or the modification of genomic locus target to form silent chromatin domains via DNA

methylation (transcriptional gene silencing, TGS) (Bologna & Voinnet, 2014). This is where *Bc*sRNA effectors hijack the plant RNAi pathway as they bind to the host plant AGO1 protein (Weiberg et al., 2013).

sRNAs non-cell autonomous action is recognised, as sRNAs are mobile molecules capable of spreading gene silencing across neighbouring cells/tissues. sRNA trafficking and spreading of RNAi effect were reported for the first time in 1998 in *Caenorhabditis elegans*, in which ingestion of exogenous dsRNAs lead to systemic gene-specific silencing (Fire et al., 1998; Timmons & Fire, 1998). Both the RNA precursors and sRNAs are capable of travelling (Sarkies & Miska, 2014), hence making the transport of sRNA effectors possible for achieving ckRNAi.

ckRNAi, a widespread mechanism during host-pathogen interactions

ckRNAi is the mechanism by which sRNAs from an external species are translocated into the cells of another species where they hijack the endogenous RNAi pathway and silence the expression of endogenous genes. It was first identified in *B. cinerea*, where *B. cinerea* sRNA (*Bc*sRNA) translocation into *A. thaliana* cells triggers the silencing of host plant immunity-related mRNAs (Weiberg et al., 2013) (Fig. 3), placing ckRNAi as important for successful establishment of *B. cinerea* infection. *Bc*sRNAs share critical similarities with the plant miRNAs binding to the plant AGO1, such as a bias for 5' U first nucleotide and the length in nucleotide. Thus *Bc*sRNAs can bind and hijack the plant RNAi machinery. In addition, *A. thaliana* mutant plants for the Ago1 protein (*atago1-27* plants) show resistance to *B. cinerea* infection, meaning that *Bc*sRNAs could not induce ckRNAi, while *A. thaliana* mutant plants for the Dicer-like protein 1 (*atdcl1-7* plants) are susceptible, suggesting *Bc*sRNAs are transported to the host, and not their RNA precursor (Weiberg et al., 2013). Besides, *B. cinerea* mutant for the two Dicer-like (DCL) proteins it possesses (DCL1 and DCL2 proteins, mutant strain *bcdcl1-dcl2* strain) fails to produce *Bc*sRNAs and shows attenuated pathogenicity (Weiberg et al., 2013). Several *Bc*sRNAs and their host mRNA targets are characterised. *Bc*siR3.2 targets MAPK mRNAs in both *A. thaliana* and *Solanum lycopersicum*. These genes are involved in plant immune response to fungal infection. For example, *Bc*siR37 can target at least 14 *A. thaliana* genes involved in the plant immune response (M. Wang et al., 2017).

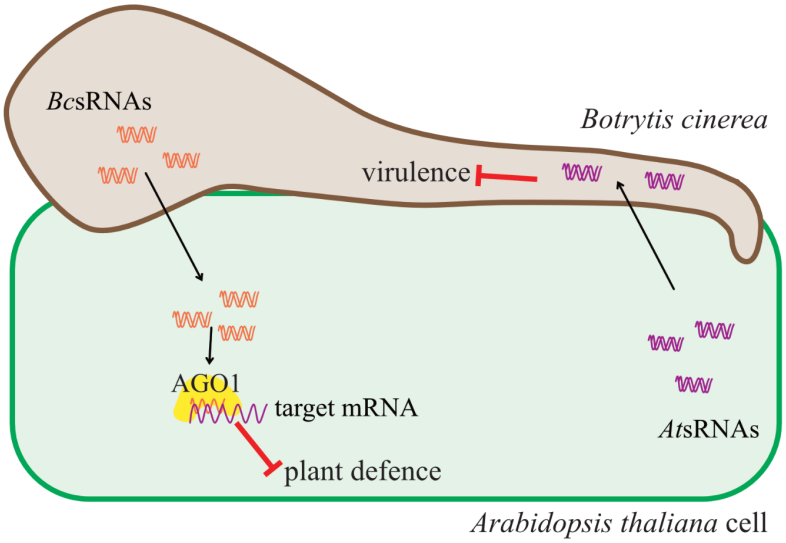

Figure 3: cross-kingdom RNA interference is bidirectional during *B. cinerea* - *A. thaliana* host-pathogen interaction.
When infecting *A. thaliana* plants, *B. cinerea* small RNAs (*Bc*sRNAs) are transported from the fungal cell to the host plant cells. By binding to the plant AGO1 proteins, they hijack the plant RNAi machinery. Thanks to sequence complementarity, they target and silence the expression of plant immunity-related mRNAs, therefore decreasing the plant immune response (Weiberg et al., 2013). This strategy is called cross-kingdom RNA interference (ckRNAi). Likewise, *A. thaliana* small RNAs (*At*sRNAs) are transported from the plant cells to *B. cinerea* cells, where they target and induce the silencing of fungal virulence-related mRNAs. Thus, ckRNAi is bidirectional during this host-pathogen interaction.

Following this discovery, ckRNAi was identified in several fungi. Among them, *Puccinia striiformis* f. sp. *tritici* and *Fusarium graminearum* use this strategy against wheat (Jian & Liang, 2019; B. Wang et al., 2017) and *Beauveria bassiana* exports a miRNA-like RNA (milRNA) that attenuates the immunity of its mosquito host and facilitates infection (Cui et al., 2019). ckRNAi appears to be widespread in the tree of life: the oomycete obligate biotroph *Hyaloperonospora arabidopsidis* manipulates its unique host thanks to sRNAs (Dunker et al., 2020), the nematode parasite *Heligmosomoides bakeri* modulates the innate immunity of mammalian cells (Buck et al., 2014), the obligate parasitic plant *Cuscuta campestris'* miRNAs act as virulence factors during infection (Shahid et al., 2018) or the ectomycorrhizal fungus *Pisolithus microcarpus* encodes a miRNA involved in symbiosis (Wong-Bajracharya et al., 2022). Some viruses release virus-derived sRNAs to interfere with the plant immune response (Zeng et al., 2019). However, ckRNAi is not only a weapon for pathogens, as it has been shown that several hosts partly rely on this strategy for defence. For example, cotton plants export miRNAs to the fungal pathogen *Verticillium dahliae* to silence

virulence-related genes (Zhang et al., 2016). Interestingly, *A. thaliana* produces sRNAs (*At*sRNAs) acting against the *Phytophthora infestans*, but the latter produces an effector suppressing the effect of the *At*sRNAs, thus enhancing the plant susceptibility to the disease (Hou et al., 2019). This perfectly illustrates the permanent arms race between hosts and pathogens. Going back to *B. cinerea* and showing another example of the continuous fight between species: during infection, *A. thaliana* sends *At*sRNAs into the fungal cells where they target and silence virulence-related genes (Cai et al., 2018), thus making ckRNAi bidirectional during the *B. cinerea-A. thaliana* interaction (Fig. 3). Importantly, *At*sRNAs are transported to the fungal cells into extracellular vesicles (EVs), which will be further discussed later.

The discovery of RNA silencing and trans-kingdom RNA transfer led to the development of two strategies of great agronomic interest called host-induced gene silencing (HIGS) and spray-induced gene silencing (SIGS) (Nowara et al., 2010; Wang & Jin, 2017). They facilitate the protection of crops against pathogens, parasites and pests. For this, plants express, or are sprayed with, double-stranded RNAs (dsRNAs) complementary to pathogen genes which will be silenced by RNAi. HIGS was reportedly successful against the powdery mildew agent *Blumeria graminis* and showed promising results against other pathogens (Nowara et al., 2010). The development of HIGS and SIGS in addition to the yet recent discovery of ckRNAi places sRNAs as central players during host-pathogen interactions and opens wide a new field of research.

LTR retrotransposons, “junk DNA”? Not really!

General knowledge about transposable elements

As detailed above, sRNAs can have different origins. Interestingly, a large proportion of *Bc*sRNA effectors involved in ckRNAi are derived from a subclass of transposable elements (TEs) called long terminal repeat (LTR) retrotransposons (Weiberg et al., 2013). TEs are mobile genetic elements present in all eukaryotic genomes, constituting relatively big fractions of these host genomes. TEs were first identified in maize in the 1950’s by Barabra McClintock (McClintock, 1950). TEs represent approximately 3 to 20 % of the genome in

fungi, up to 80 % in plants and 3 to 45 % in metazoans (Wicker et al., 2007). However, recent studies estimate the content of TEs from less than 1 % to 90 % in plant pathogenic fungi, in *F. graminearum* and *Blumeria graminis,* respectively (Cuomo et al., 2007; Frantzeskakis et al., 2018). These elements independently transpose to other loci and invade the host genomes. They were initially thought of as genomic parasites or "junk DNA" or "selfish DNA" whose presence only leads to detrimental effects such as disrupting coding regions, modifying gene expression, or chromosomal rearrangements, which are always eliminated by selection (Makałowski et al., 2019). It is now accepted that the presence of TEs and their transposition in genomes are drivers of evolution and adaptation by participating in genome plasticity (Dubin et al., 2018). Classified according to their transposition mechanisms, we distinguish two classes of TEs (Fig. 4a). The class I, or retrotransposons, uses an RNA intermediate which is later reverse-transcribed into DNA and integrated elsewhere in the genome, thus increasing the copy number of the element in the given genome ("copy/paste" mechanism), a mechanism shared with retroviruses. The class II, or DNA transposons, does not use RNA and follows a "cut/paste" mechanism, meaning they can effectively be excised from their genomic location and inserted somewhere else in the genome, hence not increasing their copy number during their transposition mechanism (Makałowski et al., 2019). TEs can be further classified hierarchically according to structural characteristics, sequence similarities, and transposition mechanisms as well. The class I (retrotransposons) is divided into five orders: LTR, DIRS (*Dictyostelium* intermediate repeat sequence), PLE (Penelope-like elements), LINE (long interspersed elements) and SINE (short interspersed elements) (Wicker et al., 2007). Here we focus on LTR retrotransposon elements, which themselves are divided into five superfamilies. Among them, Gypsy and Copia superfamilies are present in plants, fungi and metazoans. The three other subfamilies, Bel-Pao, retrovirus and ERVs (endogenous retroviruses), are only present in metazoans (Llorens et al., 2009).

A zoom on LTR retrotransposons

LTR retrotransposons have a complex, but well-studied structure, due to extensive work in the model organisms *Saccharomyces cerevisiae* and *Drosophila melanogaster* (Nefedova & Kim, 2017; Pachulska-Wieczorek et al., 2016). These elements carry two long terminal repeats (LTRs) flanking the internal coding region, which gave them their name (Fig. 4b). The central core element contains at least two coding regions: *Gag* and *Pol*,

responsible for transposition (Havecker et al., 2004). Gag and Pol proteins carry diverse functions, all indispensable for the retrotransposon reverse transcription and transposition (Fig. 4c), while the transcription is achieved by the cellular Polymerase II and regulated by a promoter in the 5' LTR and a terminator in the 3' LTR. In some LTR retrotransposons, additional open reading frames (ORFs) are present in the internal coding region in sense or antisense orientation (Vicient & Casacuberta, 2020). However their function is still unknown (Havecker et al., 2004).

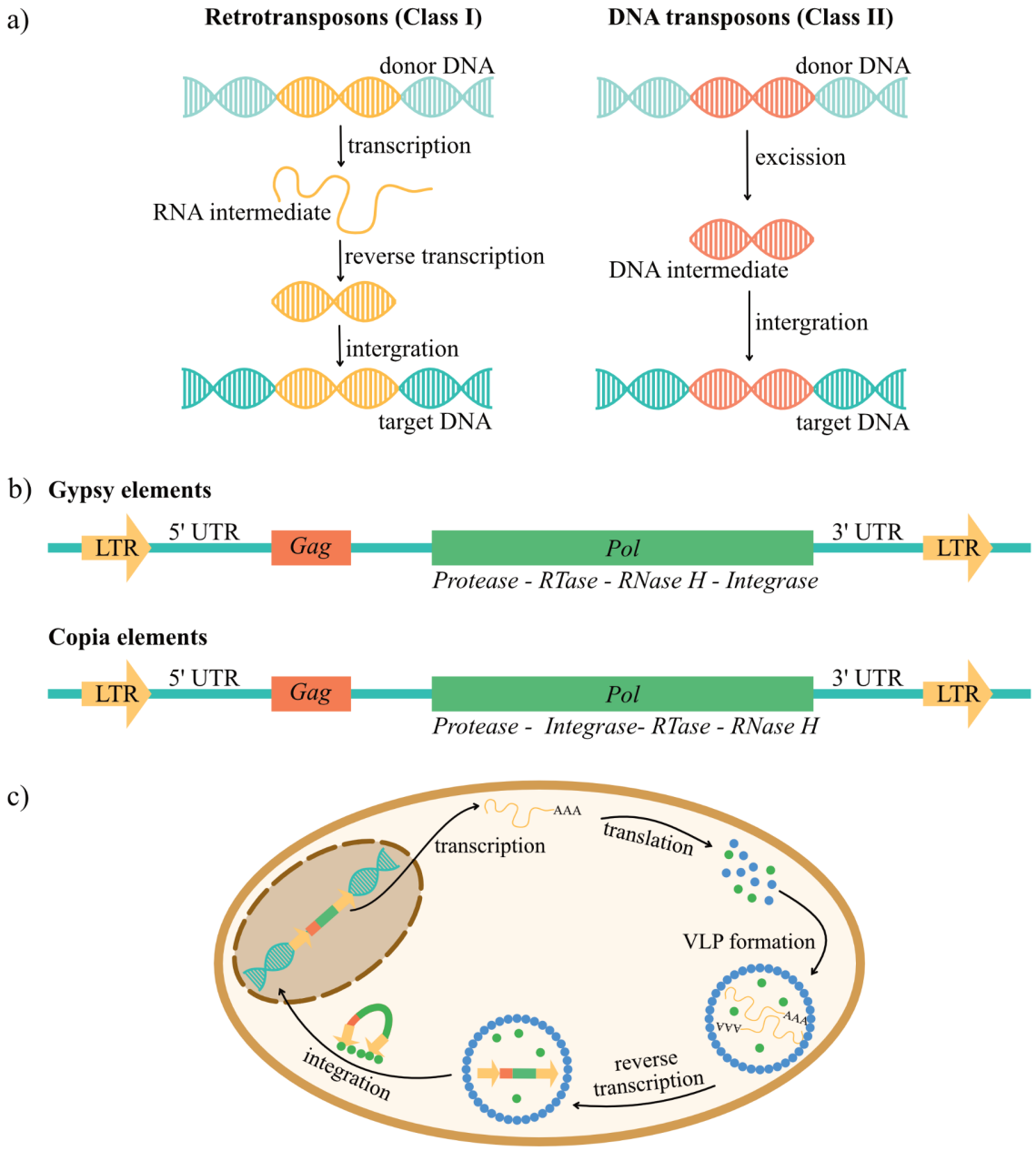

Figure 4: LTR retrotransposons are a superfamily belonging to transposable elements (TEs).
a) Retrotransposons have an RNA intermediate which is reverse-transcribed in DNA before being integrated in a new genomic locus. DNA transposons are excised from their genomic locus and

integrate in another location. **b)** The two main superfamilies of LTR retrotransposons, Gypsy and Copia, have very similar structures. They are flanked by two identical LTR regions and the central core which codes for *Gag* and *Pol*, necessary to the transposition (Havecker et al., 2004). *Gag* encodes for the capsid and nucleocapsid, structural proteins with RNA-binding properties, which form virus-like particles (VLPs). *Pol* encodes for a polyprotein with several enzymatic functions as it carries a reverse transcriptase (RTase), a ribonuclease H (RNase H), a protease, a polymerase-like and an integrase (IN) domain. **c)** The life cycle of LTR retrotransposons occurs as follows. The RNA transcription of the element is achieved by the cellular Polymerase II and regulated by a promoter in the 5' LTR and a terminator in the 3' LTR. This RNA is translocated in the cytoplasm where it is translated into VLPs and Pol. The protease domain of Pol releases itself and cleaves the different fragments, to the exception of the RNase H and the RTase domains which remain together (all domains are represented by green discs). RNA molecules are loaded into VLPs, where the RTase synthesises the cDNA. Then, the cDNA is imported back to the nucleus and the integrase inserts it into the genome. Figure 5c. was redrawn, by permission from Rightslink®: Springer Nature, Genome biology, Figure 1 of "The diversity of LTR retrotransposons", Ericka R Havecker, Xiang Gao & Daniel F Voytas, Copyright © 2004, BioMed Central Ltd.

Cohabitation between host genomes and transposable elements

Strategies for transposable element control

To avoid genome invasion and consequent damages, host organisms have developed strategies for TE control. It involves diverse epigenetic processes such as DNA methylation, chromatin remodelling thanks to histone modifications and post-transcriptional silencing by RNAi (*e.g.* well-known piRNAs in mammals) (Slotkin & Martienssen, 2007). Fungi have developed three types of mechanisms for TE control. First, identified in *N. crassa*, is the repeat-induced point (RIP) mutation defence mechanism by which C (cytosine) bases are mutated into T (thymine) within duplicated sequences (Gladyshev, 2017). Second, the methylation induced premeiotically (MIP) mechanism, identified in *Ascobolus immersus*, triggers methylation thus silencing of TEs (Daboussi & Capy, 2003). The two first mechanisms solely occur during the sexual phase, in the time window between fertilisation and the fusion of the two haploid nuclei from both parent cells (*i.e.* called karyogamy). While they have similarities, both mechanisms have different outputs with MIP being reversible but not RIP. The last type of mechanism includes quelling and meiotic silencing by unpaired DNA (MSUD), which are both controlling TEs via RNA-mediated silencing, akin to PTGS, and are triggered by the detection of aberrant RNAs.

RIP mutation defence mechanism occurs specifically in haploid nuclei dividing by mitosis before karyogamy (Gladyshev, 2017). This mechanism detects duplicated sequences

(*i.e.* two copies of one TE) in chromosomal DNA longer than approximately 0.4 kb, without being influenced by the transcriptional state, the origin, and relative as well as absolute position in the genome (however, closely located repeats are most easily detectable). RIP mutates C bases into T, within duplicated sequences, on both DNA strands (van Wyk et al., 2021). In *B. cinerea*, RIP shows a preference of mutating CpA to TpA and mutating CpT to TpT (Amselem et al., 2015). While RIP targets duplicated sequences, it can occasionally spread onto the neighbouring non-duplicated regions. Thus, some RIPed genomes have larger portions affected by this mechanism (van Wyk et al., 2019). RIP precise mechanism remains elusive. However, observations in *N. crassa* indicate it is likely to happen via a two-steps mechanism: the C base would be methylated on the 5th atom resulting in a 5-methylcytosine (5mC), then followed by N4-deamination of the 5mC to yield a T base (Gladyshev, 2017).

Benefiting from transposable elements in host-pathogen interactions

Pathogens are permanently evolving to keep up with their host in the arms race in which they are engaged. This following paragraph illustrates how pathogens have found ways to make the best out of TEs, as drivers of adaptive evolution. Over the last decades, many studies have improved the reputation of TEs, and it was shown that TE activities are intrinsically bound to genome plasticity and adaptive evolution. Genome restructuration caused by TEs can take different shapes depending on the insertion loci (in coding regions, in introns and so on), and can impact the expression of the surrounding genes by, for example, leakage of their silencing mechanisms. Natural selection retains beneficial adaptations resulting from TE transposition while deleterious ones impairing the host fitness are eliminated.

One way TEs can be beneficial for the host is called cooption, or molecular domestication. Here, the TE sequence as a whole, or only some parts of it, are repurposed to serve host cellular functions. In several organisms, TE-encoded proteins (*i.e.* Gag and Pol) are hijacked by the host cell to achieve new functions. One famous example is the variability, diversity and joining (V(D)J) recombination, a conserved process of the adaptive immune system occurring in all jawed vertebrates by which a theoretically infinite collection of antibodies is created in T and B cells (Gellert, 2002). The proteins Rag1 and Rag2 are major components of this process as they catalyse DNA rearrangements, and both are clearly identified as coopted proteins (Jangam et al., 2017). Yet to be fully established, it seems the

class I CRISPR-Cas system which protects bacteria and archaea from phages and plasmids has also emerged from TE domestication (Krupovic et al., 2014).

Sequencing of several filamentous fungal phytopathogen genomes and their analysis has led to the emergence of the two-speed genome model (Dong et al., 2015; Raffaele & Kamoun, 2012). These genomes are compartmentalised with two types of architecture: TE-rich but gene-spare regions and TE-spare but gene-dense regions. Nevertheless, TE-rich regions are enriched in Avr genes (*i.e.* Avr genes), major players during infection. This organisation allows the TE-rich compartments to evolve fast, thus driving high evolution of Avr genes and adaptation to the hosts (Plissonneau et al., 2017). Such correlation between TEs and Avr genes has been found in *Fusarium oxysporum* (Ma & Fedorova, 2010), *Magnaporthe oryzae* (Huang et al., 2014), *Zymoseptoria tritici* (Fouché et al., 2020; Lorrain et al., 2021) or *V. dahliae* (Torres et al., 2021) to name only a few. It is known that some TEs are de-repressed when the host undergoes stress. For example, the wheat pathogen *Z. tritici* TEs are de-repressed under infection, thus changing the expression of the surrounding Avr genes (Fouché et al., 2020). Interestingly, TEs have also been linked to the pathogen's host range. The evolution of new effector variants allows fungi to overcome host plant immunity of resistant cultivars, thus broadening their host range. Different strains from the same species showing major genomic rearrangement due to TEs also show different host ranges (Mat Razali et al., 2019). In *M. oryzae*, the causative agent of the blast disease in Poaceae crops, transposable elements are linked to the gain or loss of genes involved in host specialisation (Yoshida et al., 2016). Similarly to the fungal two-speed genome, the evolution of several plant genes involved in the immune response is linked to TEs (Seidl & Thomma, 2017). Thereby, alteration of gene expression and structural changes caused by TEs might be useful on both sides of the war and drive the co-evolution of both plants and phytopathogens.

However, recent genomic analysis of several fungal phytopathogens shows the two-speed model is not shared by all (Torres et al., 2020). TEs and Avr genes do not always co-localise and their evolution does not always correlate. Moreover, more than two compartmentalised types of genomic architectures can exist. On the other hand, *Blumeria graminis*, an agent responsible for powdery mildew, displays an "one-speed" genome with a lack of compartmentalisation (Frantzeskakis et al., 2018).

Jumping back to our model organism, previous study shows that different *B. cinerea* wt strains can display different phenotypes (Martinez et al., 2003) and the presence of TEs

has been proposed as an explanation for these observations. As a matter of fact, it was proposed that *B. cinerea* wt field isolates could be divided into two subpopulations depending on the presence of two TEs. *B. cinerea transposa* strains are carrying both Gypsy and Copia elements (previously called Boty and Flipper, respectively) which both belong to the LTR retrotransposon category. Conversely, *B. cinerea vacuma* strains would not carry any of these elements. Compared to the *transposa* strains, the *vacuma* ones are characterised by a faster mycelial growth rate, negatively correlated with aggressiveness (Martinez et al., 2003, 2005). In another study, hundreds of *B. cinerea* wt isolates collected from different hosts, all in Greece, were studied. The presence of LTR retrotransposons was assessed by PCR and four genotypes were identified (*vacuma*, *transposa*, carrying only Gypsy or only Copia elements), which all occured in sympatry (*i.e.* occurring at the same time and space) (Samuel et al., 2012). Remarkably, the dominance of certain genotypes on particular host species was observed, suggesting a role for LTR retrotransposons in host infection and host preference. Interestingly, *vacuma* strains caused higher incidence on latent infections compared to *transposa* strains. Altogether this suggests the LTR retrotransposons have an important role to play in *B. cinerea* aggressiveness. Moreover, as mentioned before, the majority of *Bc*sRNA effectors derive from LTR retrotransposons (Weiberg et al., 2013), more precisely they are produced from the mRNA transcribed from LTR retrotransposons, proposing another example of how TEs can be recruited in the arms race. Yet the relationship between *B. cinerea* aggressiveness and LTR retrotransposons remained to be studied in depth, which was one research axis during my doctoral project. Supporting our hypothesis, retrotransposon-derived sRNAs from the rice blast fungus *M. oryzae* were found to be upregulated under stress and during plant infection (Raman et al., 2013), suggesting a beneficial role for retrotransposon-derived *Bc*sRNA, potentially also during infection.

Intercellular communication, the extracellular vesicle highway

While we know that *Bc*sRNAs originate from LTR retrotransposons and we know *Bc*sRNAs' action on host plant immunity through ckRNAi, their way of transport remains unknown. In *C. elegans*, sRNA trafficking requires identified channel proteins (Sarkies & Miska, 2014), for which the exact mechanism remains unclear. In addition to protein

channel-dependent RNA transport, other hypotheses are currently under the examination of the scientific community. Among them are extracellular vesicles (EVs), a mechanism allowing long-distance transport and, importantly, environmental protection for their cargoes. Indeed, RNAs are considered as fragile as they are easily degradable by RNAses and the plant apoplast where *Bc*sRNA must travel contains RNAses carrying anti-pathogen functions (Galiana et al., 1997; Hugot et al., 2002).

EVs are spherical nanoparticles secreted in the extracellular environment by organisms from all branches of the tree of life (Deatherage & Cookson, 2012). First observed in the 1960's in platelet cell samples, they were described as "platelet dust" (Wolf, 1967). For long, they were considered as cell debris or secreted disposals. However, EVs are now extensively studied for their newly discovered biological function: cell to cell communication (Meldolesi, 2018). Made of a phospholipid bilayer, EVs contain various cargoes such as nucleic acids or proteins (Raposo & Stahl, 2019) (Fig. 5). Their ability to travel over long distances allows them to mediate "messages" from a cell to another in an intra- or inter-organismal way.

Extracellular vesicle subtypes and biogenesis

Based on their biogenesis and morphologies, EVs are classified into three subgroups (Fig. 5). Due to the fact that proteins secreted via EVs are lacking signal peptides, EV biogenesis pathways are termed as unconventional secretion pathways (USP), in opposition to the conventional secretion pathway (CSP) where proteins are transported in vesicles from the endoplasmic reticulum to the Golgi apparatus, before being released in the extracellular space upon vesicle fusion with the plasma membrane (Viotti, 2016). Most of EV knowledge comes from mammalian or even human-based studies. The first and smaller type of EVs are called exosomes and are estimated to be 30 to 150 nanometres (nm) of diameter (Colombo et al., 2014). Exosomes are the most studied mammalian EVs (Oliveira et al., 2013). They are generated from late endosomes, where the invagination of the membrane creates intraluminal vesicles (ILVs), forming an organelle now called multivesicular body (MVB) (Zhang et al., 2019). MVBs can fuse to lysosomes, leading to the degradation of the content, or to the plasma membrane, hence releasing the exosomes in the intercellular space. Intra-luminal budding of the late endosome membrane requires the endosomal sorting complex required for transport (ESCRT) (Hurley, 2015). This machinery, first described in yeast, is conserved to

mammals, and comprises four complexes (ESCRT-0, -I, -II, and -III), which act sequentially and form the ILVs thanks to their membrane remodelling capacity (Schmidt & Teis, 2012).

Second, microvesicles (MVs, also named shedding vesicles or ectosomes) are produced by direct outward budding of the plasma membrane, forming cytosolic protrusions which detach and get released in the extracellular space. Due to their biogenesis, their size range varies largely, from 100 to 1,000 nm of diameter (Tricarico et al., 2017). Distinct and localised changes in the protein and lipid components of the plasma membrane trigger changes in curvature and rigidity, thus causing the budding movement from which MVs results.

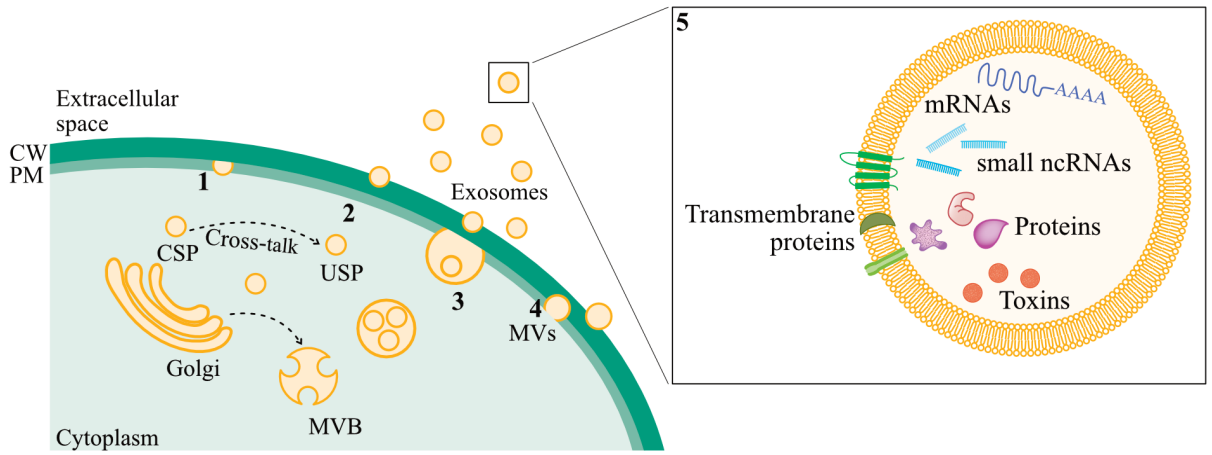

Figure 5: Extracellular vesicles are secreted via several pathways and contain various cargoes. Model drawn based on fungal studies. To be released in the extracellular space, all types of EVs need to cross the fungal cell wall (CW). **1.** The post-Golgi conventional secretion pathway (CSP) allows the secretion of proteins carrying signal peptides in the extracellular space thanks to the fusion of vesicles with the plasma membrane. **2.** Studies in *S. cerevisiae* (Sec4p) suggest a cross-talk between the CSP and unconventional secretion pathways (USP) for the release of EVs in fungi. The points **3** and **4** represent the USP. **3.** The late endosome, which originates from the trans-Golgi network, undergoes membrane invagination, thus creating intraluminal vesicles (ILVs). The organelle containing ILVs is named the multivesicular body (MVB). Exosomes are released from the MVB upon fusion with the plasma membrane (PM). **4.** Microvesicles (MVs) are released by direct budding of the PM. **5.** EVs are nanoparticles made of a lipid bilayer and were shown to contain various cargoes such as mRNAs or small ncRNAs (tRNAs-derived sRNAs, miRNA-like RNAs, sn/snoRNAs), proteins (transmembrane or soluble), or toxins.

The last type of EVs is apoptotic bodies. They are 800 to 2,000 nm of diameter and are released by cells undergoing programmed cell death by indiscriminate surface blebbing of the plasma membrane (Yáñez-Mó et al., 2015). In mammals, apoptotic bodies were disregarded in common EV research and their functions were underestimated. They are now

suggested to carry immunity related functions, similarly to exosomes and MVs (Kakarla et al., 2020). Taken all together, EVs represent a complex and heterogeneous population of particles varying not only in size but also composition, cargoes and functions, as it will be described in the following paragraphs.

EVs are secreted by cells in "normal" conditions as well as stress or pathological conditions, and these conditions are reflected in the EVs. In mammals, EVs have been linked to disease (*e.g.* diabetes or cancer) (Minciacchi et al., 2015; Pardo et al., 2018). As their content varies according to the secreting cell state, it raises the possibility to use EVs as biomarkers for diagnosis tools (Chen et al., 2018). Another promising side of EVs related to human health is on the therapeutic side, as EV-based technologies could allow cell-targeted drug delivery (Elsharkasy et al., 2020).

EV secretion and uptake

EV secretion occurs via plasma membrane restructuration and major architecture remodelling. To this goal, membrane proteins are recruited to the secretion loci. While the release process remains partially blurred, several proteins have been identified as important, such as SNAREs, Rab GTPases, syntenins and tetraspanins (TET) (Abels & Breakefield, 2016).

MVBs are generated from the late endosomes and therefore utilise the endosomal machinery such as ESCRT proteins (Hurley, 2015). However, ESCRT-independent mechanisms for MVB and exosome formations have been suggested (Oliveira et al., 2013). TETs are transmembrane proteins enriched within the membranes of late endosomes, MVBs and exosomes, and are believed to play crucial roles during exosome formation (Abels & Breakefield, 2016). In mammals, the TET protein CD63 is used as an exosome protein marker. MV formation does not take place in the late endosomal compartment, nevertheless the ESCRT machinery has been linked to MV biogenesis (Colombo et al., 2014; Tricarico et al., 2017), suggesting cross-talks between MV and exosome biogenesis. Even though these secretion pathways are termed as unconventional, knock out of proteins involved in the conventional secretion pathway leads to reduction of EV production or altered cargo content (Oliveira et al., 2010; Panepinto et al., 2009). Altogether, these indicate that EV biogenesis and secretion is a complex mechanism involving the cross-talk (Fig. 5) of many pathways

and is more complicated than initially thought. Although the majority of this knowledge does not arise from fungal models, similar pathways are expected to be involved as these proteins are highly conserved from yeast to mammals, and fungal mutants failing to produce any EVs are not existing yet. Moreover, MVB-like structures were observed in several fungi such as *C. neoformans* (Rodrigues et al., 2008) or *Golovinomyces orontii* (Micali et al., 2011).

Fungi carry an extra layer outside the plasma membrane, the cell wall. The cell wall defines the cell structure and provides physical and osmotic protection, its structure being a fine balance between rigidity and plasticity (Nimrichter et al., 2016). Fungal cell walls are mainly composed of the polysaccharides chitin and glucans, glycoproteins, and pigments. Chitin and glucans constitute an inner robust layer while the outer layer is more flexible with a composition varying among species. The observation of EV secretion raises the question of how they can traverse the cell wall. The mechanisms for this are still unclear but three main hypotheses are proposed (Brown et al., 2015). First, EVs could be mechanically pushed out at loci where the physical properties of the cell wall (*e.g.* thickness or pores) would allow the secretion. Second, active remodelling via cell wall modifying enzymes could clear a path for EV release. Indeed, EVs secreted by *S. cerevisiae* were found to be involved with cell wall remodelling (Zhao et al., 2019). Finally, EVs could be released by channels to which they could be guided by structural cable proteins present on the cell wall. In fact, Tubulin was found in EVs from different fungal species (Rodrigues et al., 2008; Vallejo et al., 2011). All three possibilities could also co-exist, but what seems clear is that viscoelasticity and composition of the cell wall matter more than initially thought (Walker et al., 2018). Moreover, it could be that EVs are sufficiently malleable, to allow deformation and passage through pores or channels smaller than their diameter. Nevertheless, liposomes containing an antifungal drug were shown to cross the cell wall in order to deliver the drug, indicating that fungal EVs should be able to pass the call wall for secretion (Walker et al., 2018).

When released in the extracellular space, EVs travel for various amounts of time and various distances before reaching the target cells. Sole interaction with the recipient cell or cargo discharge in the cytosol triggers physiological changes of the cell (Colombo et al., 2014). Although no mechanism is clear, it was proposed that EV internalisation by the recipient cells happens via either endocytosis or fusion with the plasma membrane. In

mammals, different types of endocytosis exist and have been observed to take up EVs. For example, clathrin-mediated endocytosis was identified for neurons, macropinocytosis by microglia, or cholesterol- and lipid raft-dependent endocytosis in tumour cells (Abels & Breakefield, 2016). Interestingly, the type of endocytosis seems cell specific. On the other hand, targeting of the recipient cell is also likely to happen via activation of pathways through specific membrane protein-receptor interaction (van Niel et al., 2018). Indeed, EVs from platelet cells interact specifically with macrophages and endothelial cells, and EVs from neutrophils interact only with platelets, macrophages and dendritic cells (Cocucci et al., 2009). Thus it seems that, at least in mammals, target cell specificity is determined by the enrichment of specific proteins present at the surface of EVs, thus guiding a specific interaction with the recipient cells. Concerning the uptake of fungal EVs, weak knowledge is accumulated, but similar mechanisms are expected to take place. *C. abicans* EVs were shown to colocalize at the plasma membrane of macrophages and dendritic cells, with the GM1 lipid raft marker, thus suggesting a lipid-raft mediated uptake (Vargas et al., 2015), presumably with an enrichment of specific proteins on the surface of EVs.

Methods and inherent challenges to EV isolation

Due to the novelty of the field, leading to a lack of optimised methods and knowledge, and to the small size of EVs, EV isolation reveals to be a true challenge. Currently, the most used isolation protocol is differential ultracentrifugation (DUC) (Monguió-Tortajada et al., 2019). This method consists in consecutive filtrations and centrifugations steps with increased strength and speed each time, to sequentially get rid of cells, debris and so on, before finally pelleting the vesicles (Zhou et al., 2020). DUC appears as the gold standard for EV isolation, as it does not require specific technologies and is easily achievable in any laboratory. However, this method is not specific to any particular type of particles and the EV samples are not pure from contaminants (*e.g.* protein aggregates). Thus, this method allows the enrichment in EVs but not the purification. To enhance sample purity, samples can be run on density gradient fractionation. For example, B-cell-derived exosomes density on sucrose gradient is around 1.13 to 1.19 $g.ml^{-1}$ (Théry et al., 2002). Several other methods are currently being optimised for better EV purity and EV subtype-specific isolation. Immuno-affinity capture-based precipitation (Zhou et al., 2020), requiring knowledge on EV protein markers (*e.g.* tetraspanins for mammalian exosomes, van Niel et al., 2018), purifies

specific types of EVs, while size-exclusion chromatography separates particles based on their size by filtration through a matrix. More recently, companies have been marketing kits for EV (mainly exosomes) isolation (*e.g.* precipitation-based or size-exclusion chromatography) and interestingly, EVs isolated from the same material but with different kits show differences in sizes, electrical charges or protein contents (Patel et al., 2019).

The very small size of exosomes or MVs makes them fall under the detection threshold of classical microscopy; therefore, electron microscopy is the favourite method for EV direct visualisation. However, advances in light scattering technologies led to the creation of a device called nanoparticle tracking analysis (NTA) which measures the size distribution of concentration of nanoparticles (Dragovic et al., 2011). This device is equipped with captors capable of spotting and tracking the movement of individual nanoparticles. Following the physical laws of Brownian motion and statistical analysis, it can calculate nanoparticle sizes. However, measurement is not specific to any nanoparticles (does not differentiate EVs from protein aggregates) thus the device can be equipped with fluorescent lasers, for specific measurements of fluorescently labelled EVs (*e.g.* transgenic strain GFP-TET).

Because of the inherent challenges of working with nanoparticles and the great increase of publications dealing with extracellular vesicles, the International Society for Extracellular Vesicles (ISEV) created a first guideline of minimal information for studies of extracellular vesicles in 2014 (MISEV) (Lötvall et al., 2014), which is regularly updated as progress is made in the field (Théry et al., 2018; Witwer et al., 2021). The MISEV groups a number of criteria and important controls which should be applied to EV studies in order to conclude on EV cargoes or functions.

Diversity of cargoes and possible loading mechanisms

It is admitted that the physiological state of a cell influences EV release and this is reflected in EV cargo composition (Colombo et al., 2014). Thus, unravelling EV content is key to understanding their functions. However, as no protocol allows the perfect isolation of one specific EV subtype, only heterogeneous populations are studied. Hence, composition and cargo descriptions are not strict to an EV subtype.

The proteins involved in EV formation, such as the ESCRT complex and protein partners or TET proteins, are expected and were found in EV proteomes. As these proteins are enriched inside EVs and are specific to an EV subtype, they are used as biomarkers (van

Niel et al., 2018). As previously mentioned, the TET protein CD63 is a marker of mammalian exosomes, such as the *A. thaliana* Tetraspanin 8 (TET8) (Cai et al., 2018). Numerous studies have assessed the human EV proteome and from their compilation several online databases arose, such as ExoCarta, Vesiclepedia or EVpedia. In mammals, the loading of proteins into EVs starts to be understood and is mediated by different pathways. Proteins undergoing ubiquitination as a post-translational modification are recognised by ESCRT -0, -I and -II, which possess ubiquitin binding domains and then loaded into exosomes (Frankel & Audhya, 2018; Schuh & Audhya, 2014). Ubiquitin-independent pathways are also reported and involve ESCRT -III for example (Mir & Goettsch, 2020). In addition, the human TET CD63 has also been linked to ESCRT-independent sorting of proteins (van Niel et al., 2018), showing a complex interplay. Less is known about fungi, however, Ascomycetes and Basidiomycetes genomes, such as *Colletotrichum lindemuthianum* or *B. cinerea*, were shown to code for three TET protein families (Lambou et al., 2008). Interestingly, in *B. cinerea* in *M. oryzae*, the tetraspanin *Pls1* gene is required for formation of the appressoria penetrating structure, thus *Pls1* is important for virulence (Gourgues et al., 2003). Nevertheless, none of them has been identified as fungal EV markers yet.

The first evidence of nucleic acid presence in EVs and more precisely exosomes was a major breakthrough in 2007. mRNA transported into mammalian exosomes was taken up in the recipient cells and translated into protein, showing the RNA EV cargoes stay functional (Valadi et al., 2007). Since then, several species of RNA have been identified in EVs from different organisms, such as microRNAs (miRNAs), non-coding RNAs (ncRNAs), transfer RNAs (tRNAs) and tRNA-derived sRNAs, ribosomal RNAs (rRNAs), but mainly focusing on mammalian EVs (Janas et al., 2015). To date, diverse classes of sRNAs such as miRNA-like RNAs, small nucleolar RNAs (sn/snoRNAs), mitochondrial tRNAs and mRNAs have been observed in fungal EVs, showing a conserved mechanism for RNA transfer (Alves et al., 2019; Kwon et al., 2021; Peres da Silva et al., 2015, 2019; Rayner et al., 2017). Considering the fact that some RNA species are enriched inside EVs, it highly suggests a non-random loading into EVs with a rather selective process, although some RNAs could be loaded because of their cytosolic abundancy. While no mechanism for RNA loading and sorting in fungal EVs has been discovered yet, it is also likely to occur via RNA-binding proteins (RBP). Indeed, RBPs such as RNA helicases and annexins contribute to RNA loading into plant EVs (He et al., 2021) and several RBPs were found in fungal EVs (Alves et

al., 2019). Similarly, RBPs were found to be important for miRNA loading in mammalian exosomes (Statello et al., 2018). RBPs could specifically bind to the RNAs via motif recognition in the RNA sequence. In mammalian cells a "zipcode"-like sequence of 25 nt targets mRNAs into MVs (Bolukbasi et al., 2012) and an EXOmotif targets miRNAs into EVs (Mir & Goettsch, 2020). Moreover, similarly to protein post-translational modifications, it is plausible that RNA modifications (*e.g.* uridylation or phosphorylation), or RNA secondary structure, are a mechanism participating in RNA selective loading into EVs.

Lipids constituting the EV membrane also have their importance. In mammalian cells, EV lipid composition varies from plasma membrane lipid composition, with certain types of lipids enriched, as well as lipid-raft-associated proteins. All together they confer stability and structural rigidity to EVs (Choi et al., 2013). Lipids are proposed to contribute in cargo sorting and EV formation (Mir & Goettsch, 2020) and interestingly, lipid rafts have been associated with protein and RNA sorting into mammalian exosomes (Lefebvre & Lécuyer, 2017). The lipid composition of fungal EVs is only poorly understood. In *Cryptococcus neoformans*, virulence-associated glycosphingolipids were identified (Rodrigues et al., 2007), analysis of *Histoplasma capsulatum* EVs revealed to contain many different lipids (Albuquerque et al., 2008) and *Paracoccidioides brasiliensis* EVs contain 33 phospholipids among other lipid types (Vallejo et al., 2012), altogether this indicates a complex lipidic composition. Interestingly, EVs from *H. capsulatum* grown on different media showed different lipid compositions (Cleare et al., 2020), illustrating how the environment can impact EV composition.

Fungal extracellular vesicles and host-pathogen interactions

Following the great interest shown in mammalian EVs and more specifically in cancer cells (Maas et al., 2017), fungal EVs have drawn scientists' attention. Fungal EV secretion has been proposed since the 70's with microscopic observations of changes in membrane architecture or the presence of particles in *Aspergillus nidulans*, *C. neoformans, Candida albicans* and *Schizosaccharomyces pombe* (Rizzo, Rodrigues, et al., 2020). However, the first direct characterisation of fungal EV was in 2007 in *C. neoformans,* the yeast-like pathogenic fungus responsible for cryptococcosis in humans (lung disease) (Albuquerque et al., 2008; Rizzo, Chaze, et al., 2020; Rodrigues et al., 2007). Following this, EVs have been identified

in approximately twenty fungal species from yeast to filamentous fungi (Rizzo, Chaze, et al., 2020). They have been later identified in *H. capsulatum,* the agent of histoplasmosis in humans (lung disease) (Albuquerque et al., 2008), *Malassezia sympodialis,* the agent of several skin diseases (Gehrmann et al., 2011), *P. brasiliensis,* the agent of paracoccidioidomycosis (Vallejo et al., 2011), *Cryptococcus gattii,* another agent responsible for cryptococcosis (Bielska et al., 2018), or *Sporothrix brasiliensis* responsible for sporotrichosis in cats and humans (Ikeda et al., 2018), and many others. All these species are yeast-like fungi or dimorphic fungi (*i.e.* existing in both yeast-like and mould forms) and are causing diseases in humans, which explains the interest they spark.

Proteomic analyses of fungal EVs from these species which show a great molecular diversity (*e.g.* enzymes, sterols, polysaccharides or pigments) suggest a role for fungal virulence in interfering with the host immune response (Oliveira et al., 2013). Comparison of fungal EV proteomic profiles shows the enrichment of certain sets of protein functions such as cell wall biogenesis, plasma membrane, stress responses, transport, signalling and, remarkably, pathogenesis (Bleackley et al., 2019). Remarkably, *M. sympodialis* EVs were shown to have an immunobiological activity as they modulate host cell physiology, thanks to allergen cargoes that induce a host immunity-related response (Gehrmann et al., 2011). One well known example is *C. neoformans* EVs which are coated with a capsule mainly composed of the glucuronoxylomannan (GXM) polysaccharide, which is essential for virulence (Chang et al., 1996; Rodrigues et al., 2007). GXM is known to have immunosuppressive and anti-phagocytic effects on its murine host (Feldmesser et al., 2000). Concerning host-pathogen communication, fungal EVs are currently described as having two actions on the host immune system: they either support the host infection or stimulate a host immune response (Kwon et al., 2020). Interestingly, *C. gattii* vesicles mediate pathogen-pathogen communication and facilitate a mechanism important for virulence called division of labour (Bielska et al., 2018).

Regarding filamentous fungi, less knowledge is accumulated but similar immuno-modulatory functions are to be expected (Bleackley et al., 2019). Nevertheless, EVs have been described in filamentous phytopathogen fungi *Alternaria infectoria* (environmental fungus but also an opportunistic human pathogen) (Silva et al., 2014), *F. oxysporum f. sp. Vasinfectum* (cotton pathogen) (Bleackley et al., 2020), *Z. tritici* (wheat pathogen) (Hill &

Solomon, 2020), *Colletotrichum higginsianum* (Brassicaceae pathogen) (Rutter et al., 2022), *Ustilago maydis* (agent of the corn smut) (Kwon et al., 2021) and *Penicillium digitatum* (citrus mould) (Costa et al., 2021). Analyses of EV proteomes from phytopathogens belonging to the F*usarium spp.* suggest the presence of phytotoxins and protein effectors (Bleackley et al., 2020; Garcia-Ceron et al., 2021). Moreover, *P. digitatum* EVs as well were found to carry a phytotoxic compound important for infection (Costa et al., 2021). In addition, MVBs were observed by TEM at plant-pathogen interfaces, in *G. orontii* haustoria (*i.e.* fungal structure penetrating the host plant cells and allowing feeding) when infecting *A. thaliana* (Micali et al., 2011), in *A. thaliana* cells when infected by *B. cinerea* (Cai et al., 2018), or in barley cells infected by *Blumeria graminis f. sp hordei* (An, Ehlers, et al., 2006; An, Huckelhoven, et al., 2006), strengthening the idea of an EV-mediated cross-kingdom communication in fungal-plant interactions.

Unfortunately, the knowledge on plant pathogenic fungal EVs remains poor. However, EVs have already been proposed to be important for plant-pathogen interactions, as bacterial and plant EVs were characterised in different species (Boevink, 2017). Several gram-negative bacterial pathogens such as *Xanthomonas campestris* pv *campestris*, *Xylella fastidiosa*, or *Pseudomonas syringae* were shown to produce EVs (then called OMVs, for outer membrane vesicles) *in planta* during infection, strongly suggesting a role in cross-kingdom interactions between the host and the pathogen (Rybak & Robatzek, 2019). Moreover, some of these OMVs were shown to contain cargoes such as secreted virulence factors and to have immuno-modulatory effects on the plant host.

Cross-kingdom communication via EVs seems bidirectional, as plant EVs were demonstrated to be released too. In 2009, and for the first time, plant EVs were isolated from sunflower seeds (Regente et al., 2009) and these EVs are enriched with the lectin protein, a case of non-classical secretion to plant apoplast (Pinedo et al., 2012). Further study on sunflower EVs shows their capacity to be taken up by the fungal pathogen *S. sclerotiorum* and to inhibit fungal growth, illustrating an inter-species communication during host-pathogen interaction (Regente et al., 2017). During *Phytophthora capsici* infection, *A. thaliana* also sends secondary siRNAs to the pathogen, inside EVs, to potentially silence transcripts and confer resistance (Hou et al., 2019). *A. thaliana* EVs (*At*EVs) isolated from *P. syringae*-infected plants were shown to contain antimicrobial proteins and are marked by the

penetration 1 (PEN1) protein, a t-SNARE protein mediating the fusion and secretion of vesicles at the pathogen penetration site (Rutter & Innes, 2017). On the other hand, *B. cinerea*-infected *A. thaliana* plants secrete TET8-marked EVs (Cai et al., 2018), drawing a parallel with the mammalian CD63 used as biomarkers (van Niel et al., 2018) and suggesting that TET8-EVs are exosomes. Plant scientists are currently divided on which marker represents which class of EVs and which methods and controls are the best for "proper" EV studies (Rutter & Innes, 2020). There is without a doubt room for improvement considering the challenges associated with EV studies and the lack of optimised tools for non-mammalian systems, as the fungal EV field is still in its infancy.

EVs are now under the spotlight in ckRNAi such as plant-pathogen interactions, as they were proven to transport virulence effectors and RNAs (Kwon et al., 2020; Samuel et al., 2015; U. Stotz et al., 2022). Fungal and plant EVs contain different species of RNAs, from mRNAs to tiny RNAs which are proposed to mediate plant-pathogen communication (Alves et al., 2019; Baldrich et al., 2019; Kwon et al., 2021; Peres da Silva et al., 2015; Rayner et al., 2017).

Aims of the thesis

The fungal pathogen *B. cinerea* is the causative agent of the grey mould disease which touches more than 1400 plant species, including important crops. During infection, *B. cinerea* small RNAs (*Bc*sRNAs) are sent to the host plant cells, where they hijack the plant RNAi pathway and silence plant immunity genes, a strategy named cross-kingdom RNAi. Interestingly, a large amount of *Bc*sRNAs are originating from LTR retrotransposons.

Previous studies found that *B. cinerea* strains either carry or lack LTR retrotransposons and suggested an impact on disease severity. Therefore, in the first part of my thesis, we aimed to investigate in depth the relationship between *B. cinerea* aggressiveness and LTR retrotransposons (Fig. 6). To explore this, we used 6 *B. cinerea* wt field isolates, carrying or lacking such elements. With pathogen assays and sRNAseq we aimed to identify a correlation between aggressiveness, *Bc*sRNA production, and the presence/absence of LTR retrotransposons. Moreover, we wanted to clarify if some isolates are really lacking LTR retrotransposons. Last, we inserted a LTR retrotransposon into a strain devoid of any. What is the impact on aggressiveness and to which extent does ckRNAi contribute to pathogenicity? Does it restore the production of derived *Bc*sRNAs? Do they successfully achieve ckRNAi and what are the consequences on the host plant transcriptome?

One major question arising from ckRNAi is the transport of such sRNA effectors from one organism to the other. As they transport diverse cargoes in an inter-organismal manner, extracellular vesicles (EVs) have attracted our attention. However, the fungal EV field is still in its infancy and whether *B. cinerea* secretes EVs was never studied. Thus, the second aim of my thesis was to investigate if *B. cinerea* EVs (*Bc*EVs) are the means of transport of *Bc*sRNAs (Fig. 6). Our very first goal was to optimise a protocol for *Bc*EV isolation. Does *B. cinerea* release *Bc*EVs and what are their characteristics? If yes, can LTR retrotransposon-derived *Bc*sRNAs be found inside *Bc*EVs? What other sRNAs are present? To answer these questions, we performed nuclease protection assays combined with sRNAseq analysis. Last, do *Bc*EVs carry immuno-modulatory functions? Do they trigger a response when applied to host plants?

Altogether, we aimed to better understand mechanisms surrounding ckRNAi, from the origin of *Bc*sRNAs to their transport, in order to dissect one of *B. cinerea*'s most fascinating virulence strategies.

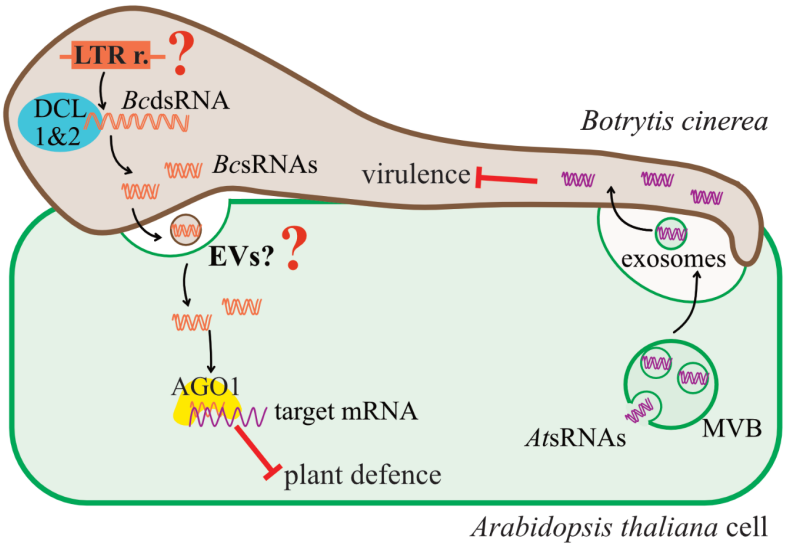

Figure 6: Schematic representation of the RNA mediated cross-kingdom communication between *B. cinerea* and *A. thaliana*, highlighting the two central questions of my doctoral thesis.
During infection, both *B. cinerea* and *A. thaliana* use ckRNAi either as an attack or a defence strategy, respectively. ckRNAi relies on the action of sRNAs into the other organism's cells where they target and silence mRNAs in the recipient cells (Cai et al., 2018; Weiberg et al., 2013). *Bc*sRNAs were shown to be processed by Dicer 1 and 2 proteins before entering the plant cells where they hijack the plant RNAi pathway by binding to the plant AGO1. *At*sRNAs were shown to be transported to *B. cinerea* cells into exosomes, a type of EVs. A large proportion of *Bc*sRNAs are expressed from LTR retrotransposons (named LTR r. in the scheme). The two axes explored during my thesis are represented by the red question marks. **1.** However, the importance of such elements for *B. cinerea* virulence remained unclear, and exploring this was the first goal of my doctoral studies. **2.** Moreover, the mechanism by which *Bc*sRNAs are shuttled to *A. thaliana* cells remains unknown, and understanding this was one goal of my doctoral studies. We hypothesised a transport via EVs.

Results

LTR retrotransposons as novel pathogenicity factors for *B. cinerea*

The first part of my dissertation is based on work accomplished by Dr. Antoine Porquier and myself, which resulted in a publication where we share the first author position: "**Retrotransposons as pathogenicity factors of the plant pathogenic fungus *Botrytis cinerea***" published in *Genome Biology* (part of Springer Nature) the August 16th, 2021 (Porquier et al., 2021). The article is licensed under a Creative Commons Attribution 4.0 International licence. A copy of this licence is available here: http://creativecommons.org/licenses/by/4.0/. Only a selection of the article results are presented here and the figures are either used in their original form or slightly modified.

B. cinerea wild-type strains carrying LTR retrotransposons are more aggressive

LTR retrotransposons belong to the class I of transposable elements, which are classified in two superfamilies called Gypsy and Copia. *B. cinerea* is no exception and a previous study identified 83 full-length copies of LTR retrotransposons, themselves classified into 9 consensus classes (Fig. 7), in the reference strain B05.10 (Porquier et al., 2016). Full-length copies of LTR retrotransposons (of several kb long) contain the two full LTR flanking regions, with the central core region coding for genes essential for the element's transposition. We observe the presence of the *Gag* gene coding for the proteins that will form the virus-like particles (VLPs) in which the retrotransposon is reverse-transcribed before integration, and the presence of domains coded into the *Pol* coding sequence, such as reverse transcriptase, ribonuclease H (RNase H), retropepsin-like aspartate protease, and integrase (IN). The 9 consensus sequences were defined based on their sequence similarities to characterised eukaryotic transposons (Porquier et al., 2016). Interestingly, 7 of the 9 consensus classes carry an additional ORF coded in antisense (Fig. 7).

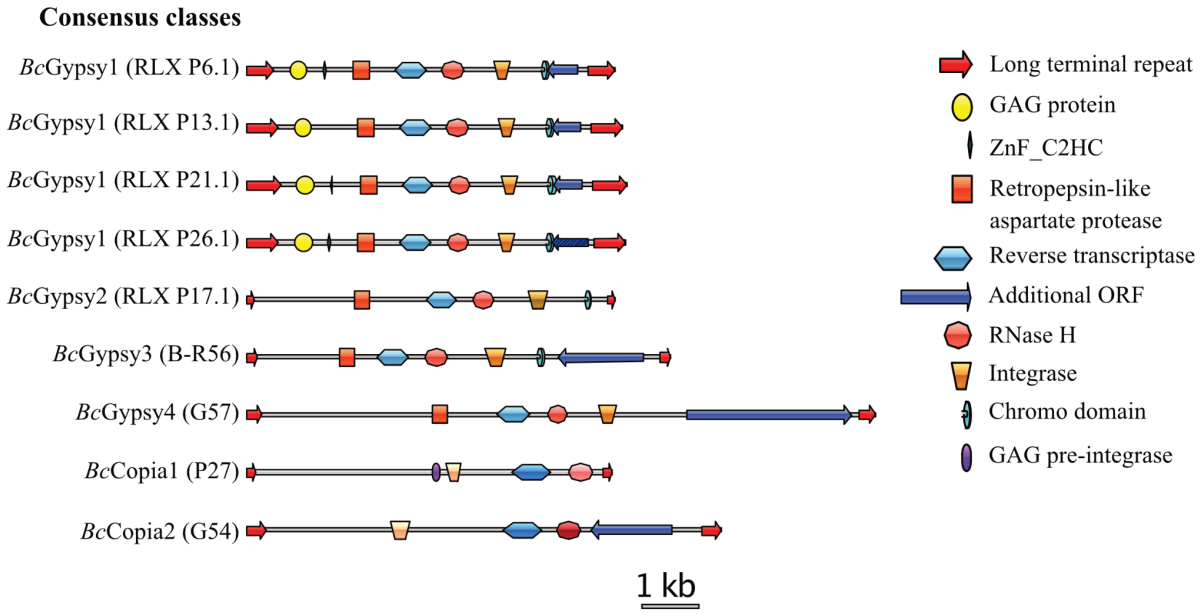

Figure 7: Conserved domains of LTR retrotransposons in B05.10 representing the nine consensus classes.

All nine consensus classes of LTR retrotransposons obtained from Porquier et al., 2016 are represented with their conserved domains and additional ORFs. To note, the consensus P26.1 additional ORF was previously characterised (Zhao et al., 2011) but was not found by our analysis, however we predicted another putative additional ORF, represented by the dashed arrow.

Based on this published LTR retrotransposon collection consisting of the 83 full-length copies, we performed a phylogenetic analysis, and identified six subfamilies, which we named *Bc*Gypsy1 to 4 and *Bc*Copia1 to 2 (Fig. 8). The phylogenetic tree was constructed based on sequence alignments, using the neighbour joining method and Jukes-Cantor nucleotide distance, and a Bootstrap analysis was run with 500 replicates.

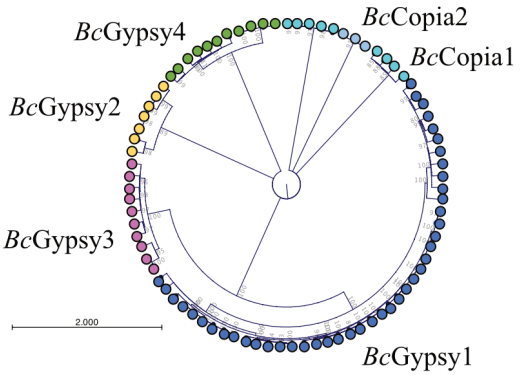

Figure 8: LTR retrotransposons are classified in six subfamilies.

Phylogenetic analysis of the 83 known LTR retrotransposon copies led to the identification of six subfamilies, *Bc*Gypsy1-4, *Bc*Copia1-2, in the strain B05.10.

Using previously published sRNAseq data (raw data available at: NCBI GEO: GSE45323, GSE45321) from *B. cinerea*-infected *Solanum lycopersicum* (tomato) and infected *A. thaliana* plants (Weiberg et al., 2013), we found that LTR retrotransposon-derived *Bc*sRNAs were produced in great majority by *Bc*Gypsy1, *Bc*Gypsy3 and *Bc*Gypsy4 (Fig. 9a and 9b). Remarkably, during both infection of *A. thaliana* and *S. lycopersicum* plants, *Bc*Gypsy3-derived *Bc*sRNAs represented more than 80 % of the reads and the peak of abundance was at an early infection time point (between 24 to 72 hours post-infection) (Fig. 9a and 9c).

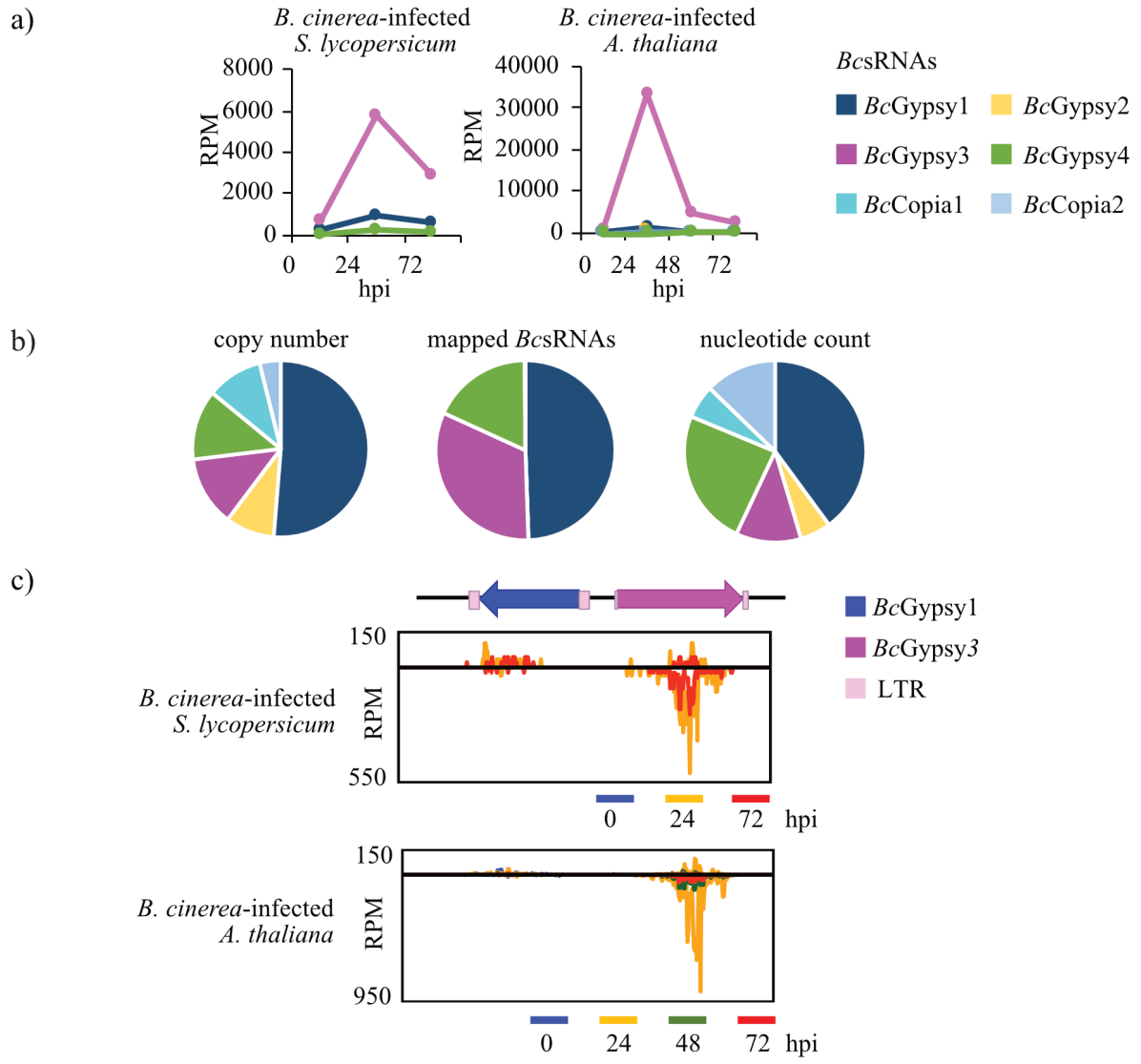

Figure 9: The majority of LTR retrotransposon-derived *Bc*sRNAs produced during early infection derive from *Bc*Gypsy1 and *Bc*Gypsy3 elements.

a) LTR retrotransposon-derived *Bc*sRNA abundance of the six subfamilies (*Bc*Gypsy1-4, *Bc*Copia1-2) at different time points of *S. lycopersicum* or *A. thaliana* host plant infection. **b)** Copy number, nucleotide count, and mapped *Bc*sRNAs of the six LTR retrotransposon subfamilies *Bc*Gypsy1-4,

*Bc*Copia1-2. **c)** *Bc*sRNA maps at the *Bc*Gypsy1/*Bc*Gypsy3 locus at different time points of *A. thaliana* or *S. lycopersicum* host plant infection. Bars above line represent sense and below line antisense reads. The raw data are available at NCBI GEO: GSE45323, GSE45321.

Noticeably, mapping of *Bc*sRNAs on a genomic locus having both *Bc*Gypsy1 and *Bc*Gypsy3 in vicinity showed that the *Bc*sRNAs are mainly produced by the element central coding region rather than the LTR flanking regions themselves (Fig. 9c). All these observations are in line with LTR retrotransposon-derived *Bc*sRNA mediated ckRNAi importance for establishing *B. cinerea* early infection by downregulating the host immune defence (Veloso & van Kan, 2018, Weiberg et al., 2013). In other words, LTR retrotransposons might be important for pathogenicity.

In this study, we used a collection of 6 different wt strains (named: D08_H24, D13_TS, D14_KF, N11_KW, B05.10 and D13_TF), which were isolated on different host plants and at different geographical origins (Table 1).

Strain ID	**Acronym**	**Host plant origin**	**Geographical origin**
B05.10	B05.10	Grapevine	Italy
N11_K_W14	N11_KW	Grapevine	Norway
D13_T_F_Nb-16	D13_TF	Strawberry	Germany
D14_K_F_Na-2	D14_KF	Strawberry	Germany
D13_T_S_Nb-7	D13_TS	Strawberry	Germany
D08_H_8_04	D08_H24	Strawberry	Germany

Table 1: The six *B. cinerea* wt isolates were collected from different plant hosts and geographical origins.

All 6 isolates were grown on nutrient-rich media (*e.g.* with malt extract) and no phenotypic differences were observed, with the exception of the D13_TF isolate, which grew faster (Fig. 10a) and did not develop sclerotia, the structure responsible for survival in unfavourable periods and the maternal parent for the sexual reproduction cycle, when grown in the dark (data not shown). By designing primers binding to the 6 LTR retrotransposon subfamilies we defined, we performed a genotyping PCR informing us on the presence or

absence of such elements in all 6 *B. cinerea* strains. Strikingly, 3 strains (B05.10, D13_TF and N11_KW) showed the presence of all six LTR retrotransposon subfamilies while the 3 other strains (D08_H24, D13_TS and D14_KF) were negatively tested for all six subfamilies (Fig. 10b). This result allowed the separation of these 6 *B. cinerea* wt strains into two groups, depending on the presence or absence of LTR retrotransposons.

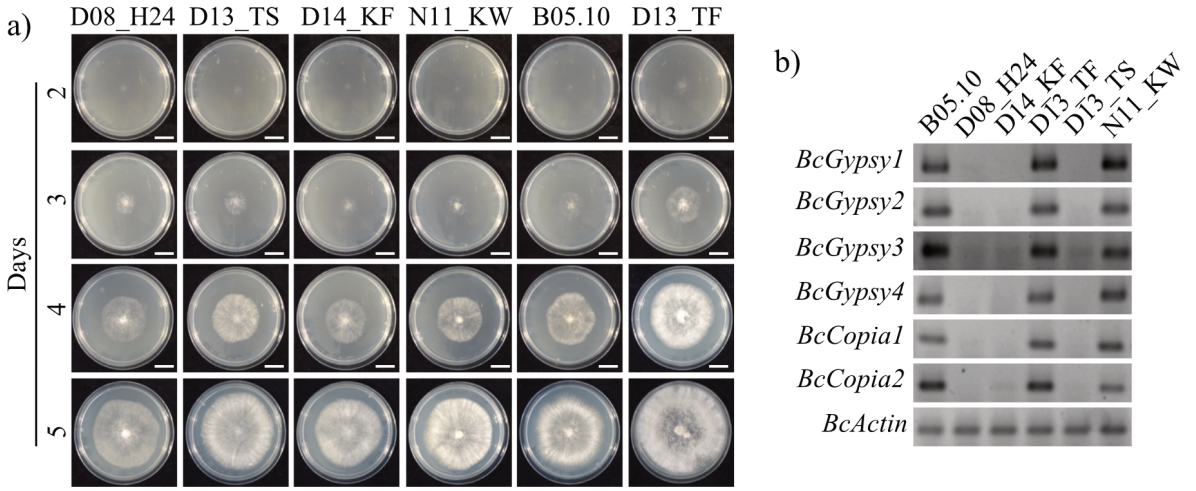

Figure 10: *B. cinerea* wt isolates separate in two groups depending on the presence or absence of LTR retrotransposons.

a) Growth phenotypes of the six *B. cinerea* strains. Scale bars indicate 20 mm. **b)** Genotyping PCR of the six LTR retrotransposon subfamilies in the six *B. cinerea* strains.

To assess the role of LTR retrotransposons for virulence, we performed pathogen assays on detached *S. lycopersicum* leaves by drop inoculation of *B. cinerea* conidium suspensions, coming from the 6 different wt strains. This was performed on *S. lycopersicum* plants as this host was shown to be responsive to LTR retrotransposon-derived *Bc*sRNAs, thus relevant for this assay (Weiberg et al., 2013). 24 hours post-inoculation, leaf discs were collected around the lesions and stained with Trypan Blue, allowing the visualisation of the primary lesion formation (staining of apoptotic cells and of *B. cinerea* mycelium). The 3 LTR retrotransposon-negative strains showed weaker primary lesions than the 3 LTR retrotransposons-positive strains (Fig. 11a). In accordance with this, the lesion area quantification after 48 hours showed similar results. Indeed, the 3 strains lacking LTR retrotransposons were significantly less aggressive than the 3 strains carrying LTR retrotransposons (Fig. 11b). With this, we identified a positive relationship between *B. cinerea* aggressiveness and the presence of LTR retrotransposons.

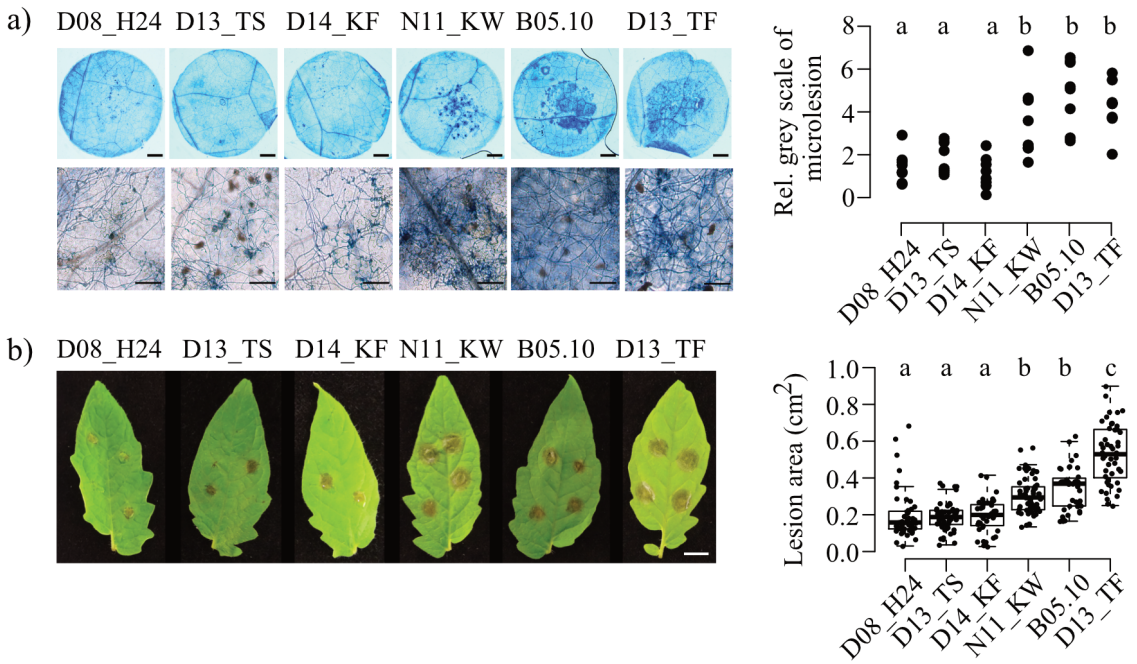

Figure 11: *B. cinerea* wt isolates carrying LTR retrotransposons are more aggressive.
a) Pathogenicity assay of the six *B. cinerea* strains on *S. lycopersicum* leaves quantifying microlesion area by Trypan Blue staining at 24 hpi. Microlesions in Trypan Blue images were quantified in eight leaf discs per strain as relative grey scale (rel. counts) in relation to the total leaf disc. Scale bars in leaf disc images indicate 1 mm, and 100 µm in higher magnification images. **b)** Pathogenicity assay of the six *B. cinerea* strains on *S. lycopersicum* leaves indicating lesion area of > 20 infection sites at 48 hpi. Scale bar indicates 1 cm. For **b)** infection experiments were repeated three times with similar results. In **a)** and **b)** a significant difference is indicated by letters and was tested by one-way ANOVA using Tukey HSD test with $p < 0.05$.

Most aggressive *B. cinerea* strains produce large amounts of LTR transposon-derived *Bc*sRNAs

As we found a positive correlation between aggressiveness and LTR retrotransposon-derived *Bc*sRNAs, we aimed to better understand it by looking at sRNA levels. Thus, we sequenced the sRNAs of all 6 wt strains, from mycelium growing in axenic cultures. By comparing the mapping of the 6 sRNA profiles, we highlighted that only the 3 most aggressive strains produced relatively abundant amounts of transposon-derived *Bc*sRNAs (Fig 12a). Quantification of different sRNA classes, after filtration of rRNAs, which were the most abundant type of sRNAs, showed that the 3 most aggressive strains produced higher amounts of *Bc*sRNAs derived from all LTR retrotransposons (between 2.0 % and 16.0 %) than the 3 less aggressive strains (between 0.03 % and 0.1 %) (Fig. 12b).

Remarkably, the great majority (> 99.4 % in the most aggressive strain) of transposon-derived *Bc*sRNAs mapped to LTR retrotransposons (Table 2), thus DNA transposon-derived *Bc*sRNAs were only in minor proportion.

strain ID	raw reads	mapped to *B. cinerea*	LTR retrotransposon	TIR	MITE	others	rRNA	tRNA	snoRNA	mRNA
B05.10	35019101	28297807	1567425	1728	193	6774	18451665	2455545	1211362	1370252
D08_H24	34354403	7837357	1167	8	118	251	4500870	647822	577125	612682
D13_TF	33309078	27958988	212398	143	20	596	17281638	6376382	296112	987626
D13_TS	73013067	56132095	21534	53	302	1593	37683927	5694422	1696385	3753954
D14_KF	33245869	24055355	2193	0	155	1344	13222189	2042417	765340	4340108
N11_KW	42575595	33352275	1197000	400	34	6252	21583999	4926181	383479	2480260

Table 2: Number of reads mapping to *B. cinerea* reference genome, to different retrotransposon subfamilies or to different sRNA species, in the sRNAseq performed on the 6 different isolates.

Size profiles of all *Bc*sRNAs from the 6 wt strains showed a preference for 21-to-22 nt-long sRNAs (Fig. 12c), and LTR retrotransposon-derived *Bc*sRNAs only coming from the 3 most aggressive strains showed the same preference as well, accompanied by a 5' first nucleotide base bias for Uracil (Fig. 12d). Those two features are typical of plant endogenous sRNAs which associate with AGO1 (Mi et al., 2008). This is in line with *Bc*sRNAs hijacking the plant RNAi pathway in order to induce ckRNAi. sRNA analysis indicates that the less aggressive strains are not producing significant amounts of LTR retrotransposon-derived *Bc*sRNAs, strengthening the relationship between LTR retrotransposons and pathogenicity. It is interesting to note that the strain D13_TF, while having the biggest lesion sizes with the pathogen assay (Fig. 11b), did not show the largest amount of LTR retrotransposon-derived *Bc*sRNAs (Fig. 12d). Hence, D13_TF enhanced aggressiveness could simply be due to its faster growth (Fig. 10a).

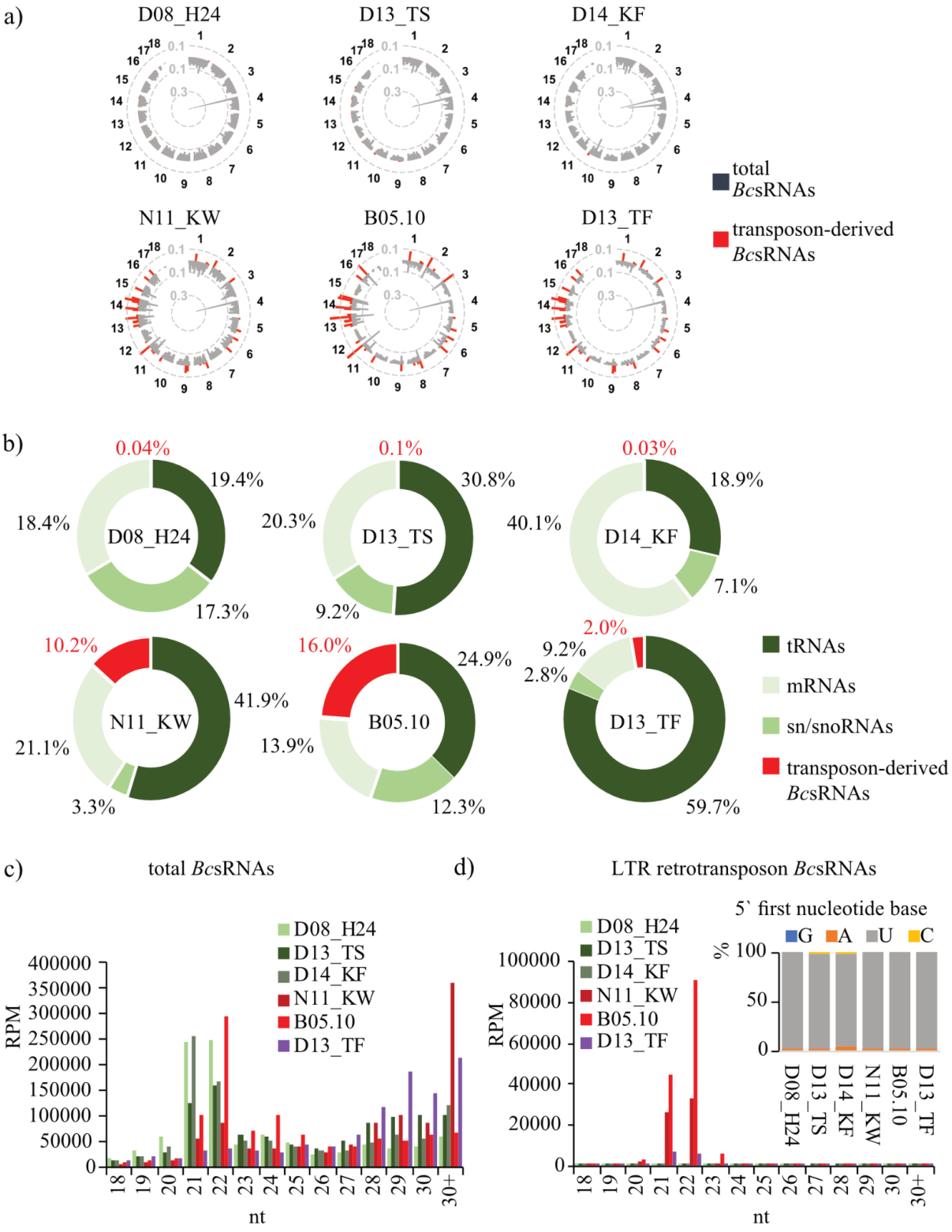

Figure 12: Comparative sRNAseq analysis of the six *B. cinerea* wt isolates reveals either the expression or the absence of LTR retrotransposon-derived *Bc*sRNAs.

a) Genome-wide *Bc*sRNA maps of the six *B. cinerea* strains, coverage represented as log(RPM). **b)** Relative composition of *Bc*sRNAs mapping to distinct genomic loci with numbers giving the relative percentage. **c)** Size profiles of total *Bc*sRNAs in the six *B. cinerea* strains. **d)** Sizes profiles

and 5′ first nucleotide distribution of LTR retrotransposon *Bc*sRNAs in the six *B. cinerea* strains; in **c)** and **d)** reads per million (RPM).

Less aggressive *B. cinerea* strains solely carry mutated and silenced versions of LTR retrotransposons

In order to confirm the fact that 3 strains are devoid of LTR retrotransposons, according to our genotyping PCR (Fig. 10b), we re-sequenced the genomes of D08_H24 and D14_KF, two of the least aggressive isolates. Using hybrid Nanopore long-read in combination with Illumina short-read sequencing techniques, followed by pairwise genome alignment and synteny analysis with the published B05.10 genome, we obtained nearly gapless genomes as shown by the whole genome chromosomal alignment analysis on B05.10 reference genome (Fig. 13a) (van Kan et al., 2017). Using the REPET pipeline, a tool to analyse repeats in genomes (Flutre et al., 2011), we identified only 1 Copia element, for which D08_H24 carried 14 full-length copies and D14_KF carried 10. No Gypsy element was identified. To complete the analysis, we performed BlastN searches in the two newly sequenced genomes and the genome of the reference B05.10. We used REPET-annotated full-length copies found in B05.10 as queries and allowed a minimum alignment length of 400 nt, thus allowing the finding of shorter (*i.e.* truncated) copies. With this method we identified several truncated Copia and Gypsy elements, in all 3 analysed genomes. From these analyses we found that D08_H24 and D14_KF do carry LTR retrotransposons, but less elements and more truncated elements in comparison to B05.10 (Fig. 13b and 13c).

When comparing the CG % of full-length LTR retrotransposons between these 3 strains, we found that all full-length elements from D08_H24 and D14_KF have a low GC content, around 20 %. In opposition, B05.10 full-length elements segregate in two groups, one with a low GC % as well (< 30 %) and one group with a high % (> 40 %) (Fig. 13d). Low GC content in transposons can be the sign of repeat-induced point mutation (RIP), a fungal defence mechanism by which C bases are mutated into T within duplicated sequences, solely taking place during the sexual reproduction cycle (Gladyshev, 2017; van den Berg & Maruthachalam, 2015). If RIP identifies and targets two identical copies of one LTR retrotransposon (= duplicated sequences), it mutates both elements on their full-length, meaning from one LTR to the other, with the coding sequence in the middle. RIP occurring in *B. cinerea* shows a preference of mutating CpA to TpA and mutating CpT to TpT (Amselem

et al., 2015), which alters the frequency of certain dinucleotides within the mutated sequences.

a)

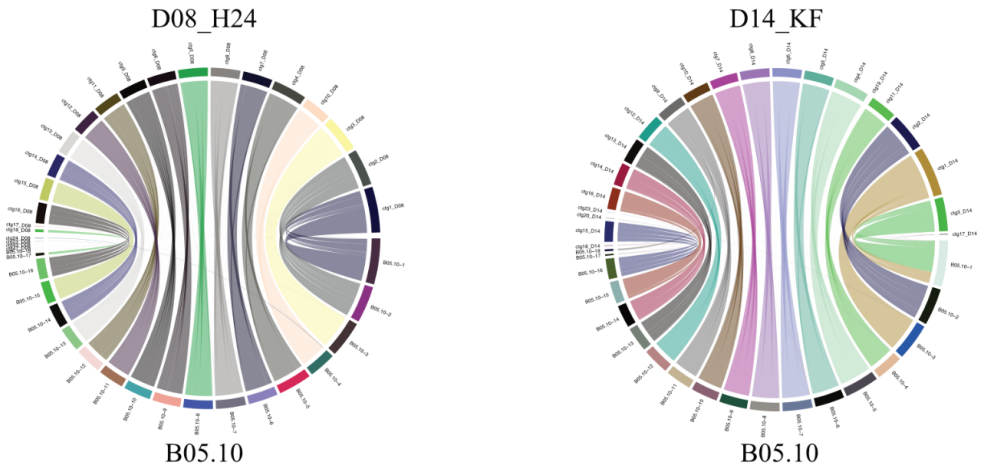

b)

	B05.10	D08_H24	D14_KF
scaffolds	18	49	28
genome size (Mb)	42.630	42.735	42.737
full-length LTR retrotransposons (REPET)	83	14	10
overall GC content (%)	33.48	14.85	19.06
LTR retrotransposons (BLASTn > 400 nt)	178	53	87
overall GC content (%)	31.69	16.22	17.24
LTR retrotransposon *Bc*sRNAs (RPM)	55458.75	111.24	14.76

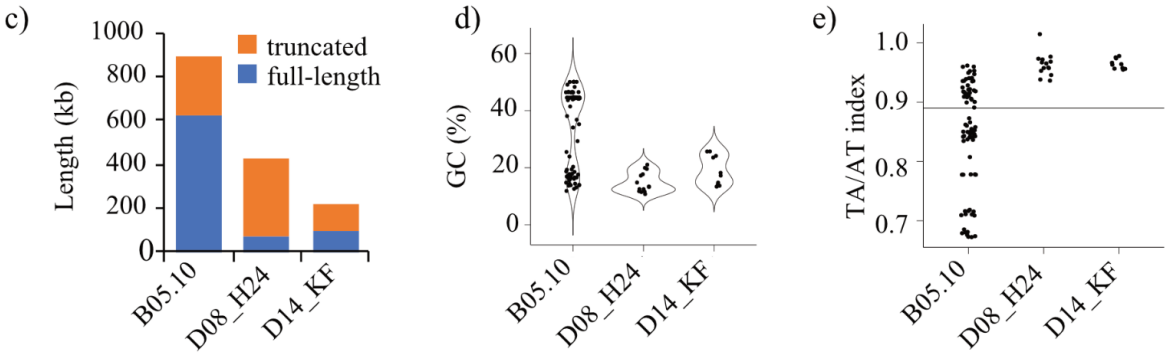

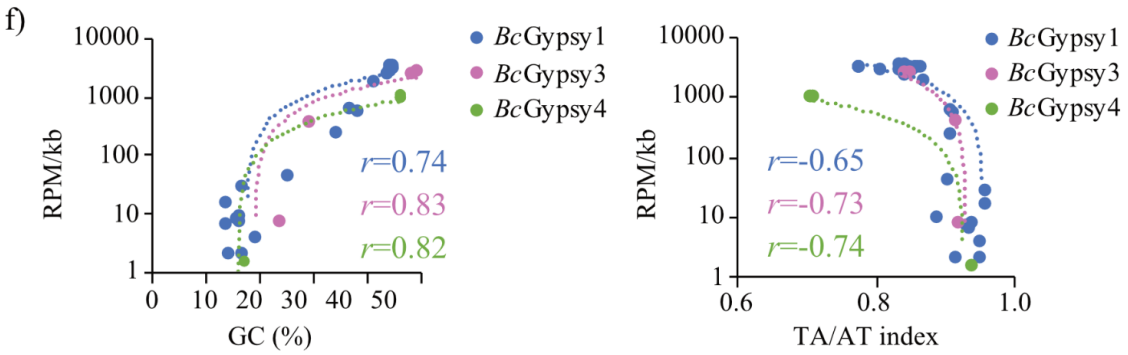

Figure 13: Comparative genome analysis of LTR retrotransposons shows the existence of RIPed and truncated copies.

a) Whole genome chromosomal alignment analysis. For **b** to **e)** Comparative analysis of LTR

retrotransposons identified in the strains B05.10, D08_H24 and D14_KF, and differences in the level of copy numbers, truncation, GC content (%), and the TA/AT dinucleotide ratio with threshold line shown at 0.89. **f)** Correlation analysis between LTR retrotransposon *Bc*sRNA read abundance and GC content (%) or TA/AT dinucleotide ratio of the strain B05.10. r gives the Pearson correlation coefficient.

Thus, to identify RIP's occurrence within the LTR retrotransposon full-length copies, we calculated TA/AT ratios, with high TA/AT ratio indicating a low GC content and therefore RIP. While we found dispersed ratio values for B05.10, D08_H24 and D14_KF ratios were all above 0.89, a threshold that indicates RIP (Hane & Oliver, 2008) (Fig. 13e). This is likely to explain why no signal was detected on the genotyping PCR (Fig. 10b), as these strains carry LTR retrotransposons but their full sequences were heavily mutated by RIP, thus the primers we used could not bind the elements. The B05.10 isolate carries both intact full-length copies of LTR retrotransposons and RIPed (full-length or truncated) elements and interestingly, over the ten copies of *Bc*Gypsy3, only two are intact (data not shown). Correlation analysis between the expression of LTR retrotransposon-derived *Bc*sRNAs (from *Bc*Gypsy1, 3 and 4, the most expressed ones) and the GC content was positive in B05.10 (Fig. 13f), which is in line with RIP leading to transcriptional silencing in fungi (Gladyshev, 2017). Still in B05.10, expression of LTR retrotransposon-derived *Bc*sRNAs negatively correlated with the TA/AT ratios (Fig. 13f). Altogether we showed that the less aggressive *B. cinerea* strains do carry LTR retrotransposons but they all have a low GC content due to RIP mutations and consequently do not express derived *Bc*sRNAs.

The *Bc*Gypsy3 element enhances plant infection

To demonstrate our concept of LTR retrotransposons being important for a stronger aggressiveness, we chose a transgenic approach and inserted a full-length GC-rich non-RIPed LTR retrotransposon into a less aggressive strain. We cloned the *Bc*Gypys3 element from B05.10, as it is the LTR retrotransposon producing the biggest amounts of *Bc*sRNAs and transformed it into D08_H24 as this strain does not carry any full-length *Bc*Gypsy3 elements. We constructed different types of elements into a fungal expression vector containing a 4.98 kilobase *Bc*Gypys3 without the LTR flanking regions, as they do not encode for *Bc*sRNAs and are essential for reverse-transcription and thus transposition of the element, which we wanted to avoid. We made two constructs of *Bc*Gypys3, under the control of constitutive promoters, single-stranded *Bc*Gypys3 ss*Bc*Gypys3) and double-stranded *Bc*Gypys3

(ds*Bc*Gypys3) which is supposed to enhance the production of sRNAs. We used an empty vector as a negative control (EV #18) (Fig. 14a). All the elements were transformed into *B. cinerea* D08_H24 following the homologous recombination method and transgenes were inserted into the *Nitrate reductase D* (*Bc*niaD) locus, known for *B. cinerea* transformation without impacting its virulence (Schumacher, 2012). Additionally, ds*Bc*Gypys3 was also randomly inserted in *B. cinerea* D08_H24 genome (rand*Bc*Gypys3), instead of *Bc*niaD. For all, two or four individual transformants were collected, which showed similar growth on nutrient-rich solid medium (Fig. 14b). A genotyping PCR was performed to control the correct insertion of *Bc*Gypys3 transgene into the *Bc*niaD locus (Fig. 14c).

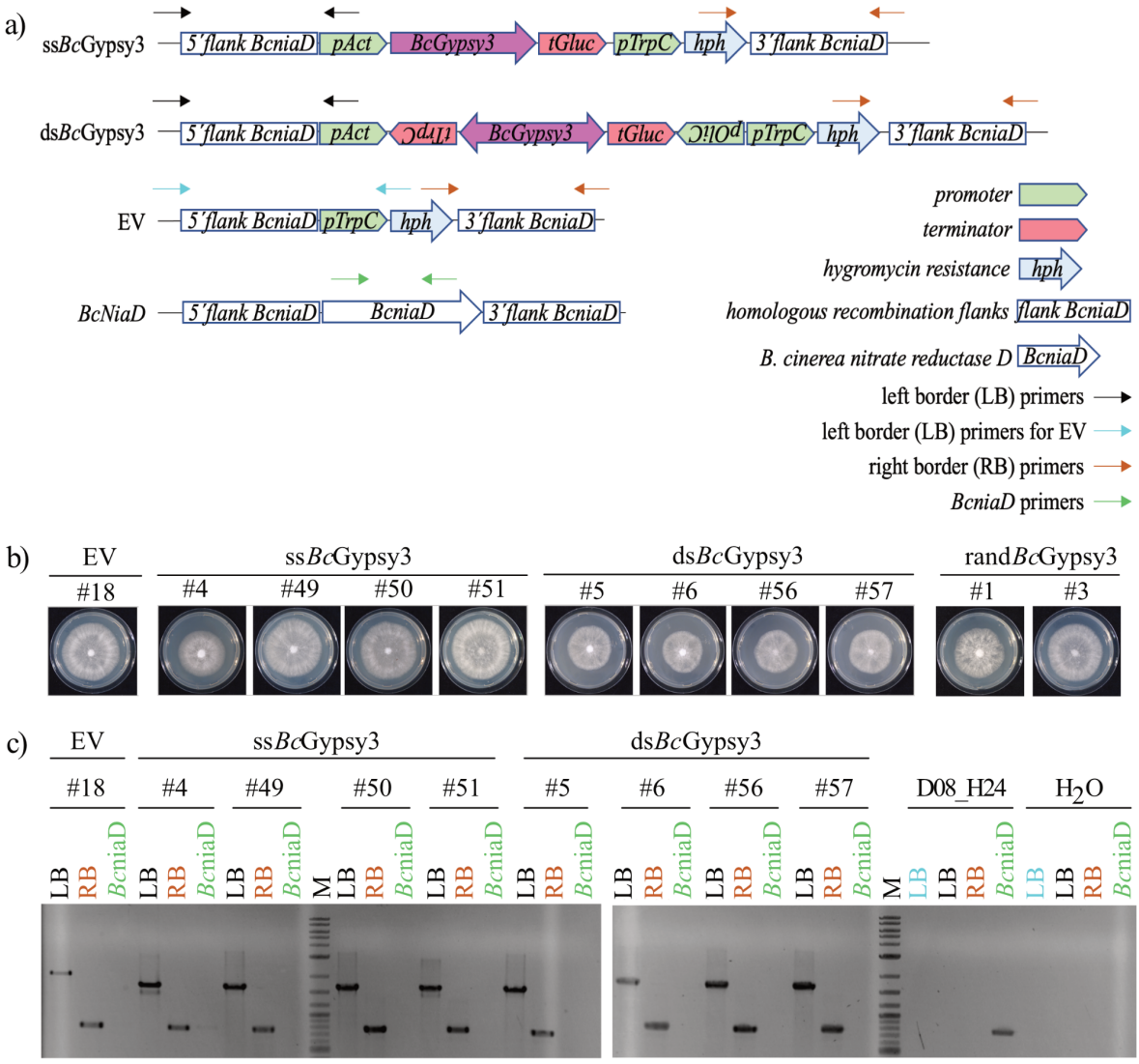

Figure 14: Generation of *Bc*Gypsy3 transformants in the D08_H24 wt strain.

a) Cloning strategy for different *Bc*Gypsy3 transgene and empty vector (EV #18) control.

b) Genotyping PCR of the integrated *Bc*Gypsy3 transgene into the *Bc*niaD locus. M: 1 kb DNA ladder. **c)** Morphological phenotypes of D08_H24 *Bc*Gypsy3 transformants.

We then assessed the level of expression of *Bc*Gypsy3 by RT-qPCR in all selected transformants, targeted and randomly inserted (Fig. 15). Interestingly, a difference in *Bc*Gypsy3 mRNA levels was observable between ss*Bc*Gypsy3 and ds*Bc*Gypsy3 constructs, albeit non-significant. All transformants reached a *Bc*Gypsy3 mRNA level similar to the that of B05.10, except for one rand*Bc*Gypys3 transformant (#1) which had a threefold expression.

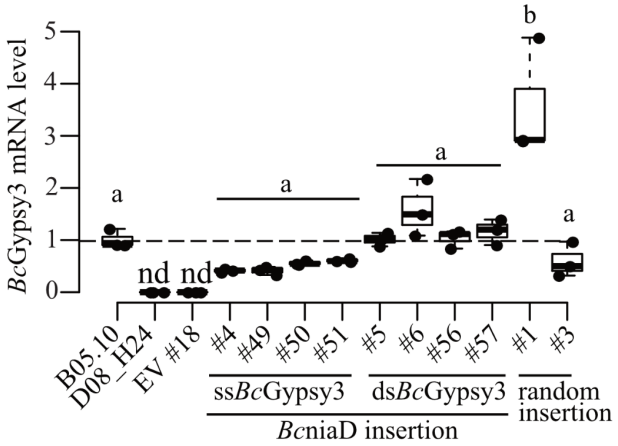

Figure 15: *Bc*Gypsy3 transformants express *Bc*Gypsy3 mRNA in similar or higher levels than B05.10.

*Bc*Gypsy3 mRNA expression in single strand ss*Bc*Gypsy3 (#4, #49, #50, #51), double strand ds*Bc*Gypsy3 (#5, #6, #56, #57) or empty vector (EV #18) transformants with the *Bc*Gypsy3 transgene inserted in the *Bc*niaD locus of D08_H24. Further, randomly inserted ss*Bc*Gypsy3 (rand*Bc*Gypsy3) transformants #1, #3 into the D08_H24 genome, as well as the wild-type strains D08_H24 and B05.10 are shown. Data points represent three biological replicates. A significant difference as indicated by letters was tested by one-way ANOVA using Tukey HSD test with $p < 0.05$.

To estimate the impact of *Bc*Gypsy3 transgene on aggressiveness, we performed pathogen assays on detached *S. lycopersicum* leaves by drop inoculation of conidium suspensions. Two out of four independent transformants of ss*Bc*Gypys3 showed significantly bigger lesion sizes than the empty vector negative control (EV #18), while all four independent transformants of ds*Bc*Gypys3 showed significantly bigger lesion sizes than the empty vector (Fig. 16a and b). This could be explained by the higher expression of *Bc*Gypsy3 in the ds*Bc*Gypys3 transformants (Fig. 15). Concerning *Bc*Gypsy3 random insertion

transformants, #1 which had a high level of *Bc*Gypsy3 mRNA (Fig. 15) showed bigger lesion sizes than the wt strain D08_H24, a less aggressive strain (Fig. 16c); however, #3 showed similar lesion sizes than D08_H24 probably due to the low level of *Bc*Gypsy3 mRNA (Fig. 15). Interestingly, there seemed to be a correlation between the *Bc*Gypsy3 mRNA level and (Fig. 15) and the lesion size (Fig. 16b).

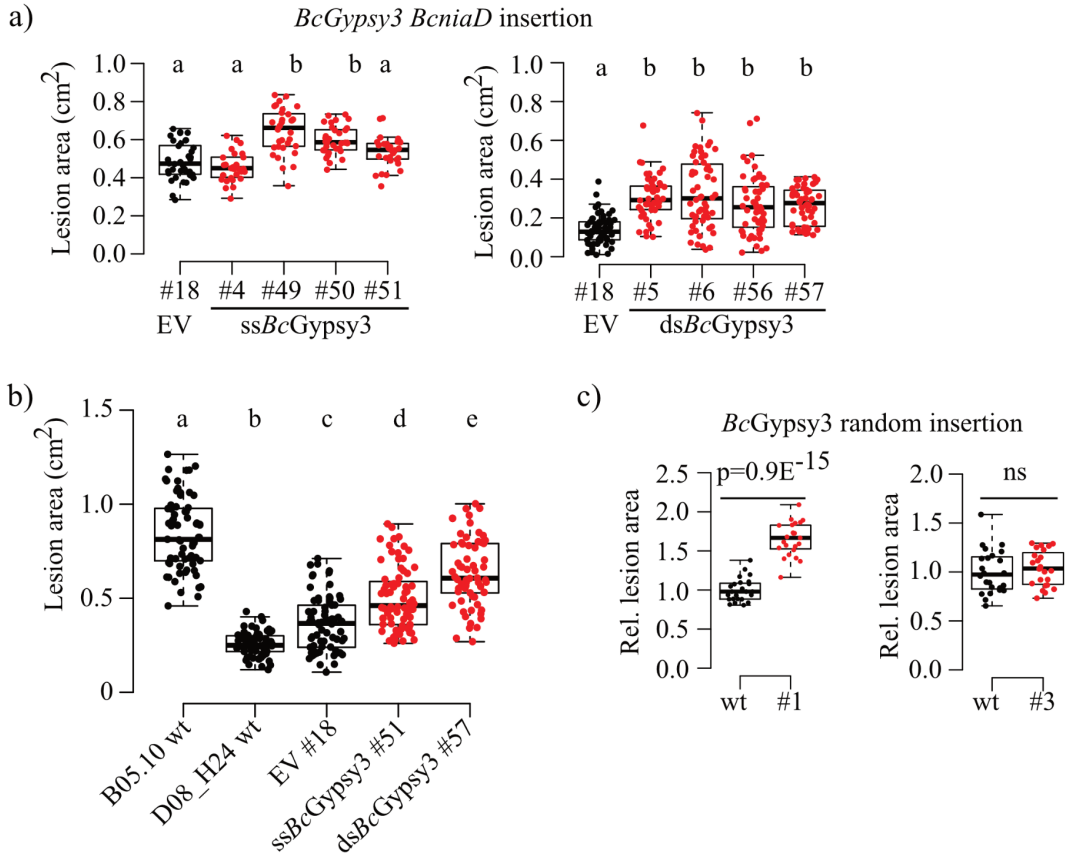

Figure 16: *Bc*Gypsy3 transformants show enhanced aggressiveness compared to D08_H24.
a) Pathogenicity assay with dropped spore suspension of *Bc*Gypsy3 transformants on *S. lycopersicum* leaves quantifying lesion area of > 20 infection sites at 48 hpi. A significant difference as indicated by letters was tested by one-way ANOVA using Tukey HSD test with $p < 0.05$. **b)** Replication of *S. lycopersicum* leaf pathogenicity assay with dropped spore suspension of *Bc*Gypsy3 transformants and *B. cinerea* D08_H24 and B05.10 wt strains. Lesion areas of > 20 infection sites were quantified at 48 hpi. A significant difference as indicated by letters was tested by one-way ANOVA using Tukey HSD test with $p < 0.05$. **c)** Pathogenicity assay with agar plugs of rand*Bc*Gypsy3 transformants on *S. lycopersicum* leaves quantifying lesion area of minimum 8 infection sites at 48 hpi. Significant difference was tested by a two-sided Student's t test. For all, similar results were obtained in two independent infection experiments.

To rule out any importance of the LTRs in this mechanism and more precisely in the expression of *Bc*Gypsy3 mRNA, we cloned the 258 bp of the 5' LTR flanking region and used it instead of the constitutive promoter we used before, in one new ds*Bc*Gypys3 construct and transformed it into the *Bc*niaD locus of D08_H24 (Fig. 17a). Indeed, 5'LTRs are responsible for the transcription regulation of the retrotransposons as they contain the promoter (Havecker et al., 2004). We selected two individual transformants (5'LTR*Bc*Gypsy3 #2 and #3), controlled the transgene insertions via genotyping PCR (Fig. 17b) and their growth on rich solid medium (Fig. 17c).

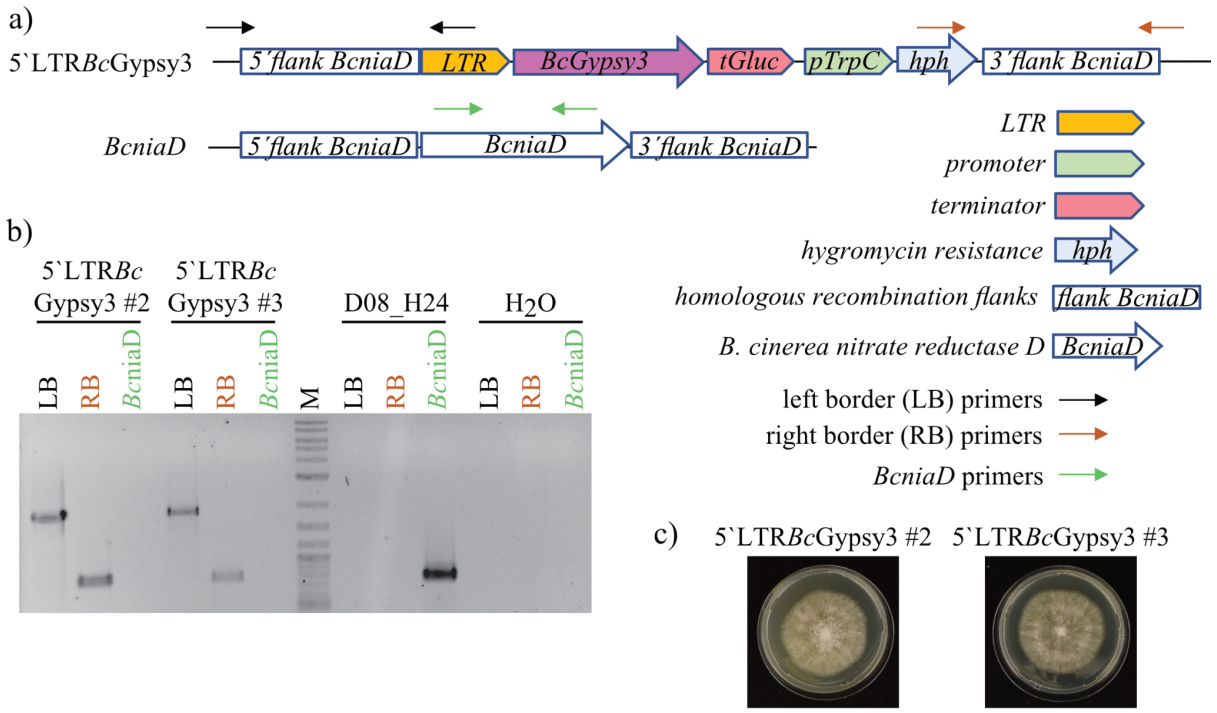

Figure 17: Generation of 5'LTR *Bc*Gypsy3 transformants in the D08_H24 strain.
a) Cloning strategy for 5`LTR*Bc*Gypsy3 transgene. **b)** Genotyping PCR of the integrated 5`LTR *Bc*Gypsy3 transgene into the *Bc*niaD locus. M: 1 kb DNA ladder. **c)** Morphological phenotypes of D08_H24 5` LTR *Bc*Gypsy3 transformants.

We then assessed the level of *Bc*Gypsy3 mRNA by RT-qPCR, which did not reach the level of *Bc*Gypsy3 mRNA in B05.10 (Fig. 18a). For both transformants, we obtained bigger lesion sizes than the ones induced by the empty vector control (EV #18) (Fig. 18b).

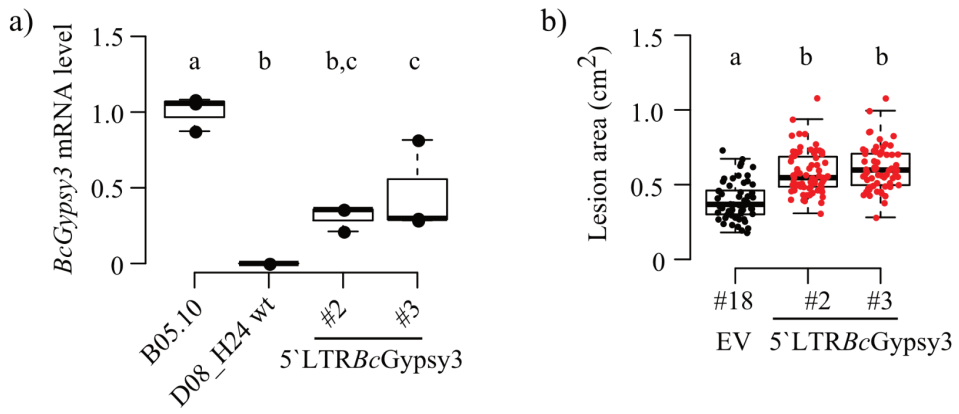

Figure 18: 5'LTR *Bc*Gypsy3 transformants show enhanced aggressiveness compared to D08_H24.

a) *Bc*Gypsy3 RNA expression in 5` LTR *Bc*Gypsy3 (#2, #3). Data points represent three biological replicates. Significant difference as indicated by letters was tested by one-way ANOVA using Tukey HSD test with $p < 0.05$. **d)** Pathogenicity assay with dropped spore suspension of 5` LTR *Bc*Gypsy3 transformants or EV transformant (EV #18) on *S. lycopersicum* leaves quantifying lesion area of > 50 infection sites at 48 hpi. Significant difference as indicated by letters was tested by one-way ANOVA using Tukey HSD test with $p < 0.01$.

All *Bc*Gypsy3 transgenic strains showed enhanced aggressiveness compared to the negative control (EV #18) or D08_H24. Taken altogether, these results indicate a possible positive relationship between the level of *Bc*Gypsy3 mRNA and the aggressiveness reflected by the lesion sizes.

To conclude on this hypothesis, we performed a sRNAseq analysis on one ss*Bc*Gypys3 transformant (#51), one ds*Bc*Gypys3 transformant (#56), one random insertion *Bc*Gypys3 transformant (#1) and the empty vector control (EV #18). In accordance with the RT-qPCR (Fig. 15), *Bc*Gypys3-derived *Bc*sRNAs were slightly more abundant in ds*Bc*Gypys3 transformants than ss*Bc*Gypys3 transformants (Fig. 19). Interestingly, *Bc*Gypsy3-derived *Bc*sRNA levels in ds*Bc*Gypys3 transformants did not reach the level of the wt B05.10 even if their *Bc*Gypys3 mRNA levels were similar (Fig. 15 and 19). Moreover, sRNAseq analysis revealed that *Bc*Gypys3-derived *Bc*sRNAs expression in the random insertion *Bc*Gypys3 transformant (#1) was 10 times higher than in the other transformants where the *Bc*niaD locus was used (Fig. 19). Moreover, this was consistent with the RT-qPCR where *Bc*Gypys3 transformant (#1) showed the higher *Bc*Gypys3 mRNA level (Fig. 15).

Overall, all *Bc*Gypys3 transformants showed enhanced *Bc*Gypys3 derived *Bc*sRNA production accompanied by enhanced aggressiveness, clearly supporting the role of pathogenicity factor of this LTR retrotransposon.

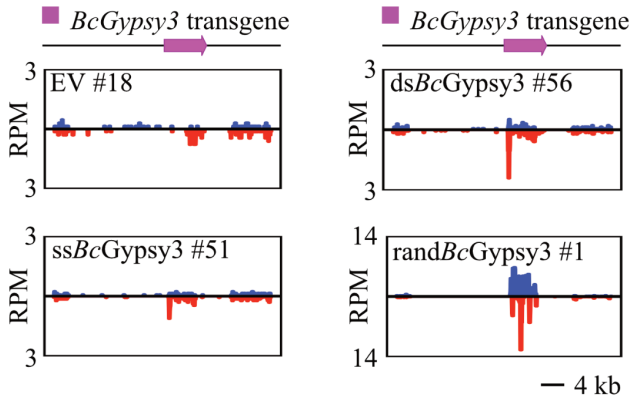

*Bc*Gypsy3 *Bc*sRNAs (RPM)	
EV #18	22.6
ss*Bc*Gypsy3 #51	27.5
ds*Bc*Gypsy3 #56	59.2
rand*Bc*Gypsy3 #1	499.8
B05.10	17550.5

Figure 19: Insertions of *Bc*Gypsy3 transgenic constructs result in expression of derived *Bc*sRNAs.

sRNAseq analysis at the *Bc*Gypsy3 transgene locus representing ss*Bc*Gypsy3 (transformant #51), ds*Bc*Gypsy3 (transformant #56), rand*Bc*Gypsy3 (transformant #1), or empty vector (transformant EV #18), with blue bars indicating sense and red bars indicating antisense reads. The table shows normalised read counts (RPM) of *Bc*Gypsy3 *Bc*sRNAs.

The main action of *Bc*sRNA effectors is to hijack the plant RNAi pathway and target plant genes to silence them (Weiberg et al., 2013), and inserting *Bc*Gypys3 into a less aggressive strain induced enhanced aggressiveness, supposedly via the action of *Bc*Gypys3-derived *Bc*sRNAs. To explore this, we chose to use the random insertion *Bc*Gypys3 transformant (#1) (also named rand*Bc*Gypsy3 #1) and first assessed the expression of 3 previously characterised *Bc*sRNAs (*Bc*siR3.1, *Bc*siR3.2 and *Bc*siR20) (Weiberg et al., 2013), all produced from *Bc*Gypys3, by stem-loop RT-PCR (Varkonyi-Gasic et al., 2007). All three were indeed expressed in rand*Bc*Gypsy3 #1 in comparison to the wt strain D08_H24 which does not carry anyGC-rich and intact (*i.e.* active) *Bc*Gypys3 copies (Fig. 20a).

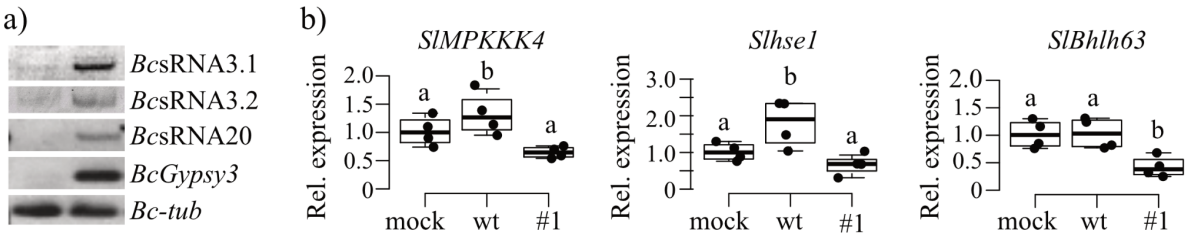

Figure 20: *Bc*Gypsy3 transgene insertion leads to downregulation of the *S. lycopersicum* target mRNAs.

a) Stem-loop RT-PCR showed *Bc*sRNA3.1, *Bc*sRNA3.2 and *Bc*sRNA20 expression in the rand*Bc*Gypsy3 #1. *Bc*Gypsy3 mRNA expression and *BcTub* were used as controls. **b)** qRT-PCR of *S. lycopersicum* target mRNA expression after water treatment (mock), infection with D08_H24 wt or rand*Bc*Gypsy3 #1. Each data point represents a biological replicate.

The mRNA levels of the 3 known targets, in *S. lycopersicum* (Weiberg et al., 2013), of these *Bc*sRNA effectors were measured by RT-qPCR under infection with either rand*Bc*Gypsy3 #1, D08_H24 and compared to a mock treatment (Fig. 20b). The first target is *Mitogen-activated protein kinase kinase kinase 4 (SlMAPKKK4)* mRNA. MAPKs are molecules involved in signalling cascades important for numerous processes, including immunity. In plants, MAPK cascades mediate signals received by membrane receptors, such as PAMPs binding PRRs, to downstream components to conduct responses, such as triggering PTI (Bigeard et al., 2015). MAPK signalling is important for PTI induction but might also be involved in the interplay between PTI and ETI (Thulasi Devendrakumar et al., 2018). The second target is the *Class E vacuolar protein-sorting machinery protein hse1 (Slhse1)* (gene accession: *Solyc09g014790*) mRNA. HSE1 protein is part of the ESCRT-0 complex and is involved in the recruitment of the ESCRT-I complex to the outer membrane of the MVBs and is the receptor responsible for ubiquitination-mediated cargo sorting into the MVBs (Schmidt & Teis, 2012). Thus, silencing of *Slhse1* would impact the MVBs and EV trafficking. As EVs are involved in plant defence against pathogens (Rutter & Innes, 2018), they seem like a relevant target for *B. cinerea*. Remarkably, one identified *A. thaliana* sRNA achieving ckRNAi in *B. cinerea* targets a vacuolar protein sorting involved in vesicular trafficking as well (Cai et al., 2018). The third target is the *Basic helix-loop-helix (Bhlh)63 transcription factor* (gene accession: *Solyc03g120530*) mRNA. Except its most probable role in transcription regulation, nothing is known on this particular transcription factor, although we can speculate a possible role in plant immune response. All three targeted mRNAs

showed downregulation under rand*Bc*Gypsy3 #1 infection compared to wt D09_H24 infection (Fig. 20b).

Similarly, the mRNA levels of the known targets of *Bc*sRNA3.1 and *Bc*sRNA3.2, in *A. thaliana* were measured by RT-qPCR under either rand*Bc*Gypsy3 #1 or D08_H24 infections and compared to a mock treatment. In *A. thaliana*, *Bc*sRNA3.2 targets both *Mitogen-activated protein kinase 1* (*AtMPK1*) and *Mitogen-activated protein kinase 2* (*AtMPK2*). Like previously, MAPKs are involved in the signalling pathway of PTI, thus in the immune response. *AtMPK1* mRNA level showed a significant downregulation, and *AtMPK2* showed a tendency to decrease, upon rand*Bc*Gypsy3 #1 infection compared to D08_H24 infection (Fig. 21).

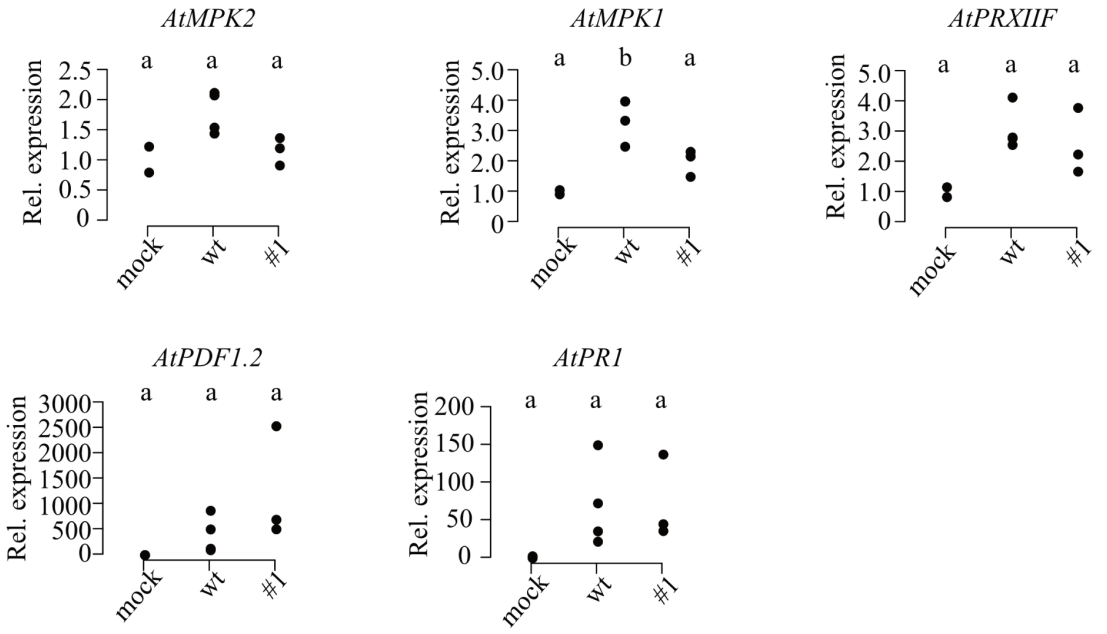

Figure 21: *Bc*Gypsy3 insertion leads to the downregulation of target mRNAs, but not of control non-targeted mRNAs, *A. thaliana* plants.
qRT-PCR analysis of *A. thaliana* target mRNAs after no-infection (mock) or after infection with D08_H24 wt or rand*Bc*Gypsy3 #1. *AtPDF1.2* and *AtPR1* were used as *B. cinerea*-inducible genes in *A. thaliana* and these genes were not predicted targets of *Bc*sRNAs. Each data point represents a biological replicate.

*Bc*sRNA3.2 targets an oxidative stress-related gene, *peroxiredoxin* (At*PRXIIF*), which is crucial in regulating the redox homeostasis and root growth of *A. thaliana* under stress

(Finkemeier et al., 2005). Comparable to *AtMPK2*, *AtPRXIIF* only showed a slight tendency under rand*Bc*Gypsy3 #1 infection compared to D08_H24 infection (Fig. 21). As a control, two *A. thaliana* genes involved in pathogen response, but which are not targeted by *Bc*Gypsy3-derived *Bc*sRNAs, were measured as well by RT-qPCR. *AtPlant Defensin* (*AtPDF1.2*) and *AtPathogenesis-related protein* (*AtPR1*) did not shown any downregulation in rand*Bc*Gypsy3 #1 compared to D08_H24 infection (Fig. 21). The silencing of the plant targets supports our model and illustrates how *Bc*Gypys3-derived *Bc*sRNAs can manipulate the host.

To gather additional knowledge on the impact of *Bc*Gypys3 on the host plant mRNA transcriptome, we infected *A. thaliana* plants with either rand*Bc*Gypsy3 #1 or D08_H24 (Fig. 22a) and performed an RNAseq followed by a differential gene expression analysis. With a false discovery rate (FDR) cut-off at 0.05, it appeared only a few genes were identified as differentially expressed, 7 genes were up- and 8 genes were downregulated under rand*Bc*Gypsy3 #1 infection compared to D08_H24 infection (Fig. 22b). Two genes involved in auxin signalling were downregulated, the *Small auxin upregulated RNA 78* and the *Catalase* (*AtCAT2*). It was shown in other studies that *A. thaliana* susceptibility to *B. cinerea* is increased with repression to auxin signalling (Llorente et al., 2008), which is in line with our finding. Moreover, the cysteine protease *Response to dehydration 21* was also downregulated, and together with (*AtCAT2)* they both are known resistance factors of *A. thaliana* against *B. cinerea* infection (Shindo et al., 2012; Yuan et al., 2017). On the other hand, upregulated genes related to stress response comprised: the transcriptional repressor *Jasmonate-Zim-Domain (JAZ)5* which is a negative regulator of *A. thaliana*'s defence against *B. cinerea* (Jiang & Yu, 2016) and the transcriptional repressor and *NF-X-LIKE 1* which is a negative regulator of defence against fungal toxins (Asano et al., 2007, 2008). Down and upregulations of such genes are beneficial for *B. cinerea* infection and are a consequence of *Bc*Gypys3 transgene, thus showing its importance for manipulating the plant host gene expression, presumably by cross-kingdom RNAi.

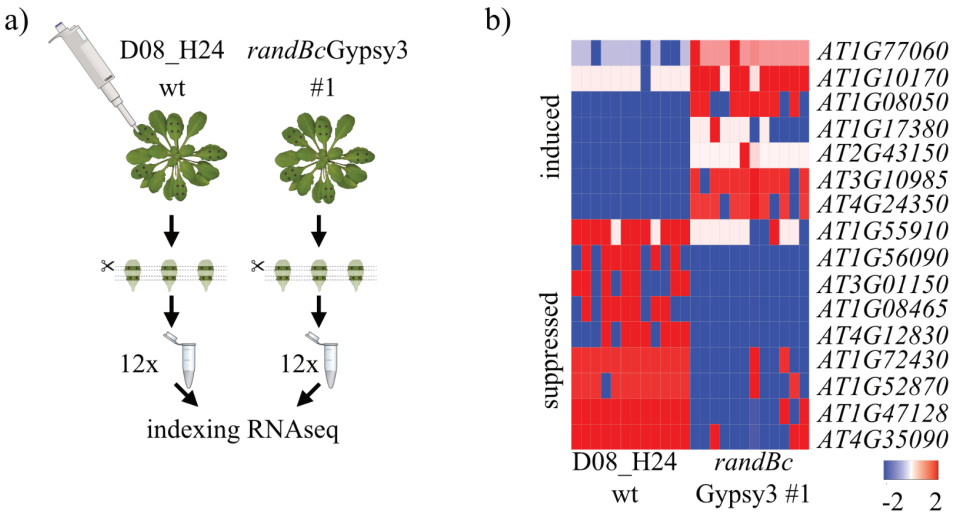

Figure 22: *Bc*Gypsy3 transgene induces a modulation of the host plant transcriptome.
a) Scheme of the RNAseq experiment, with infecting *A. thaliana* either with D08_H24 wt or rand*Bc*Gypsy3 #1 comprising 12 biological replicates for each treatment. **b)** Heat map showing differentially expressed *A. thaliana* genes comparing infection with D08_H24 wt or rand*Bc*Gypsy3 #1.

Altogether, in this study we could show that LTR retrotransposons are playing the role of pathogenicity factors in the fungal phytopathogen *B. cinerea* and in particular, the *Bc*Gypys3 element from which a large amount of *Bc*sRNAs are expressed. These *Bc*sRNA effectors are translocated into the host plant cells to achieve ckRNAi and silence host plant immunity-related genes. Naturally occurring *B. cinerea* strains carry only relics of LTR retrotransposons mutated by the genome protection mechanisms RIP, and do not produce *Bc*sRNA effectors, hence are less aggressive. By inserting *Bc*Gypys3 into a less aggressive strain we could restore the expression of *Bc*sRNA effectors and enhance the aggressiveness.

Characterisation of *B. cinerea* extracellular vesicles

B. cinerea produces extracellular vesicles in axenic culture

For an early successful infection, *B. cinerea* relies on cross-kingdom RNAi (ckRNAi), a strategy in which *Bc*sRNAs are transported in the host plant cells and hijack the plant RNAi pathway to silence the expression of plant mRNAs related to the immune response (Weiberg et al., 2013). No mechanism for *Bc*sRNA transport to the host cells has been identified and we hypothesised that *Bc*sRNAs are loaded and travel into *B. cinerea* EVs (*Bc*EVs). Thus, the first step was to optimise a method for *Bc*EVs isolation, from the aggressive reference strain B05.10 which carries GC-rich LTR retrotransposons, thus produces *Bc*sRNAs deriving from these elements. The most common and approachable method for EV isolation is differential ultracentrifugation (DUC). It relies on the sequential sedimentation and separation of all components present in a liquid culture. With this method each step increases the centrifugation speed and filtration strength, eliminating sequentially mycelium, cell debris and apoptotic bodies, and finally MVs (Li et al., 2017). In our protocol, the final ultracentrifugation step was done at 100,000 g-force for 60 min (at 4 °C) and pelleted *Bc*EVs. This raw extract of *Bc*EVs was washed in MES buffer with a last ultracentrifugation, resulting in a sample we called crude *Bc*EVs (Fig. 23a).

To investigate whether *B. cinerea* secretes *Bc*EVs, we first performed DUC on *in vitro* axenic liquid cultures. For this, conidia were inoculated into liquid media and cultivated for several days until enough biomass was obtained and thus numerous *Bc*EVs would be produced and released in the culture supernatant. The first trials were made either with nutrient-rich liquid media, alone or supplemented with plant extract, as it could enhance *B. cinerea* growth and hypothetically enhance *Bc*EV secretion. These generated highly thick and viscous cultures, which made the DUC protocol extremely difficult to complete. Isolation from this type of culture, performed until the protocol final steps, did not result in *Bc*EV containing samples (data not shown). All tested media are referenced in a table (Annexe 1).

Because no *Bc*EVs could be isolated in these conditions, and because the cultures were highly viscous, we hypothesised that this was due to the thick extracellular glucan matrix that *B. cinerea* secretes, which would enclose *Bc*EVs and thus prevent isolation. To solve this we used a modified version of Czapek Dox minimal liquid media to decrease the

C/N sources ratio, which is known to reduce the glucan matrix secretion (Leal et al., 1979; Maas & Powelson, 1972; Pielken et al., 1990). These cultures were indeed less viscous, therefore only this minimal liquid media was used for *B. cinerea* liquid culture. However, it is important to note that not all liquid cultures could easily pass through all DUC protocol steps, showing that *B. cinerea* still secreted some extracellular matrix. Overall, this method reached a 60 to 70 % rate of success, revealing *Bc*EV isolation to be challenging.

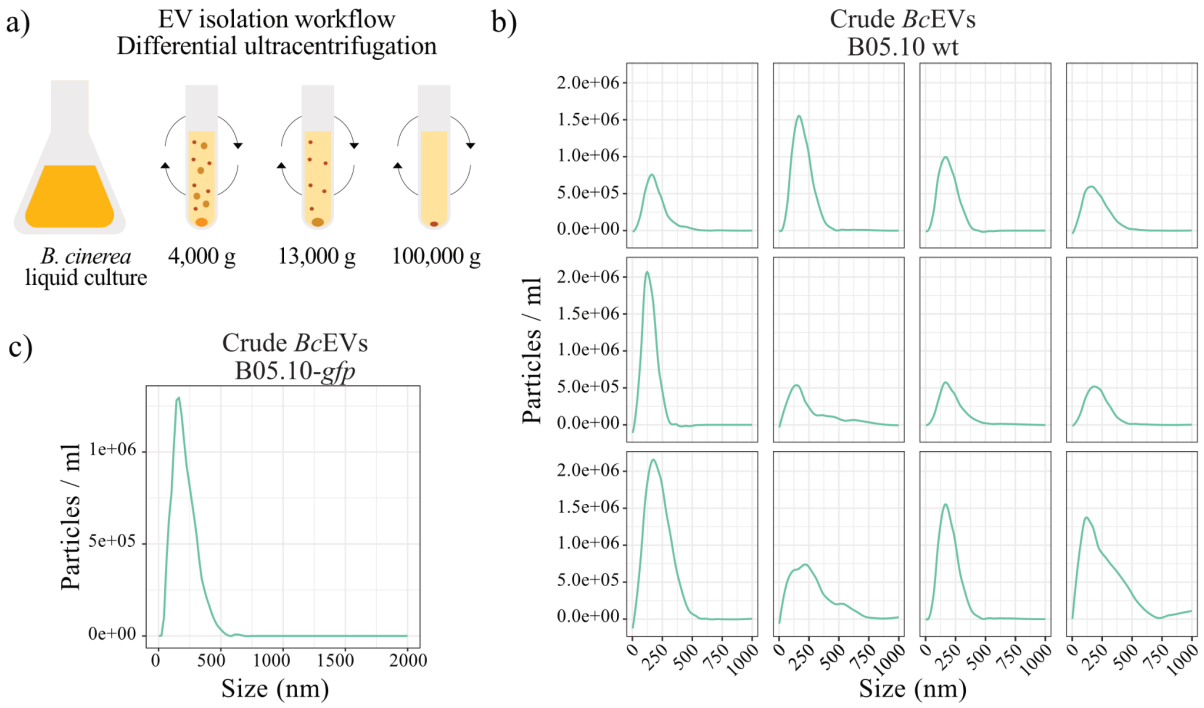

Figure 23: *B. cinerea* secretes *Bc*EV nanoparticles in liquid cultures.
a) Schematic representation of *Bc*EV differential ultracentrifugation (DUC) isolation protocol. *Bc*EVs were isolated from liquid culture supernatant which undergoes sequential steps of centrifugations with increasing speeds, in order to get rid of mycelium, apoptotic bodies and microvesicles before pelleting crude *Bc*EV samples. **b)** Crude *Bc*EV size profiles, measured with NTA, of 12 B05.10 *B. cinerea* liquid culture biological replicates either in different panels or overlayed. Concentration and size heterogeneity among samples were observed. **c)** Crude *Bc*EVs isolated from B05.10-*gfp* strain, in two biological replicates, showed a similar profile to crude *Bc*EVs isolated from B05.10 wt. For **b** and **c)** the graphical outputs do not represent the raw data but are smoothed following the locally weighted least squares regression ("loess") model.

Crude *Bc*EVs were isolated from 12 independent axenic liquid cultures (of the B05.10 reference strain) and analysed by nanoparticle tracking analysis (NTA). The mean sizes ranged from 133 to 200.5 nm in diameter and for all samples taken together, the median was 184 nm and a mean of 220.7 nm (Fig. 23b, Table 3). Even if all the peaks were centred on the

same size (nm, x axis), heterogeneity could still be observed (Fig. 23b). *Bc*EV concentrations (particles per ml) seemed rather heterogeneous (Table 3), reflecting the variation of efficiency among several *Bc*EVs isolations, and were globally surprisingly low considering the quantity of liquid culture from which they were isolated (700 to 1000 ml). For example, from one *C.neoformans* EV isolation (cells resuspended in 10 ml), 20 to 50 more particles are recovered (Rizzo et al., 2021). Culture conditions and EV concentrations of other fungal species were collected from publications and are referenced in a table, for comparison (Annexe 2). The rather poor *Bc*EV yields showed again the challenging aspect of isolating *Bc*EVs.

Biological replicates	**Median size (nm)**	**Mean size (nm)**	**Concentration (particles/ml)**
1	177.5	204.8	4.23E+05
2	133	146	1.28E+06
3	177	235.6	3.99E+05
4	200.5	233.8	3.86E+05
5	191	211	3.66E+05
6	198	222	1.24E+06
7	200.5	258.3	5.18E+05
8	198	224.4	7.60E+05
9	184	237.7	1.15E+06
10	198	224.4	7.60E+05
11	178	190.3	6.18E+05
12	193	213.2	4.00E+05

Table 3: Sizes and concentrations of *Bc*EVs from the 12 independent biological replicates represented in Fig. 23b. Measurements were performed by NTA.

Experiments were conducted on two strains, either the aggressive B05.10 reference wt strain, which carries GC-rich LTR retrotransposons, or the same strain but genetically modified to encode for cytoplasmic GFP and the resistance cassette to hygromycin, which we called B05.10-*gfp* strain. Both strains showed comparable phenotypes when grown on agar

plates under light or darkness and in minimal medium liquid culture (data not shown). NTA measurements of crude *Bc*EVs isolated from the B05.10-*gfp* strain, in two biological replicates, showed size profiles with an average median of 184 nm and an average mean of 207 nm (Fig. 23c). This shows that insertions of the *Gfp* coding gene and the antibiotic resistance cassette did not impact the production and biogenesis of *Bc*EVs; therefore, both strains were used similarly to conduct the experiments.

Transmission electron microscopy (TEM) of negatively (with 1 % uranyl acetate) stained crude *Bc*EV samples (isolated from the B05.10-*gfp* strain) displayed spherical structures similar to extracellular vesicles, which were not present in the growth medium alone (Fig. 24a) showing they originated from *B. cinerea*. *Bc*EV diameter measurements manually performed with the software Fiji showed sizes mainly ranging from 25 nm to 91 nm (Fig. 24b), with a median of 48.63 nm and mean of 50.46 nm. EVs, and more particularly exosomes, are usually bigger than what we observed (Colombo et al., 2014). However, negative staining for electron microscopy involves dehydration which causes shrinking of the vesicles, potentially explaining the smaller size (Bachurski et al., 2019; Szatanek et al., 2017; van Niel et al., 2018). To visualise *Bc*EVs secretion from *B. cinerea* hyphae, we performed scanning electron microscopy (SEM) of mycelium collected from axenic liquid cultures used for vesicle isolation (B05.10 wt strain). The images showed spherical particles, of approximately 150 to 200 nm in diameter, budding out of the hyphae resembling what would be *Bc*EVs (Fig. 24c). Interestingly, the first SEM attempt was revealed to be ineffective as pictures displayed mycelium hidden by a “net” structure (data not shown), thus hiding possible *Bc*EVs as well. We believe these structures were in part the extracellular glucans secreted by *B. cinerea*. This issue was solved by performing acetone dehydration with graded baths during sample preparation.

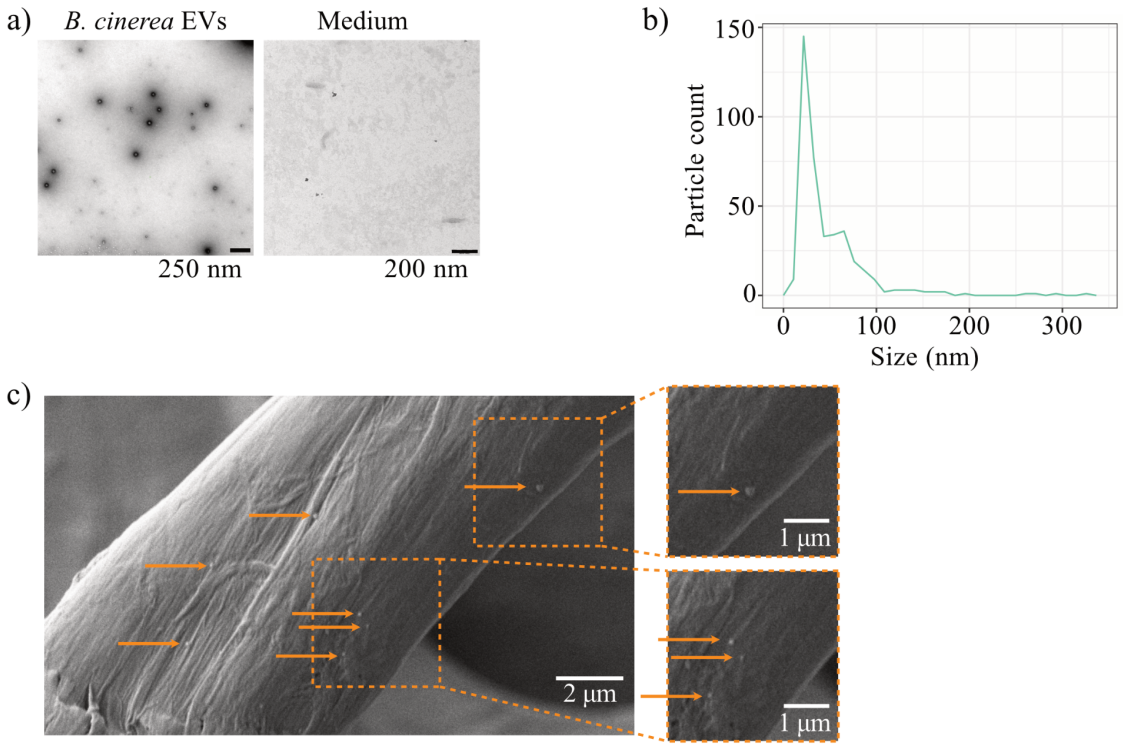

Figure 24: *Bc*EVs are spherical and released from the hyphae.
a) TEM imaging of crude *Bc*EVs isolated by DUC showed spherical nanoparticles, which are not present in *B. cinerea* growth medium alone. **b)** Size profile of crude *Bc*EVs manually measured from TEM pictures, with a median size at 48.63 nm. **c)** SEM picture of *B. cinerea* hyphae growing in liquid culture, displayed *Bc*EVs, of approximately 150 to 200 nm, getting released in the extracellular space.

*Bc*EVs isolated from axenic cultures co-purify with *Bc*sRNAs

To determine if *Bc*sRNA effectors, actors of ckRNAi, are transported to the host plant via *Bc*EVs, we performed a stem-loop RT-PCR on two previously characterised *Bc*sRNAs: *Bc*siR3.1 and *Bc*siR20 (Weiberg et al., 2013). Stem-loop RT-PCR is one of the most popular techniques for detecting small RNAs, it is based on two steps: first, the sRNA is reverse transcribed with a specific stem-loop primer and second, it is amplified by PCR (Varkonyi-Gasic et al., 2007). As stem-loop RT-PCR requires to be performed separately for each sRNA because of the RT primer specificity (hence to divide the *Bc*EV sample) and as *Bc*EVs were not massively abundant; we decided to restrict the experiments to two *Bc*sRNAs. Both *Bc*sRNAs were detected in crude *Bc*EVs (isolated from the B05.10-*gfp* strain), as well as in a total sRNA sample from mycelium (Fig. 25).

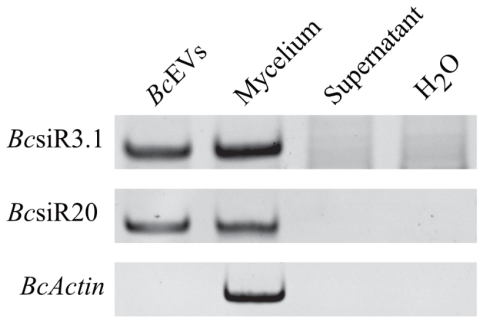

Figure 25: *Bc*sRNAs co-purify with *Bc*EVs after DUC isolation.
Stem-loop RT-PCR showed the presence of *Bc*siR3.1 and *Bc*siR20 in crude *Bc*EV sample and mycelium, while standard oligodT RT-PCR detected *BcActin* in mycelium only, suggesting a sorting mechanism into *Bc*EVs. Both negative controls were performed using H_2O instead of RNA template.

BcActin mRNA was only present in the mycelium, suggesting that not all *B. cinerea* cellular RNAs are packed inside *Bc*EVs, therefore an active and selective loading process might take place. RNA extracted from the last ultracentrifugation supernatant was used as a negative control. Neither *Bc*sRNA 3.1 and 20 nor *Actin* mRNA were detected, showing that all present RNAs co-precipitate with *Bc*EVs particles during the ultracentrifugation (Fig. 25). With this result we found evidence that *B. cinerea* sRNA effectors, which are transported into the host plant cells during infection, co-purify with *Bc*EVs *in vitro*.

*Bc*EVs and *Bc*sRNAs are relatively resistant to diverse treatments

To assess the intravesicular localisation of *Bc*sRNAs and rule out the possibility of co-precipitation, we performed nuclease protection assays (in both *Bc*EVs isolated from the B05.10 reference strain or the B05.10-*gfp* strain). To reach this aim, each crude *Bc*EV sample was equally divided into three to four aliquots, which all receive different treatments. These treatments sequentially and selectively alter different types of molecules (lipids, proteins and finally nucleic acids, when all treatments are performed) in order to show that *Bc*sRNAs are protected into *Bc*EVs (Buck et al., 2014; Cai et al., 2018; Valadi et al., 2007). Indeed, solely treating *Bc*EV samples with a nuclease, in combination or not with proteinase K (to make protein-protected RNAs accessible to the nuclease), cannot lead to the degradation of any intravesicular RNAs but only of the RNAs present outside which co-purified with *Bc*EVs. But if vesicles are first disrupted with a detergent such as Triton X-100 (whose action perturbs lipids/membranes), in addition to mechanical/physical treatments (heat, vortex), the

RNA content should be released outside the vesicles and accessible for degradation. For this assay, one aliquot was always kept untreated on ice, remaining as crude *Bc*EVs as a control. Directly after the treatments, sRNAs were extracted and stem-loop RT-PCRs were performed on all the aliquots to detect the presence of one *Bc*sRNA (*Bc*siR20). Because *Bc*EV concentrations are low and because we split the samples into several aliquots, we chose to detect only one sRNA to avoid being under the stem-loop RT-PCR detection limit.

For the first trial, the *Bc*EV sample was divided in three reactions and the aliquots were either non-treated, RNase A-treated or Triton X-100 - RNase A-treated. *B*csiR20 was detectable in all three aliquots (Fig. 26a). However, RNase A cleaves only single-stranded RNAs and *B*csiR20 could be double-stranded. Thus, in a second assay we used Micrococcal nuclease (MNase) which degrades single and double-stranded DNA and RNAs in an endo-/exo-nuclease manner. Here again, *B*csiR20 was detected in all three aliquots (Fig. 26b). However, single or double-stranded *B*csiR20 could be bound to proteins which would protect it from MNase degradation. Hence, in a third assay a fourth aliquot was added and a proteinase K degradation step included. Unexpectedly, *B*csiR20 was detected once again in all aliquots (Fig. 26c and d). In all assays, a 1 % final concentration of Triton X-100 was used, similarly to another study conducted on *At*EVs (Cai et al., 2018), which should not impair nuclease activity. To ensure this, Triton X-100 - MNase treated total RNA was either directly run on a gel to visualise total RNA, or used for detecting *B*csiR20 by stem-loop RT-PCR. In both cases the presence of the detergent did not prevent MNase activity (Fig. 26e). As further proof, we cloned and sequenced the stem-loop RT-PCR product of *Bc*siR20 from two treated *Bc*EV samples (proteinase K – MNase and Triton X-100 – proteinase K – MNase). Both sequencing results showed a perfect alignment to *Bc*siR20 (Fig. 26f). These results showed that *Bc*siR20 was not degraded by MNase, even in the presence of Triton X-100 which supposedly disrupts *Bc*EVs and leaves the *Bc*sRNAs accessible for degradation. Altogether this suggests that *Bc*siR20 is surprisingly stable and might be located inside *Bc*EVs, and, moreover that *Bc*EVs have an unexpected resistance to detergent treatment.

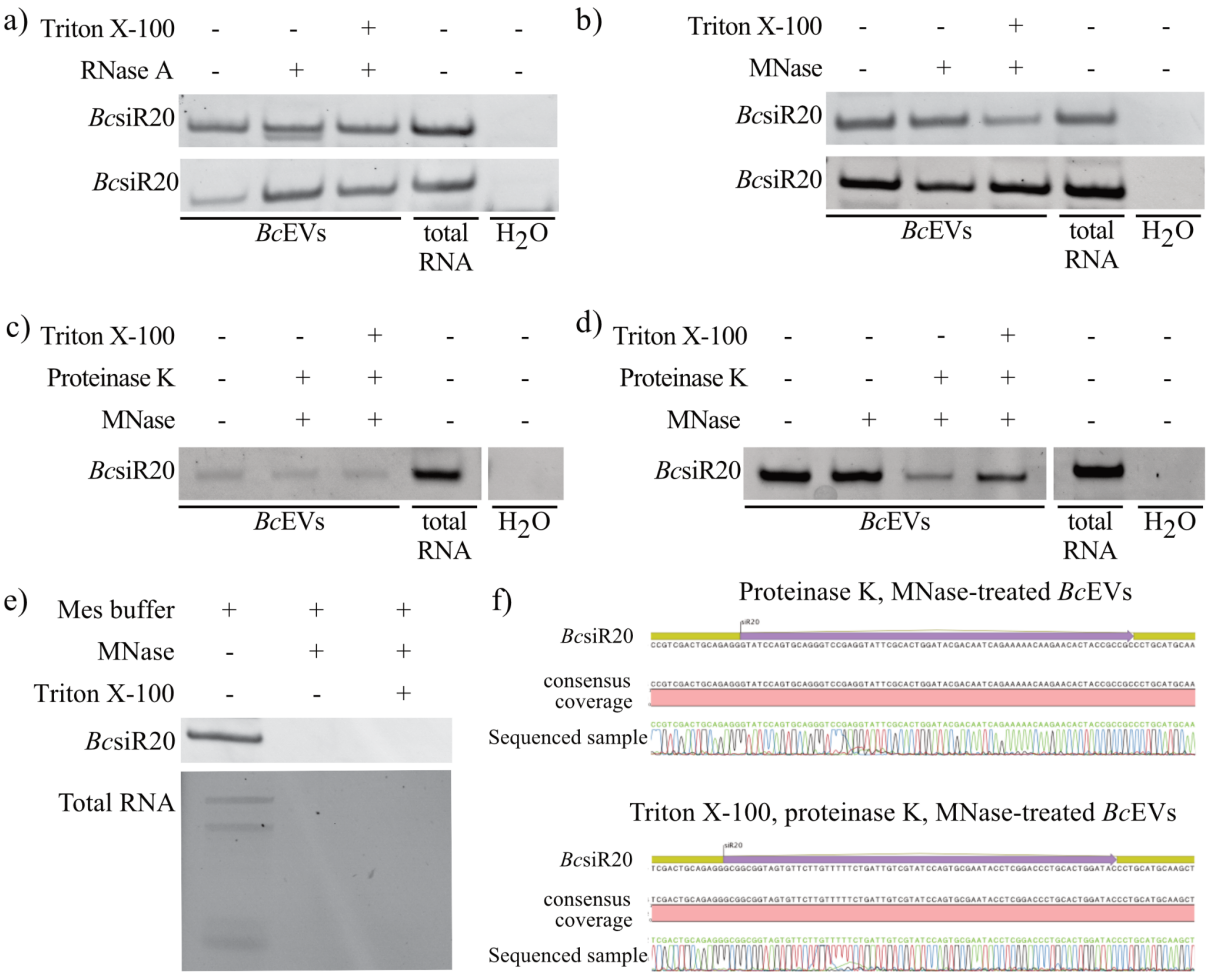

Figure 26: *Bc*sRNAs are protected from nuclease degradation.
Nuclease assays were performed to show the intravesicular location of *Bc*sRNAs. Different treatments were applied to crude *Bc*EV samples before detection of *Bc*siR20 by stem-loop RT-PCR. No treatment led to loss of the PCR signal. **a)** Crude *Bc*EV samples were treated with Triton X-100 and/or RNase A. Two biological replicates are displayed. **b)** Crude *Bc*EV samples were treated with Triton X-100 and/or MNase. Two biological replicates are displayed. For **c** and **d)** Crude *Bc*EV samples were treated with Triton X-100 and/or proteinase K and/or MNase. **e)** Total RNA extracted from *B. cinerea* mycelium was treated with MES buffer (*Bc*EV resuspension buffer) and/or Triton X-100 and/or MNase, to confirm the activity of MNase under these conditions, the sample was either ran directly on a gel or used for a stem-loop RT-PCR, to ensure the activity of MNase under these conditions. **f)** Two *Bc*siR20 bands were cut out from the gel and sequenced to control the true presence of the sRNA after treatments. In both situations, the sequenced PCR fragments fully matched the *Bc*siR20 sequence.

To rule out the alternative that *Bc*siR20 presence after Triton X-100 treatment would be due to *B*cEVs being resistant to the detergent, we analysed the particles with NTA after all treatments (experimental set-up like in Fig. 22c), on three biological replicates. While crude *Bc*EVs and proteinase K - MNase-treated *Bc*EVs show similar size profiles and

concentrations, *Bc*EVs exposed to Triton X-100 were more numerous and significantly smaller, with, remarkably, very homogeneous sizes (Fig. 27a and b).

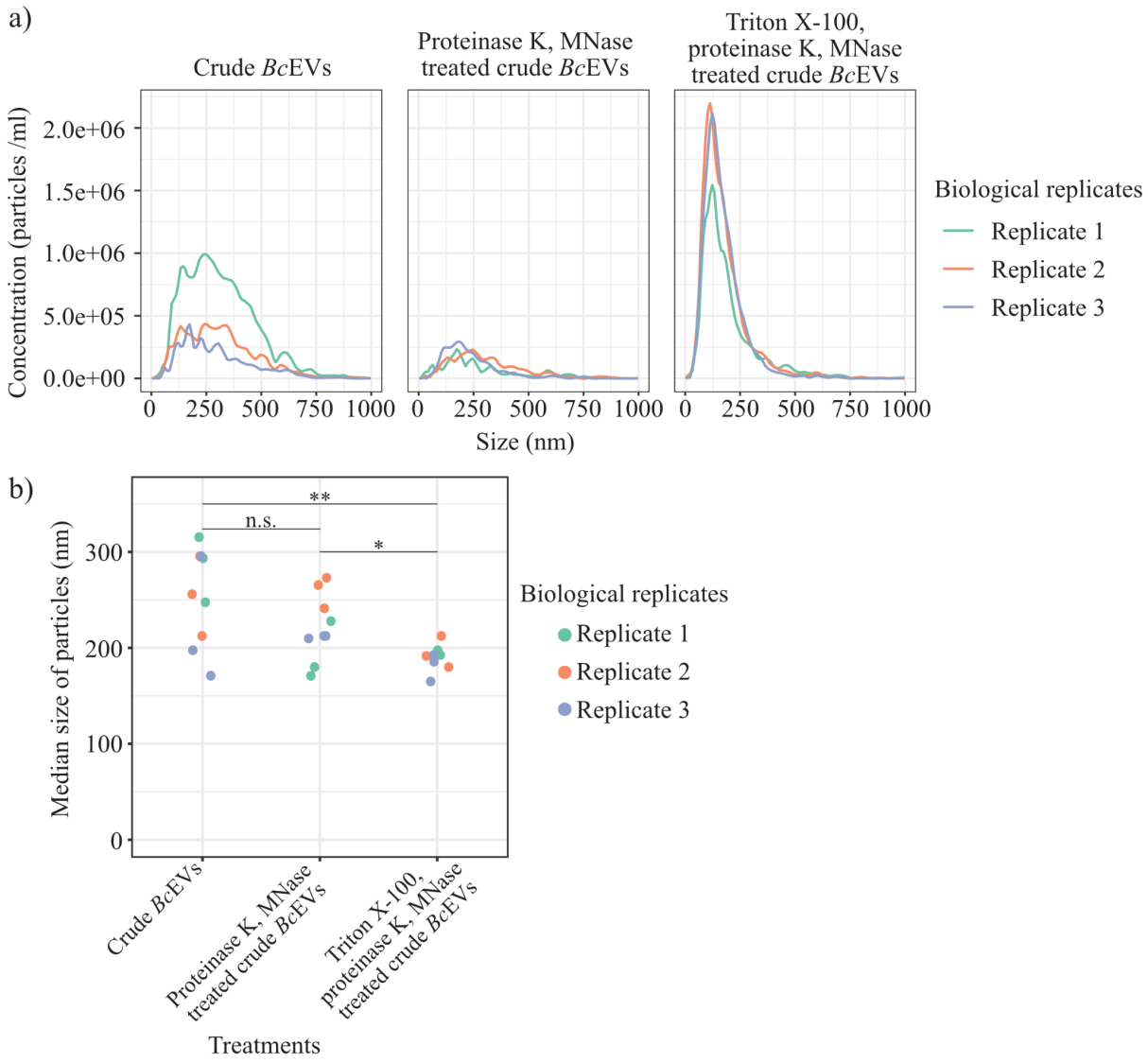

Figure 27: *Bc*EVs seem resistant to Triton X-100 treatment.
Three biological replicates of crude *Bc*EV samples were split in three aliquots, and treated or not treated with proteinase K and MNase, or with Triton X-100, proteinase K and MNase. *Bc*EV size profiles of the three replicates were measured with NTA. **a)** Results are presented with a line plot, and the data were smoothed following the loess regression method, **b)** or a dot plot. Significant differences indicated by * ($p \leq 0.05$) or ** ($p \leq 0.01$) and no difference by n.s. ($p > 0.05$), were tested by a paired Wilcoxon test.

We hypothesised that Triton X-100 triggers a restructuring of *Bc*EV membrane lipids which first solubilise, thus releasing part of the intravesicular content in the environment/buffer, and then reassemble into membrane-enclosed particles (here of smaller

sizes) while re-enclosing some of the RNA molecules. This could explain why *Bc*siR20 was still detectable by stem-loop RT-PCR (Fig. 26 a to d). This hypothesis is also supported by the very homogenous sizes of Triton X-100-exposed *Bc*EVs measured by NTA (Fig. 27b). Taken together, the data suggest an intravesicular localisation of the *Bc*siR20 effector and show an unexpected resistance of *Bc*EVs to different treatments.

_Bc_EVs and _Bc_sRNAs are released during plant infection and co-purify on density gradient fractionation

As previous isolations of *Bc*EVs relied on axenic cultures and did not reflect *in planta* infection conditions, we isolated *Bc*EVs from *B. cinerea* infected *A. thaliana* plants. For this, we performed a DUC protocol on apoplastic plant wash fluid (Rutter & Innes, 2017) extracted from *B. cinerea*-infected and mock-treated plants (infected with the B05.10-*gfp* strain).

NTA measurement of EVs isolated from *B. cinerea*-infected *A. thaliana* showed a size profile with only one peak, suggesting that *At*EVs and *Bc*EVs are not differentiable by size (Fig. 28a). TEM pictures of these mixed crude EV samples depicted very heterogeneous size particle populations (Fig. 28b), most probably showing particles secreted by both *B. cinerea* and *A. thaliana*. However, numerous filamentous structures were present in all samples, most probably being bacterial flagella as this experiment is not done in sterile conditions. Thus we cannot rule out the possibility that some observed particles are EVs released from bacteria. To confirm the presence of *Bc*sRNA effectors, stem-loop RT-PCR on RNA extracted from crude EV samples was performed. EVs from *B. cinerea*-infected condition contained *Bc*siR3.1 and 20 (Fig. 28c), while the mock-treated condition did not.

To enhance EV purity, we added a step of density gradient fractionation after apoplastic wash fluid extraction and DUC. Crude EVs were loaded and ran through an Optiprep™ (non-ionic iodixanol-based medium) gradient and 11 fractions were collected. RNA was extracted on all fractions and stem-loop RT-PCR performed. *Bc*siR20 was detected in fraction 5 which has a density of 1.15 $g.ml^{-1}$, similar to mammalian exosomes (Théry et al., 2002) (Fig. 28d). Results from previous experiments also showed a signal for *Bc*siR20 in fraction 6 (data not shown). We then assessed particle sizes in the different fractions by NTA measurements.

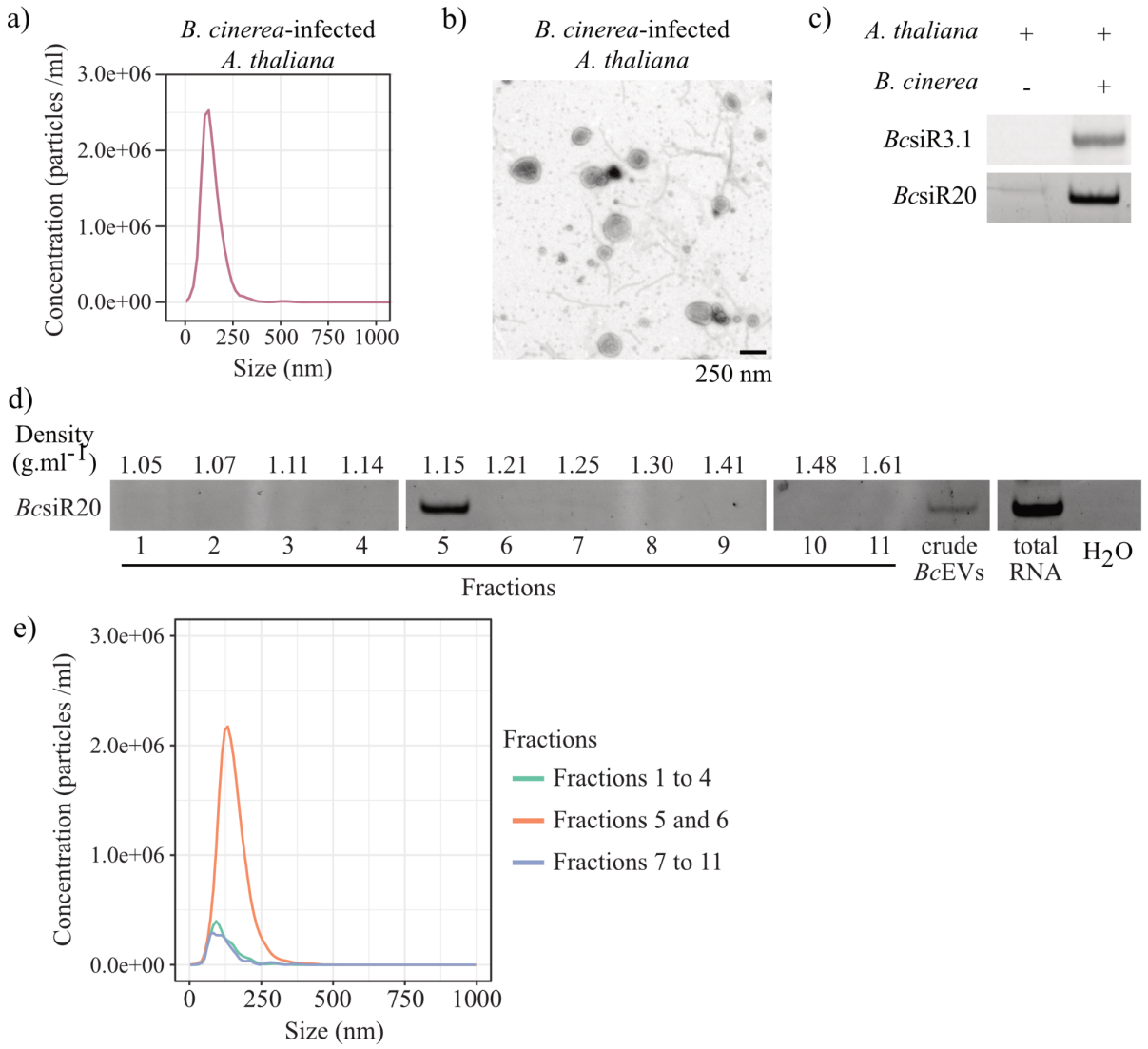

Figure 28: *Bc*sRNAs and *Bc*EVs are co-secreted during plant infection.

A. thaliana plants were infected with *B. cinerea* and after 4 days, apoplastic wash fluid was harvested, and subsequently EVs were isolated by DUC. **a)** Size profile of EVs isolated from *B. cinerea*-infected *A. thaliana* plants, measured by NTA. **b)** TEM picture of crude EVs, isolated from *B. cinerea*-infected *A. thaliana* plants, showed spherical nanoparticles of heterogeneous sizes and filamentous structures due to contaminant co-precipitation by DUC. **c)** Stem-loop RT-PCR detected *Bc*siR3.1 and *Bc*siR20 only in EVs samples isolated from *B. cinerea*-infected *A. thaliana* plants but not mock-treated *A. thaliana* plants. **d)** Stem-loop RT-PCR showed that *Bc*siR20 fractionated at 1.15 $g.ml^{-1}$ (fraction 5) after EVs isolated from *B. cinerea*-infected plants were run on density gradient. In some previous experiments *Bc*siR20 fractionated with fraction 6 (data not shown). **e)** NTA measurement of fractions 1 to 4, 5 to 6 and 7 to 8, pooled in three samples, showed the presence of nanoparticles only in fractions 5 and 6, which corresponded to the fractions containing *Bc*siR20. For **b** and **e)** the data were smoothed following the loess regression method.

Based on the PCR results, fractions 1 to 4, fractions 5 and 6 and fractions 7 to 11 were pooled in three samples. Fractions 5 and 6 showed the presence of particles/EVs while the

other fractions appeared devoid of any (Fig. 28e). Thus, *Bc*EVs and *Bc*sRNAs co-fractionated at the same density. Altogether, these results imply that *Bc*EVs and *Bc*sRNAs are secreted together during infection and support the previous observations suggesting that *Bc*EVs contain *Bc*sRNAs.

*Bc*EV treatments on *A. thaliana* plants did not induce a growth defect or an ROS burst inhibition

After isolating *Bc*EVs from both *B. cinerea* liquid cultures and *B. cinerea*-infected plants, we aimed to gain insights into *Bc*EV biological functions. For this we applied *Bc*EVs to plants and observed if it would induce a plant immune response or modulate the plant immune reaction. As *B. cinerea* can infect the model plant *A. thaliana,* we used it for the following experiments.

As a first analysis of *Bc*EV function *in planta*, we incubated *A. thaliana* 4-day-old seedlings, growing in liquid conditions, with crude *Bc*EVs isolated from three *B. cinerea* (B05.10 strain) axenic cultures constituting three biological replicates. For the treatments, we used the full amounts of isolated *Bc*EVs. The final concentrations were ranging from 2,75E+06 to 2,25E+08 particles/ml and their size profiles measured by NTA were all similar (Fig. 29a). Flagellin 22 (Flg22) and elongation factor 18 (Elf18) are PAMPs which trigger PTI response, and were used as positive controls, while the *Bc*EV resuspension buffer (MES) was used as negative control. 8 days post-treatments, the seedling weights were measured, reflecting their growth under *Bc*EV exposure. *Bc*EV-treated seedlings showed similar weights than mock-treated seedlings, while Flg22 and Efl18 treatments induced drastic growth inhibition (Fig. 29a).

Reactive oxygen species (ROS) emission is a hallmark of the early plant immune response (Bigeard et al., 2015). Therefore, we treated *A. thaliana* leaves with *Bc*EVs 2 or 12 hours before we triggered PTI with Flg22 and observed the effect on the ROS burst, thus allowing the visualisation of an immuno-modulatory effect. Indeed, as *Bc*sRNAs decrease the plant immune response by achieving ckRNAi, *Bc*EVs could have an immunosuppressive effect and might impact ROS production. At this time no NTA was available in the laboratory, thus *Bc*EVs isolated from the usual volume of *B. cinerea* axenic culture (B05.10-*gfp* strain) were diluted at 1:10 as a final concentration, which should result in a range of E+04 to E+05 particles per ml. For both time points (2 and 12 hours), no alteration

or modulation in the emissions of ROS from Flg22-*Bc*EVs-elicited leaf discs was observed compared to Flg22-elicited leaf discs (Fig. 29b). However, these results have to be taken with caution as *Bc*EVs were not controlled by NTA measurements and no biological replicates were performed.

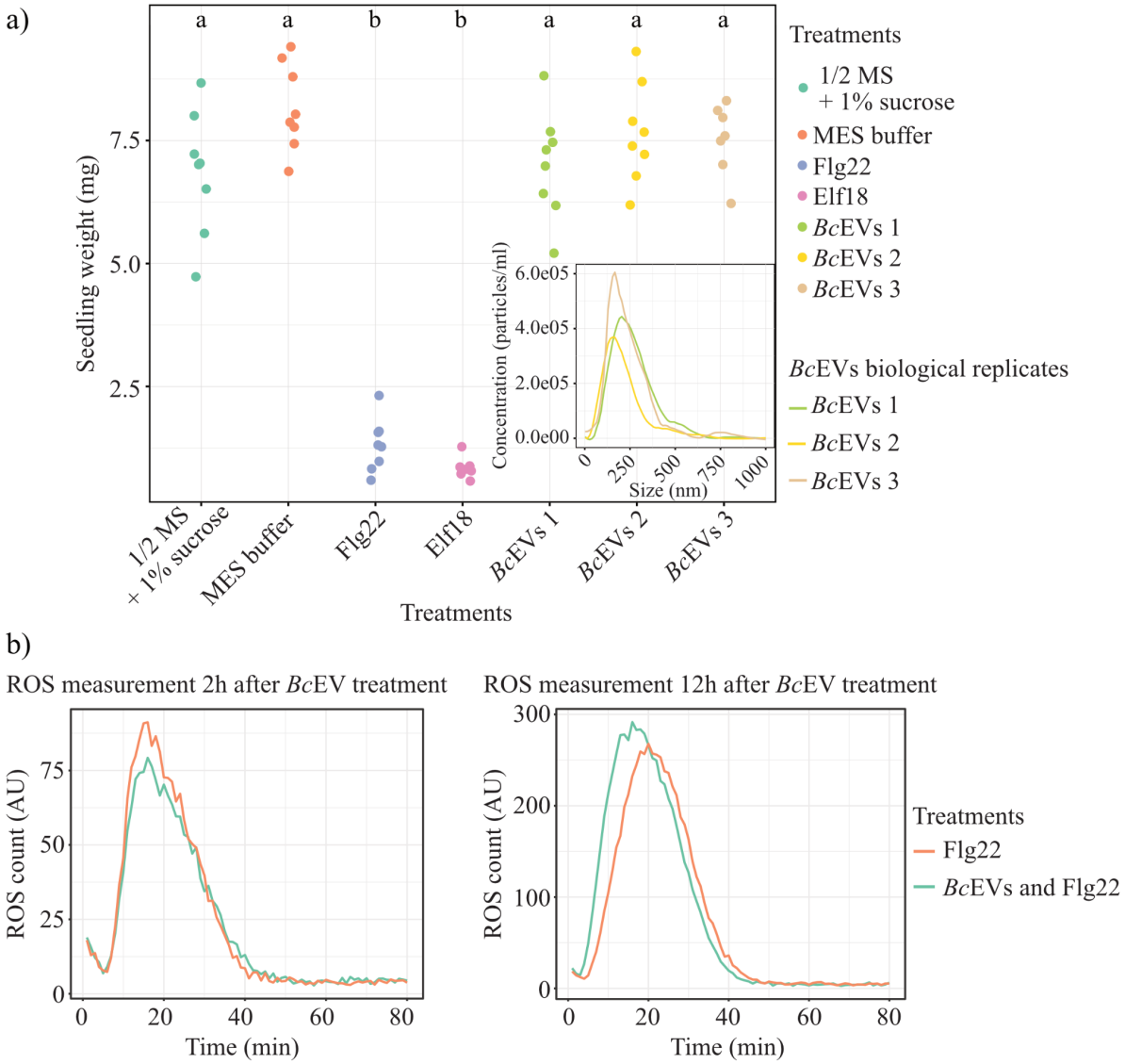

Figure 29: *Bc*EVs applied on *A. thaliana* plants do not induce a ROS burst modulation or a growth defect.

a) 4-day-old seedlings of *A. thaliana* were treated either with ½ MS + 1 % sucrose alone, or supplemented with MES buffer (negative controls), with Flg22 or Elf18 (positive controls), and with the three crude *Bc*EV samples. After 8 days, their weight was measured. *Bc*EV treatment did not induce a growth defect. The three crude *Bc*EV samples used for the growth assay showed similar size profiles, measured by NTA. The size (nm) is shown in x and the concentration (particles/ml) in y. A significant difference as indicated by letters was tested by one-way ANOVA using Tukey HSD test with $p < 0.05$. **b)** *A. thaliana* leaf discs were pre-treated with *Bc*EVs or MES buffer. 2 hours and 12 hours after, Flg22 was added and the ROS burst measured. Pre-treatments with *Bc*EVs or MES buffer

showed the same ROS response, without *Bc*EVs triggering any modulation of the response. These preliminary experiments were performed only once without biological replicates.

For both assays, *B*cEVs did not show any immunogenic or immuno-modulatory effects on plants, with the performed experimental set-ups. Whether this was truly due to *B*cEVs not having an effect on growth and ROS production is still uncertain to us, as these results are preliminary and should therefore be taken with caution.

sRNAseq revealed the sRNA profile of *Bc*EVs

As we previously found by nuclease protection assays that LTR retrotransposon-derived *Bc*sRNAs seemed to be located inside *Bc*EVs, we carried out a sRNAseq analysis on *Bc*EVs (from the B05.10 reference strain) in order to quantify such *Bc*sRNAs and identify new cargoes. Following the same strategy as for the nuclease protection assays (Fig. 26 a to d), crude *Bc*EVs were divided in two aliquots (Fig. 30). One remained crude (*i.e.* non-treated), representing the extracellular *Bc*sRNA content (sRNAs located inside the vesicles plus outside); while the second one was treated with MNase to degrade all extravesicular RNA contaminants co-purified by DUC but not the ones contained inside the *Bc*EVs, thus representing the intravesicular *Bc*sRNA content. Together with sRNAs extracted from mycelium, constituting the cellular sRNA fraction, three sRNA libraries were cloned and sequenced, in two biological replicates. Interestingly, the sRNAs from mycelium samples *v.s.* the sRNAs from *Bc*EVs samples showed different size profiles. While the cellular fraction showed peaks at 21-to-22 nt, 28-to-29 nt and 22 nt-long sRNAs, both vesicular sRNA samples (crude *Bc*EVs and MNase - *Bc*EVs) showed a major peak at 33 nt-long sRNAs, for both biological replicates (Fig. 31a). This reinforces the idea of having a particular set of sRNA selectively loaded in *Bc*EVs, as it was suggested by the absence of *BcActin* mRNA by PCR assay (Fig. 25).

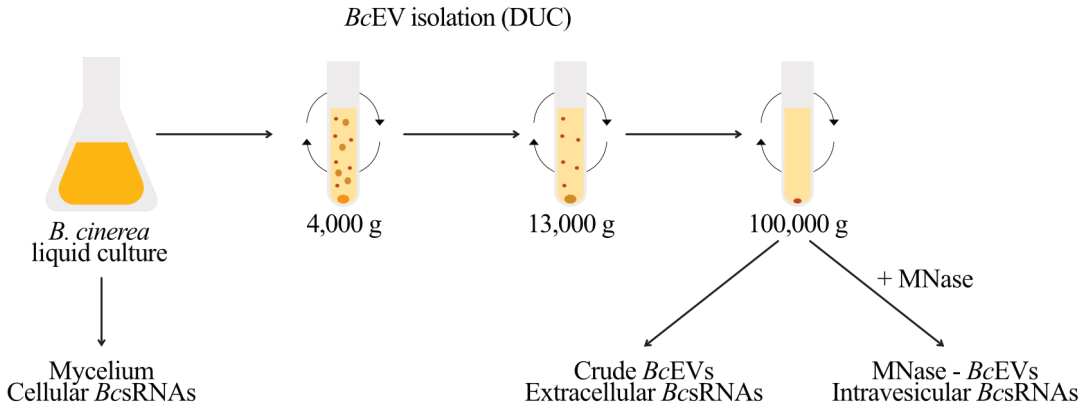

Figure 30: Schematic representation of the experimental design of the sRNAseq.
sRNAs from *B. cinerea* mycelium, crude *Bc*EVs and MNase-treated *Bc*EVs were sequenced.

After mapping the reads to the reference genome of B05.10, and filtering out the rRNAs, we quantified the relative amount of different sRNA species in all samples: sn/snoRNAs, transfer RNA-derived sRNAs or transfer RNA fragments (tRFs), mRNA-derived sRNAs and LTR retransposon-derived sRNAs. sn/snoRNAs, which are a class of sRNA functioning in the nucleolus, were present in lower % in *Bc*EVs treated or not, compared to mycelium (Fig. 31b), showing that *Bc*EV samples mainly contained extracellular RNAs. While LTR retrotransposon-derived *Bc*sRNAs were representing between 5.9 to 19.7 % of the total sRNA count in mycelium, they represented only 0.03 and 0.05 % in the MNase *Bc*EVs treated samples and 1.5 to 9.2 % in the crude *Bc*EV sample (Fig. 31b). Similar results were observed from published data from EVs isolated from *B. cinerea*-infected *A. thaliana* plants (data not shown) (Cai et al., 2018). Our sRNAseq analysis showed a depletion of LTR retrotransposon-derived *Bc*sRNA effectors in *Bc*EVs, contrary to what we were expecting, suggesting these sRNAs might use another means of transport towards the host plant cells. However, we cannot exclude that, for technical reasons, *Bc*sRNA effectors were not properly detectable with this experimental set-up.

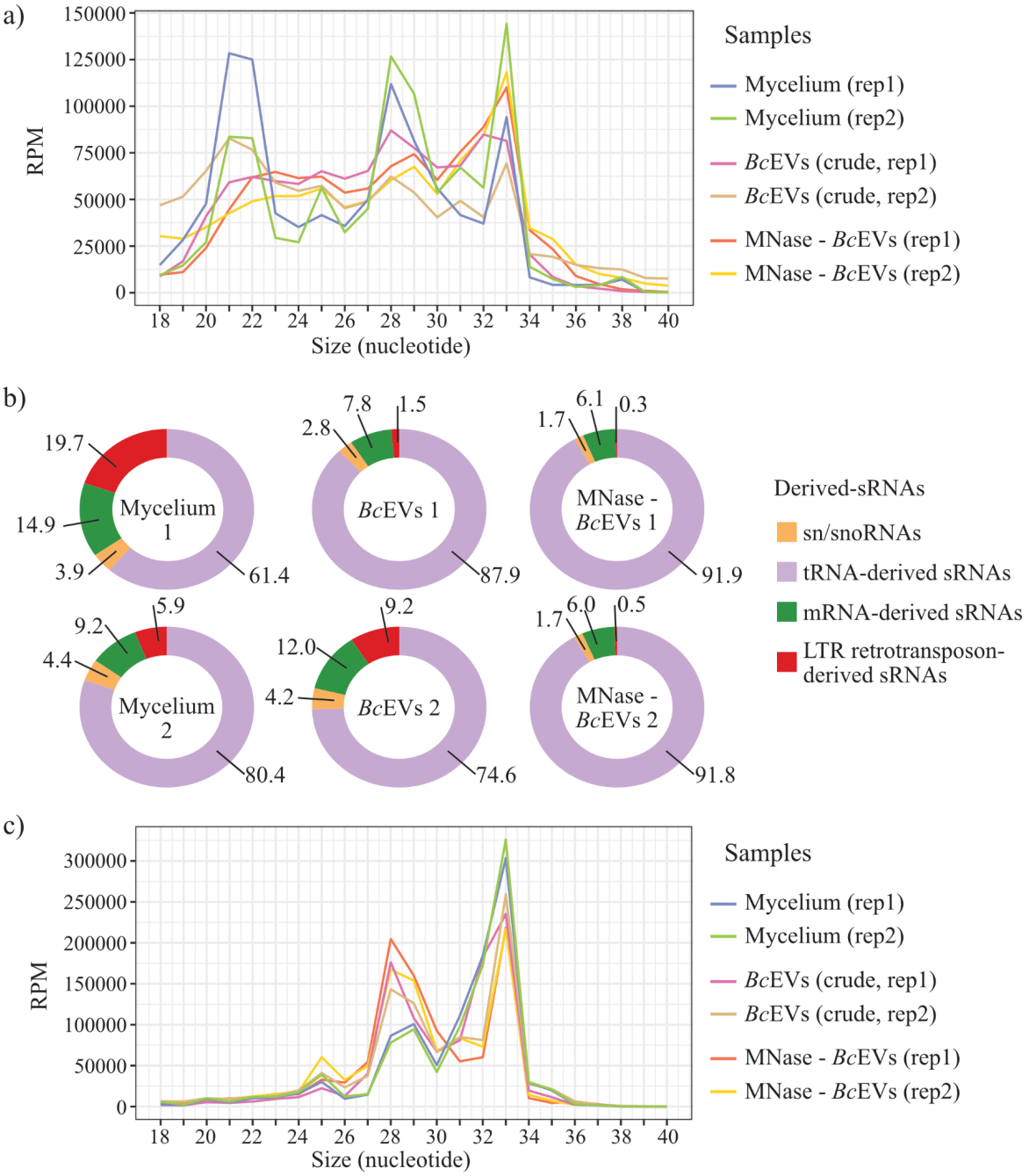

Figure 31: sRNA sequencing shows the depletion of LTR retrotransposon-derived *Bc*sRNAs and the enrichment of tRNA-derived sRNAs in *Bc*EV samples compared to mycelium.
sRNAseq was performed in two biological replicates. **a)** Total *Bc*sRNA size profiles of all samples showed different enrichments for sRNA from mycelium compared to sRNA from *Bc*EVs. **b)** Relative composition of derived-sRNAs in mycelium, crude *Bc*EVs of crude *Bc*EVs treated with MNase.. Numbers give the relative percentages. **c)** Size profiles showed an enrichment of 28-to-29 nt-long tRFs in *Bc*EVs compared to mycelium, while 33 nt-long ones were enriched in mycelium compared to *Bc*EVs.

Remarkably, we noticed an enrichment of tRFs in *Bc*EVs compared to mycelium. They represented up to 80.4 % of the cellular sRNAs but reached up to 91.9 % of the

intravesicular sRNAs (Fig. 31c). The biological replicates for mycelium and crude *Bc*EVs showed differences, but importantly the MNase-treated *Bc*EVs biological replicates were similar which comforted us in these observations.

The size profile of tRFs revealed two peaks, with either a size of 28-to-29 nt-long RNAs or 33 nt-long RNAs. Interestingly, the 28-to-29 nt tRFs were enriched in *Bc*EVs compared to mycelium, while 33 nt tRFs were depleted in *Bc*EVs compared to mycelium. This specific distribution of tRFs, and in general the different distribution of sRNAs between mycelium and *Bc*EVs, argue for a selective loading of sRNAs into *Bc*EVs.

Altogether, with this work we could show for the first time that *B. cinerea* produces and releases EVs into the extracellular space, although in rather poor amounts. We investigated the possibility of *Bc*EVs being the means of transport of *Bc*sRNA effectors, however, our sRNAseq results did not confirm this hypothesis. This could be supported by the observations of crude *Bc*EV-treatment not triggering a growth defect or a ROS burst in *A. thaliana* plants. On the other hand, we could show that *Bc*EVs and *Bc*sRNAs co-purify together *in vitro* and *in planta*. Moreover, the *Bc*sRNAs present in *Bc*EVs were protected from degradation. This pilot study opened many questions and laid the groundwork for much more experimental work on *Bc*EVs.

Discussion

Botrytis cinerea, the agent of the grey mould disease, possesses many molecular weapons for attacking host plants. *B. cinerea* is a necrotrophic pathogen feeding on dead tissues, therefore releasing numerous effectors and apoptosis-inducing compounds. However, before inducing the host plant apoptosis, *B. cinerea* requires the host cells to briefly stay alive in order to successfully establish the very early infection (Veloso & van Kan, 2018). For this, *B. cinerea* strategy is cross-kingdom RNA interference (ckRNAi). It consists in sending small RNAs (*Bc*sRNAs) into the plant host cells, where they hijack the host RNAi pathway by binding to the plant AGO1 proteins to form RISC complexes. Thanks to sequence complementarity, RISC complexes target and silence host mRNAs related to plant immunity (Weiberg et al., 2013). By decreasing the plant immune response, with a Trojan Horse-like strategy, *B. cinerea* ensures a strong beginning of infection.

Previous studies collected *B. cinerea* isolates from infected plants in the wild, and several types of genotypes were identified: *transposa* (carrying both Gypsy and Copia elements), *vacuma* (not carrying any elements), and carrying only Gypsy or Copia elements (Martinez et al., 2003, 2005; Samuel et al., 2012). Based on their observations they proposed that, depending on their LTR retrotransposon landscapes, *B. cinerea* wt strains showed different levels of aggressiveness and different preferences for plant hosts. Moreover, a large proportion of *Bc*sRNAs that hijack the plant host RNAi machinery in order to achieve ckRNAi derive from LTR retrotransposons (Weiberg et al., 2013). Altogether, these findings suggest that LTR retrotransposons have an important role to play in *B. cinerea* aggressiveness.

LTR retrotransposons as pathogenicity factors for *B. cinerea*

Summary of the main results

In this study we identified LTR retrotransposons as true pathogenicity factors. Indeed, by combining pathogen assays and sRNAseq analysis, we showed that *B. cinerea* wt strains carrying LTR retrotransposons produced *Bc*sRNA effectors and had strong aggressiveness

towards *S. lycopersicum* plants, while *B. cinerea* wt strains not carrying LTR retrotransposons did not produce *Bc*sRNA effectors and caused lighter infection symptoms. When doing full genome sequencing, it appeared that for these last strains, LTR retrotransposons were actually present but heavily mutated by RIP, a fungal genome defence mechanism, thus rendering the expression of *Bc*sRNA effectors impossible (Gladyshev, 2017). Indeed, RIP leads to mutation on the full elements (*i.e.* also the promoters) which are hence not transcribed anymore. However, the reasons why some wt strains escaped from RIP and preserved intact retrotransposons remain unknown.

As a proof of concept, we cloned a GC-rich LTR retrotransposon *Bc*Gypsy3 from the most aggressive strain (B05.10) to transform a less aggressive one (D08_H24), which did not carry any full-length, intact, GC-rich *Bc*Gypsy3 copy. This led to enhanced aggressiveness in a *Bc*Gypsy3 mRNA and *Bc*Gypsy3-derived *Bc*sRNA expression-dependent manner. Two strategies for transgene insertion were used, either targeted at the *Bc*niaD locus or randomly inserted. *Bc*Gypsy3 expression was dependent on the genomic insertion site, and while *Bc*Gypsy3 mRNA levels in some transformants were similar to the one of the B05.10 donor strain, the production of *Bc*sRNAs was not fully restored. However, we observed a positive correlation between *Bc*Gypsy3 mRNA and *Bc*sRNA levels. We performed an RNAseq analysis on D08_H24 or on *Bc*Gypsy3 transformant-infected *A. thaliana* tissues, and identified differentially up- or downregulated genes in the host plant transcriptome. In response to *Bc*Gypsy3-derived *Bc*sRNAs, a few immunity repressors were upregulated while some immunity activators were repressed, showing how *B. cinerea* can manipulate the host immunity genes. As these expression changes were observable in the presence of one LTR retrotransposon, we expect more plant genes to be regulated through *Bs*RNAs deriving from *B. cinerea'*s diverse set of transposons.

Reaching *Bc*Gypsy3-derived *Bc*sRNA production level similar to B05.10 in D08_H24 *Bc*Gypsy3 transformants

While we observed a positive correlation between *Bc*Gypsy3 mRNA levels in the transformants and lesion size (*i.e.* aggressiveness), and while some transformants showed *Bc*Gypsy3 mRNA levels similar to the one in B05.10, the amounts of *Bc*Gypsy3-derived *Bc*sRNAs did not reach the one in B05.10. Several hypotheses could explain this observation, however, it is important to keep in mind that our transformants carried only one copy of

active GC-rich *Bc*Gypsy3, while the wt isolate B05.10 carries at least two such copies, therefore having a higher production of *Bc*sRNAs.

First, we cloned and transformed different constructs containing the *Bc*Gypsy3 element, which were not fully corresponding to the wt element in B05.10. We cloned *Bc*Gypsy3 without the LTRs (to avoid transposition), in two different constructs which express either ss*Bc*Gypsy3 or ds*Bc*Gypsy3 under the control of a constitutive promoter. We also cloned *Bc*Gypsy3 with the 5' LTR but without the 3' one, which resulted in the expression of *Bc*Gypsy3 sense mRNA only, and under the control of the native promoter present in the 5' LTR. Such incomplete *Bc*Gypsy3 elements (*i.e.* without LTRs or only expressing sense mRNA) could be impaired in their expression regulation, as LTRs were shown to contain regulatory sequences in mammals and act as promoters or enhancers, even sometimes in a tissue-specific manner (Thompson et al., 2016). However, for this last construct containing the 5' LTR, the production of *Bc*Gypsy3-derived *Bc*sRNAs was not evaluated by sRNAseq, in opposition to the sRNAseq performed on the other *Bc*Gypsy3 transformants. Thus it seems important to perform such an analysis and compare it to the *Bc*sRNA levels in the other transformants to conclude on the role of LTRs in sRNA expression. Moreover, continuing with the same approach and inserting the full *Bc*Gypsy3 with both LTRs (meaning also dsGypsy3 expression) in the same less aggressive wt strain (D08_H24), and evaluating the *Bc*Gypsy3 mRNA expression and the derived *Bc*sRNA production, would complete our understanding on the regulation of *Bc*Gypsy3-derived *Bc*sRNA expression. Nonetheless, a full and intact *Bc*Gypsy (*i.e.* with both LTRs and intact coding sequences) could transpose and copy itself elsewhere in the genome. While we are currently unsure if *Bc*Gypsy3 is able to do so (*i.e.* being an autonomous retrotransposon), caution should be taken to avoid *Bc*Gypsy3 unwanted genome invasion.

Second, the *Bc*niaD-targeted transformants we used for the experiments were the first generation after transformations (insertion in this locus allows direct selection of transformants) and there is a possibility that *Bc*sRNA expression could have been higher if the transformants would have undergone several generations. Indeed, previous studies showed that the insertion of a LTR retrotransposon in a *Magnaporthe oryzae* strain which was devoid of it was followed by high expression of the derived mRNA in the early generations but a decrease in later ones, while the derived sRNAs had opposite behaviour with higher accumulation with more generations (Murata et al., 2007). Similar observations

were made in *A. thaliana* plants transformed with a LTR retrotransposon, where the derived sRNA accumulation increased from the eight generation (Marí-Ordóñez et al., 2013). However, the mechanisms underlying this phenomenon remain unclear.

Finally, we observed that *Bc*niaD-targeted insertion transformants and both random insertion transformants (loci unknown) showed different mRNA expression; thus making *Bc*Gypsy3 mRNA expression levels dependent on the insertion loci, probably because of the chromatin state being more or less transcriptionally permissive. While the randBcGypsy3 #1 transformant showed high *Bc*Gypsy3 mRNA expression, the randBcGypsy3 #2 showed the opposite; identifying both insertion loci and its chromatin state would be informative and might explain the *Bc*Gypsy3 mRNA levels. Moreover, the chromatin state of the *Bc*niaD locus might also not represent the endogenous *Bc*Gypsy3 loci in B05.10. Therefore, performing the *Bc*Gypsy3 transgene insertion in the native locus might be of interest in order to be as close as possible to the B05.10 wt isolate.

Possible positive selection for preserving LTR retrotransposons from RIP

Transposable elements (TEs) are repeated sequences present in all eukaryotic genomes which can, as their name implies, transpose in the host genomes. LTR retrotransposons are a type of TEs, which can transpose in the genome thanks to an RNA intermediate, the mRNA transcribed from the element which codes for all necessary proteins. Even though they are now recognised as drivers for evolution, transposition is chaotic and often leads to highly deleterious effects for the genome as they would, for example, induce many mutations in the DNA sequence. Therefore, host genomes use different strategies for TE control. RNAi-mediated silencing of TEs is a widespread mechanism, and in fungi is called quelling. LTR retrotransposon-derived *Bc*sRNAs are produced from the mRNA transcribed from the coding central region (*i.e.* not comprising the LTRs). Therefore, *Bc*sRNAs' first biological function is very likely to mediate silencing of the elements from which they are expressed (*i.e.* quelling) (Veloso & van Kan, 2018; Weiberg et al., 2013). On the other hand, repeat-induced point mutation (RIP) is a fungal strategy for permanent TE control, which targets and mutates duplicated sequences within the genome (*e.g.* two identical copies of one TE). While it is a powerful mechanism, it solely occurs during sexual reproduction, thus limiting its impact.

In *B. cinerea*, many LTR retrotransposons are RIPed which renders them inactive and silenced. However, some LTR retrotransposon copies, such as the one from which our *Bc*sRNAs of interest are expressed, seem to have escaped RIP, and the derived *Bc*sRNAs are beneficial for *B. cinerea* infection as they mediate cross-kingdom RNA interference. The reasons why some LTR retrotransposons have escaped RIP silencing, while the majority has been silenced, remain unclear.

As elements such as *Bc*Gypsy3 are beneficial for plant infection, even while being a threat to the fungus's fitness, it is possible that a positive selection force is preserving these elements intact. The observation that both types of strains (*transposa,* meaning carrying intact GC-rich LTR retrotransposons, or *vacuma,* meaning carrying only silenced LTR retrotransposons) are present in the wild suggests that both situations have benefits. In line with this idea, the observations made in previous studies where *vacuma* strains have a faster mycelial growth while *transposa* strains cause stronger infection symptoms, or the fact that different LTR retrotransposon landscapes can be linked to host prevalence (Martinez et al., 2003, 2005; Samuel et al., 2012). In these situations, carrying non-silenced LTR retrotransposons and carrying silenced LTR retrotransposons are both of interest for *B. cinerea* and represent two different "life styles". In addition, in the aggressive wt isolate B05.10, the *Bc*Gypsy3 superfamily comprises ten copies. Among these copies, we found that eight are mutated by RIP, therefore inactive (*i.e.* cannot transpose) and silenced (*i.e.* do not produce *Bc*sRNAs), and two copies are active, meaning they are intact and produce *Bc*sRNA effectors. This observation could argue in the direction of a positive selection for these two copies.

Datation of the GC-rich BcGypsy3 copies in B05.10

To explore the possibility of positive selection of GC-rich *Bc*Gypsy3 copies, it would be relevant to understand the age of these elements. Comparative genomic methods, and more precisely synteny analysis, allows the comparison of conserved blocks, such as chromosomes, and the identification of divergent sequences within the blocks. Comparing the loci of the two GC-rich *Bc*Gypsy3 copies in B05.10 with the same loci in D08_H24 and D14_TF (as we have their genome sequenced) would identify if these last wt isolates carry RIPed *Bc*Gypsy3 or not. If D08_H24 and/or D14_TF do not have any *Bc*Gypsy3 relics at these loci, then the GC-rich *Bc*Gypsy3 copies in B05.10 are recent coming from insertion

events and it could explain why they are not RIPed yet. On the other hand, if D08_H24 and/or D14_TF possess RIPed *Bc*Gypsy3 elements at these loci, it would argue for a protection against RIP in the B05.10 copies, in other words a positive selection pressure to keep them intact. However, it is important to note that the absence of elements at specific loci could also be due to LTR retrotransposon removal, due to homologous unequal recombination or illegitimate recombination, as it was observed in some plant species (Jedlicka et al., 2020). Yet, to perform such a comparative genomic method, it would be necessary to have sequenced the genomes of all the six wt isolates we used in our study, at least. As we are interested in repetitive elements which usually cause problems for genome assembly, genomes should be sequenced with a long read sequencing technology.

Estimating the age of all copies, in *B. cinerea* strains, would be informative on the possible events which allowed - or not - the conservation of intact elements. Investigating different LTR retrotransposon superfamilies in a large set of *B. cinerea* isolates, by synteny analysis or sequence similarity analysis (Jedlicka et al., 2020; Lorrain et al., 2021), might provide exciting results about the conservation of GC-rich *Bc*Gypsy3 copies in B05.10. However, it would also be possible that these copies are too "young" to be RIPed if no sexual reproduction has occured after their transposition/insertion events.

Impact of B. cinerea sexual reproduction on TEs, and more specially on the GC content of BcGypsy3 elements

It is difficult to estimate the occurence of asexual versus sexual reproduction of *B. cinerea* in the wild just by observing host plants in fields, because of the small sizes of *B. cinerea'*s organs (Giraud et al., 1997). However, sexual reproduction can be achieved in laboratories. Either of these reproduction strategies induce particular genetic structures which can be identified. Indeed, it is expected that a population undergoing sexual reproduction would be clonal while a population undergoing sexual reproduction would be genetically more diverse. To study population genetics, one common method is restriction fragment length polymorphism (RFLP). It consists in detecting differences between homologous DNA sequences, coming from different individuals, by detecting the presence of fragments of different lengths after digestion of these regions with specific restriction endonucleases.

RIP solely occurs during sexual reproduction. Therefore, there is also a possibility that the two GC-rich *Bc*Gypsy3 copies of B05.10 are still intact because no sexual

reproduction cycle has occured recently, in opposition to the hypothesis of a positive selection. To explore this possibility, we could evaluate the sexual reproduction occurrence in the wild by analysing several wt field isolates of the same aggressive species (B05.10, D13_TF or N11_KW), by RFLP. This analysis would require numerous isolates collected from very close geographical localisations. Previous studies have reported different reproduction behaviours in different populations. Indeed, in Champagne (France), field isolates of *B. cinerea* were found to regularly reproduce sexually, while field isolates in California seem to be mainly reproducing asexually (Fournier & Giraud, 2008). Moreover, the isolates from Champagne showed a prevalence for *transposa* strains (containing non-RIPed Gypsy and Copia copies) (Fournier & Giraud, 2008; Giraud et al., 1997). Similarly, *B. cinerea* wt isolates from Hungary reproduce sexually and *transposa* strains represent a strong majority (Váczy et al., 2008). Although these different isolates reproduce sexually, meaning that RIP can occur, they carry GC-rich TEs (*transposa* strains) which suggests a protection against RIP mechanism or a preference from RIP for some elements; but in both cases a positive selection for GC-rich copies.

Another interesting approach would be to induce *B. cinerea* B05.10 sexual reproduction in the laboratory, and analyse the GC content of the two *Bc*Gypsy3 copies expressing the *Bc*sRNAs after one, two, three or more cycles of sexual reproduction. If the GC content of the *Bc*Gypsy3 copies does not drop, RIP does not occur, and it would argue for a positive selection of GC-rich *Bc*Gypsy3 copies.

Since the discovery of domestication, the dogma about TEs has started to change and the theory of selfish DNA (theory by which TEs are parasitic DNA only causing neutral or deleterious effects which are always eliminated by selection) is now rethought. While positive selection of TEs was suggested a few times. For example, in a human population genomic study, accumulated evidence is pointing to a positive selection thanks to the observation of frequent locus-specific insertion of one TE (Rishishwar et al., 2018). However, this remains largely unknown and misunderstood.

In a study analysing 26 *Zymoseptoria* genomes (22 *Z. tritici* isolates and 4 *Zymoseptoria* closely related species), researchers found that RIP shows variation of efficiency depending of the TE type and among *Zymoseptoria* species, with 74 to 99 % of

TEs being RIPed in the different strains (Lorrain et al., 2021). The mechanism by which these TEs maintain their population stable in the genome despite RIP remains unclear. Importantly, RIP is a costly defence mechanism for the host genome and RIP can be lost (Galagan & Selker, 2004; Lorrain et al., 2021). Indeed, studies in *N. crassa* have shown that RIP has impacted the genome on gene duplication level (as RIP targets duplicated sequences) and that most if not all duplicated genes in *N. crassa* have appeared and diverged before RIP. As gene duplication is believed to be a major driver of evolution for new gene functions, RIP seems to be a costly protection mechanism.

However, by performing sequence similarity analysis, it was shown that the *Zymoseptoria* isolates carry both "old" and "recent" TEs copies, with some recent copies being RIPed, hence showing that RIP still takes place. *Z. tritici* is a fungal plant pathogen, which genome follows the two-speed model (*i.e.* TEs are associated with Avr genes). Moreover, during infection some TEs are de-repressed (Fouché et al., 2020). This suggests that, similarly to *B. cinerea transposa* strain, there is a benefit to keeping some active TEs for pathogenicity, and that maybe in *Zymoseptoria* this occurs via a positive selection.

One little step further than LTR retrotransposons

Previous studies have identified the 83 full-length copies of LTR retrotransposons present in the reference strain B05.10 and classed them in 9 consensus classes (Porquier et al., 2016). Strikingly, 7 classes out of 9 are elements having an additional ORF, coded in antisense to the transposon mRNA, and present upstream of the 3' LTR. The products of these additional ORFs are unknown. In *B. cinerea* strain T4, f *Bc*Gypsy1 encodes for an additional ORF called *brtn*, which is likely to be expressed, however its function is presently unknown (Zhao et al., 2011). The *Bc*Gypsy3 element we cloned and inserted into the less aggressive strain D08_H24 carries an additional ORF in antisense (Bcin14g04350). Thus, while the enhanced aggressiveness under *Bc*Gypsy3 transgenic insertion certainly depends on the production of derived *Bc*sRNAs, as they achieve ckRNAi, we cannot exclude this to be also partially due to a contribution from the additional ORF product. Indeed, we constructed several types of *Bc*Gypsy3 transgenes, either single strand *Bc*Gypsy3 (ss*Bc*Gypsy3) meaning they carry a constitutive promoter in 5' and only the sense mRNA is produced, or double-strand *Bc*Gypsy3 (ds*Bc*Gypsy3) with two constitutive promoters in sense and in antisense resulting in the expression of both sense and antisense mRNAs. *B. cinerea*

transformants' aggressiveness was stronger with ds*Bc*Gypsy3 constructs than with ss*Bc*Gypsy3, certainly because of the higher production of *Bc*Gypsy3-derived *Bc*sRNAs. However, in this condition the additional ORF is also transcribed and might also be translated, which could have an impact on the observed enhanced aggressiveness. Sequence analysis (*e.g.* Kosak sequence necessary for translation) and domain prediction on this additional ORF in *Bc*Gypsy3, and the others present in LTR retrotransposons, would inform us on whether these genes can be involved in virulence, for example if they would be putative effectors.

Further studies on the role of LTR retrotransposons during infection and for pathogenicity should definitely consider the additional ORFs, first by bioinformatically identifying their putative functions, second by using transgenic approaches and transforming less aggressive *B. cinerea* wt isolates with functional and GC-rich LTR retrotransposons with mutated additional ORFs, or the additional ORFs alone.

TEs in host-pathogen interaction

In nature, several cases link TEs and the pathogenicity of certain species, such as the two-speed fungal genome model, mentioned in the introduction, where TEs are driving high-speed evolution of Avr genes. The finding of *B. cinerea* LTR retrotransposons being pathogenicity factors brings a new role of such elements in pathogenic interactions. Moreover, a similar strategy is adopted by *M. oryzae*, the agent responsible for the rice blast disease, where LTR retrotransposon-derived sRNAs are upregulated under stress and during rice plant infection (Raman et al., 2013). Moreover, it is known that LTR retrotransposons are de-repressed during stress or wheat infection for the pathogen *Z. tritici*, indicating a possible positive role for infection for this fungus as well (Fouché et al., 2020). Remarkably, the parasitic nematode *H. bakeri* manipulates its host transcriptome by secreting retrotransposon-derived sRNAs in EVs (Buck et al., 2014; Chow et al., 2019). The authors of these studies argued that, possibly, selection might exploit the rapidly evolving retrotransposons to generate novel sRNAs having low risk for self-targeted effects but possible beneficial effects.

Characterisation of *B. cinerea* extracellular vesicles

While the origin of *Bc*sRNA effectors was identified, the transport of such elements to the host plant cells remains unclear. Since RNAs are easily prone to degradation and the plant apoplast contains RNases proven to be important for defence against pathogens (Galiana et al., 1997; Hugot et al., 2002), we aimed to identify how *Bc*sRNA transport could take place, in a manner conferring protection. Importantly, ckRNAi is bidirectional between *B. cinerea* and *A. thaliana*, and it was shown that *At*sRNAs were transported to the fungal cells into EVs (Cai et al., 2018). EVs are nanoparticles emitted from cells from all organisms in the tree of life, which shuttle diverse cargoes from cell to cell in an intra- or inter-organismal way (Colombo et al., 2014; Deatherage & Cookson, 2012; U. Stotz et al., 2022). Since a few years EVs are highlighted for their implication in cross-kingdom communication as several pathogenic species were shown to deliver diverse molecules to their host into EVs (Buck et al., 2014; Chow et al., 2019; Gehrmann et al., 2011; Rodrigues et al., 2007). In this study, we made the first steps into the characterisation of *Bc*EVs and looked into their sRNA content.

Summary of the main results

To study *Bc*EVs, we first optimised a DUC protocol, which allowed the isolation of crude *Bc*EV samples from *B. cinerea* axenic liquid cultures. By performing stem-loop RT-PCR, we found that *Bc*sRNAs and *Bc*EVs are co-purifying and nuclease protection assays indicated an intravesicular location of *Bc*sRNAs, but more surprisingly, suggested an unexpected resistance of *Bc*EVs and *Bc*sRNAs to different treatments. In an attempt to study a less artificial situation, we isolated EVs from *B. cinerea*-infected *A. thaliana* plants, resulting in a mixture of both *Bc*EVs and *At*EVs. Similarly to the results obtained from axenic cultures, *Bc*EVs and *Bc*sRNAs co-purified in crude *Bc*EV extract and on density gradient purification as well. To investigate the possible biological functions of *Bc*EVs, crude samples were applied to plant tissues and two types of immunity-related responses were measured. No plant reaction was observed following *Bc*EV treatment. However, the reasons for this result are still unclear. Finally, to confirm *Bc*sRNA intravesicular location and gain knowledge on *Bc*EV sRNA cargoes, we performed a sRNAseq on *Bc*EVs. Surprisingly, LTR retrotransposon-derived *Bc*sRNAs, the *Bc*sRNAs important for ckRNAi, were depleted in

*Bc*EVs compared to mycelium, contrary to our starting hypothesis. On the other hand, tRFs were enriched in *Bc*EVs compared to mycelium.

Exploring the sRNA content of *B. cinerea* extracellular vesicles

As stated above, we performed a sRNAseq on *Bc*EV samples. More exactly, we sequenced the sRNAs from *B. cinerea* mycelium, from crude *Bc*EVs and from *Bc*EVs treated with MNase prior to the sRNA library cloning, in order to degrade contaminant RNAs present outside of the vesicles. Thus the three types of samples represented: the total sRNA content, the extracellular sRNAs and the intravesicular sRNAs. These data revealed that LTR retrotransposon-derived *Bc*sRNAs were depleted inside *Bc*EVs compared to mycelium, while tRFs were enriched.

LTR retrotransposon-derived BcsRNAs seem to be depleted in BcEVs

Surprisingly, the LTR retrotransposon-derived *Bc*sRNA effectors we were interested in, were depleted in *Bc*EV samples compared to the mycelium. At least two hypotheses emerge from this observation, i) *Bc*sRNAs transport to the host plant cells does not occur via *Bc*EVs and ii) technical limitations of the experimental set-up did not allow the detection of *Bc*sRNAs inside *Bc*EVs.

***Bc*sRNAs main means of transport remains unknown**

In the case of the first hypothesis, *Bc*sRNAs would truly be depleted in *Bc*EVs and their main way of transport from *B. cinerea* to the host plant cells remains unknown. This would question the importance of *Bc*EVs for ckRNAi, and this could be supported by the low concentration yields after isolation, meaning maybe *B. cinerea* does not release considerable amounts of *Bc*EVs at all, independently of the conditions. The possibility of *Bc*sRNA secretion via RNA channels, although never identified, and the involvement of RNA binding proteins remain to be explored. To note, extracellular RNAs were found outside of EVs, in *A. thaliana* (Zand Karimi et al., 2021) or in human embryonic kidney cell lines (Sork et al., 2021), highlighting the role of soluble protein complexes. Additionally, in honey bee jelly, RNA was found in stable granules when bound to a secreted RNA binding protein (Maori et al., 2019). Moreover, RNA uptake in an EV-independent way is possible as well, such as in *C. elegans* with the Systemic RNAi defective (SID) 1/2 proteins (Sarkies & Miska, 2014),

and importantly *B. cinerea* and other pathogens were also shown to take up naked RNA (Qiao et al., 2021; M. Wang et al., 2016). Altogether, it shows that growing evidence is bringing light on EV-independent RNA secretion pathways, which should be considered for *B. cinerea* LTR retrotransposon-derived *Bc*sRNA effectors as well.

_Bc_sRNAs could not be detected in our _Bc_EV samples

In the case of the second hypothesis, it is possible that the experimental set-up used did not allow the detection of *Bc*sRNAs into *Bc*EVs, and several explanations could be the reason for it. First, if *Bc*sRNAs were modified before being secreted, this could have prevented a correct adapter ligation during the library cloning, thus rendering their sequencing difficult. Interestingly, secondary siRNAs selectively loaded into EVs from the gastrointestinal nematode *H. bakeri* are 5' poly-phosphorylated and thus require a 5' RNA phosphatase treatment before library cloning (Chow et al., 2019; White et al., 2020) and noticeably, *H. bakeri* sRNAs are derived from transposons. Moreover, RNA editing (*e.g.* A bases to I), if happening, would also be an obstacle as 0 mismatches were allowed for mapping the *Bc*sRNA reads onto the B05.10 reference genome. Considering the idea that RNA loading into EVs could be dependent on RNA modifications, and as such can impair sRNAseq, there is also a risk we missed *Bc*sRNAs in our sequencing. Thus, analysing the data set while allowing more mismatches seems like a first step towards solving this question.

Second, this analysis showed that all LTR retrotransposon-derived *Bc*sRNAs are depleted in *Bc*EVs, although it is known that not all LTR retrotransposon subfamilies are involved in ckRNAi with the same importance as they do not express derived *Bcs*RNAs in the same amount (Porquier et al., 2021). Indeed, the *Bc*sRNAs *Bc*siR3.1, *Bc*siR3.2 or *Bc*siR20 which were identified to hijack the host plant AGO1 protein, and have known plant mRNA targets, are all produced from the element *Bc*Gypsy3. Thus, it would be interesting to look at the enrichment of these specific *Bc*sRNAs or of only *Bc*Gypsy3 derived *Bc*sRNAs rather than all LTR retrotransposon-derived *Bc*sRNAs.

Third, it is important to remember how the DUC protocol used for EV isolation works. Indeed, before the last ultracentrifugation round (at 100,000 g-force) which pellets the particles we analysed during this study, there is a centrifugation step with a lower speed (at 14,000 g-force) and a filtration step (pore size approx. 200 nm) which exclude bigger particles such as microvesicles. Therefore, it could be that the LTR retrotransposon-derived

*Bc*sRNAs important for ckRNAi are transported in larger EVs than the ones we studied, such as MVs which are also known to transport RNA (Cocucci et al., 2009).

tRNA-derived sRNAs are enriched in BcEVs

The second remarkable indication we found from this sRNAseq analysis was the vesicular enrichment of short tRFs, compared to mycelium. In the past years, tRFs have emerged as a new class of sRNAs with regulatory functions, outside of their "classical" role for protein synthesis (Magee & Rigoutsos, 2020). Several types of secondary RNA products are derived from tRNAs, such as tRNA-derived sRNAs, tRNA fragments or others. For simplicity they are referred to as tRFs in this study. In humans, tRFs are involved in gene expression regulation, RNA stability, reverse transcription and more cellular processes; but also cancer or more broadly in pathophysiology (Pandey et al., 2021). Similar observations were made concerning tRFs functions in plants (Alves & Nogueira, 2021). More interestingly, tRFs were linked to cross-kingdom RNAi between bacteria and plants. Indeed, rhizobial tRFs were shown to be signal molecules regulating plant nodulation process during symbiotic interactions, moreover these bacterial tRFs seem to be binding plant AGO1 (Ren et al., 2019). While evidence is growing about the interaction between tRFs and AGO proteins, further validation is required. Remarkably, it was proposed that some *Cryptococcus* spp. might compensate for the lack of RNAi machinery with tRFs (Streit et al., 2021).

While we could not further explore the exciting perspective of tRFs being enriched in *Bc*EVs, this is not the first report of tRFs as part of EV cargoes from several species (Alves et al., 2019; Gámbaro et al., 2020; Peres da Silva et al., 2015). In humans, tRFS were found in EVs, and their function was linked to immunity via the activation of T cells (Chiou et al., 2018). The protozoan parasite *Trichomonas vaginalis* secretes EVs enriched with tRFs, which are internalised by the human host cells (Artuyants et al., 2020). While the role of tRFs once internalised in the recipient cells is still unclear, it is likely to alter the host immune response. Several pathogenic bacteria species were found to secrete OMVs enriched with tRFS with as a goal the modulation of the host immune response (Li & Stanton, 2021). tRFs have shed light onto a novel type of sRNAs with very possible cross-kingdom and immune modulatory functions. Hence, it is highly probable that *B. cinerea* tRFs present in *Bc*EVs have a function once internalised into the host plant cells. More precisely, 28-to-29 nt-long tRFs were enriched in the crude *Bc*EVs compared to mycelium, while 33 nt-long tRFs were depleted in

the same fraction. This might mean that the 33 nt-long ones have endogenous regulatory functions while the shorter ones would be specifically loaded into *Bc*EVs and destined to be important for cross-kingdom communication with the plant hosts. A first step into understanding the possible role of *B. cinerea* tRFs enriched in *Bc*EVs would be to bioinformatically predict putative plant mRNA targets, if these sRNAs were to have a ckRNAi function similar to what was observed in rhizobial bacteria (Ren et al., 2019). However, the tRFs we identified were longer than the typical 21-to-22 nt sRNAs bound by AGO proteins (Mi et al., 2008), suggesting a different mechanism than the canonical RNAi pathway.

*Bc*EV resistance to Triton X-100

*Bc*EV resistance to Triton X-100 was highly unexpected as previous EV studies used the same detergent to successfully blast EVs (Bielska et al., 2018; Cai et al., 2018; Zand Karimi et al., 2021). Triton X-100 is a nonionic surfactant (*i.e.* neutrally charged surface active agent), which lowers the surface tension between two phases (liquid/liquid, liquid/gas and liquid/solid). Thus, in biochemistry, Triton X-100 is used to solubilise and unfold proteins, dissociate aggregates or induce membrane permeabilisation by disorganising the lipid bilayer. Variable sensitivities to different detergents and different concentrations have been observed in different vesicle populations (Osteikoetxea et al., 2015). Moreover, detergent-resistant membranes and specifically Triton X-100-resistant membranes have been identified and this phenomenon is partially due to the lipid composition and the presence of lipid rafts (Mattei et al., 2015; Sot et al., 2002). Under certain conditions, only partial solubilisation occurs and major changes in the membrane architecture are observed, such as reassembly, which could explain our results. Moreover, lipid rafts are expected to be present on *Bc*EVs and the lipid composition of *Bc*EVs remains unknown. By performing more detergent treatments (*e.g.* different concentrations and different types of detergents) on *Bc*EVs, a condition where they are completely lysed could be reached. Incidentally it could also be informative on *Bc*EV lipid and lipid raft composition. Nevertheless, a lipid mass-spectrometry approach would fully unravel the composition, allowing us to further understand *Bc*EV structure and stability, and speculate on loading mechanisms as lipids and lipid rafts are proposed to be important for this last process (Lefebvre & Lécuyer, 2017; Mir & Goettsch, 2020).

***B. cinerea* EVs in cross-kingdom communication: less important than initially thought or technically challenging to study?**

Remarkably, *Bc*EV isolations from biological replicates of *B. cinerea* axenic liquid cultures always gave relatively heterogeneous results. Samples varied mostly in concentration and occasionally in size, despite being isolated from similar conditions (inoculation strength, amount of culture, time of growth etc…) and use of the same isolation protocol. Indubitably, performing a normalisation would be the best way to assess any concentration variations among biological replicates. While it was not performed in this study, it would be important to implement in the follow-up experiments for such comparison. Contrary to bacteria, measurement of the culture O.D. is not a suitable method as the fungus does not grow uniformly in the medium but rather as aggregates. One solution could be to measure the fungus biomass (pelleted during the first step of DUC), and use the weight for normalisation. However, as this material comes from liquid cultures, caution must be taken when weighing the mycelium, as retained liquid medium would interfere with a proper measurement. Drying or dehydrating the biomass before weighing would be a good alternative to avoid this problem, but the large quantity of mycelium (coming from 700 ml of 4-day-old liquid cultures) might be a problem. But even without normalisation for comparing replicates between them, while comparing to other fungal EV studies, we could see that *Bc*EV concentrations were always strikingly low compared to other fungal species.

In addition to the low secreted amounts of *Bc*EVs by *B. cinerea*, application of *Bc*EVs to plants did not result in a growth delay, or induce a ROS burst. These information together suggest a moderate to low importance of *Bc*EV for communication with the host plants. Nonetheless, while this could be due to *Bc*EVs truly not triggering any immunogenic response in *A. thaliana* plants, it can also be that *Bc*EV concentrations were insufficient to trigger a plant response, that *Bc*EVs produced in liquid cultures are not biologically functional and/or require partners lost during isolation for proper recipient cell targeting for example, or that the DUC isolation protocol damages them and impairs their functions.

Taken all together, these observations led us to think that either *B. cinerea* does not produce considerable amounts of *Bc*EVs and they are not relevant for cross-kingdom communication, or that the conditions we tested are not optimal. Similarly to our situation,

attempts to isolate EVs from *C. higginsianum* axenic cultures using a DUC protocol resulted in low EV yields (Rutter et al., 2022), which was solved by isolating EVs from *C. higginsianum* protoplasts, suggesting that EVs are produced in specific circumstances. Noticeably, EVs were isolated from *Aspergillus fumigatus* cell-wall regenerating protoplast as well (Rizzo, Chaze, et al., 2020). According to these studies, it could be that for *B. cinerea* as well, EVs are produced in specific circumstances which were not reproduced by the culture conditions we used. While it is evident that the axenic liquid cultures we used are not representing a real infection situation, it is important to note that generating protoplasts is a very artificial situation as well and the secreted EVs might be completely different to the ones released during infection. Nonetheless, for future experiments, it seems interesting to try a similar strategy and isolate *Bc*EVs from *B. cinerea* hyphae with semi-permeabilised cell walls or protoplasts. Importantly, this could mean that *Bc*EVs are not efficiently crossing the cell wall, at least not in axenic liquid cultures. With this in mind, we should also remember that *B. cinerea* secretes cell wall degrading enzymes (CWDEs) to penetrate plant tissues which could participate in making EV transport feasible.

Moreover, another exciting perspective would be to specifically look at the early host-pathogen interaction interfaces (*e.g.* first penetrating structures, appressoria), where the cell wall might be thinner or more permeable, thus more easily "crossable" for *Bc*EVs. Indeed, the cell wall, at least from the plant side, appears to be removed at the interaction interface, here haustorial interface, formed by certain pathogen species (Bozkurt & Kamoun, 2020). Moreover, MVBs were observed at the haustoria of *G. orontii* when infecting *A. thaliana* (Micali et al., 2011) and vesicles were observed in the extrahaustorial matrix between the oomycete *Hyaloperonospora parasitica* and the plant host (Mims & Richardson, 2004). First, electron microscopy techniques could inform us on the accumulation - or not - of MVBs, and consequently EV release, at the infection sites. Second, *Bc*EV isolation targeted from these specific interfaces, although extremely challenging, would give a more accurate glimpse on the *Bc*EV populations (and cargoes) and roles during plant infection.

Very conclusive evidence was provided in the direction of LTR retrotransposon-derived *Bc*sRNAs being crucial for ckRNAi, as we showed with the first results of this study. By analysing several *B. cinerea* wt isolates and transgenic strains on a

pathogenicity, genomic and transcriptomic levels we could identify LTR retrotransposon as pathogenicity factors as we made a clear link with the fungus aggressiveness. However, the means of transport of *Bc*sRNA effectors towards the host plant cells remains uncertain as *Bc*EVs were depleted in *Bc*sRNA effectors. Whether this was due to technical limitations or not is still to be clarified. Nonetheless, *Bc*EVs could be isolated and characterised, opening the field for understanding their functions, possibly related to *B. cinerea* aggressiveness.

While ckRNAi promotes infection by downregulating the plant host immune response, it is important to keep in mind that *B. cinerea* is a necrotrophic pathogen (at least after a very early stage of infection) having many resources to reach its final goal. *B. cinerea* strains D08_H24, D13_TS and D14_KF (wt) and *bcdcl1-dcl2* (mutant for both *dcl 1* and *2* genes) all fail to produce *Bc*sRNAs and show and reduced aggressiveness compared to the B05.10 wt (Porquier et al., 2013; Weiberg et al., 2013). However, these strains are still capable of infecting host plants. This shows the benefit of ckRNAi for plant infection, but also indicates that *B. cinerea* can successfully infect host plants without ckRNAi, even if it was proposed to be a crucial mechanism for establishing early hemibiotrophic infection. Therefore, it seems that our knowledge and understanding of ckRNAi only represents the tip of the iceberg and ckRNAi could be involved as well in other mechanisms such as directing some *B. cinerea* populations towards host-specialised and adapted infection strategies. This research is but a small snapshot in the bigger picture of plant pathogen interactions, and opened a window to many exciting questions I hope to see solved in the future.

Materials and methods

Botrytis cinerea strains and growth conditions

Botrytis cinerea (Persoon: Fries) B05.10 reference strain, as well as five other wild-type isolates (D08_H24, D14_KF, D13_TF, D13_TS and N11_KW) and the B05.10-*gfp* were used in this study. Routine cultivation was performed on solid nutrient-rich medium (10 $g.l^{-1}$ malt extract, 4 $g.l^{-1}$ yeast extract, 4 $g.l^{-1}$ glucose, 15 $g.l^{-1}$ agar), supplemented with hygromycin B (70 $\mu g.ml^{-1}$, Carl Roth, catalogue number: 1287.2) or nourseothricin (120 $\mu g.ml^{-1}$, Werner Bioagents, catalogue number: 5.001.000) for mutant cultivation. The plates were kept at room temperature under constant near-ultraviolet light exposure to stimulate conidia formation. For *Bc*EVs isolation, spores were grown into liquid minimal medium (20 $g.l^{-1}$ sucrose, 4 $g.l^{-1}$ $NaNO_3$, 1 $g.l^{-1}$ K_2HPO_4, 0.5 $g.l^{-1}$ KCl, 0.5 $g.l^{-1}$ $MgSO_4$ and 0.01 $g.l^{-1}$ $FeSO_4$; pH adjusted to 6.0).

Solanum lycopersicum culture conditions

Both Money Maker and Heinz cultivars were used for pathogen assays. Plants were grown under long day conditions (16 hr light/8 hr dark, 24 °C and 60 % relative humidity) in soil (Stender, catalogue number: A210) and in growth cabinets (photon flux density 85.92 $\mu mol\ m^{-2}\ s^{-1}$).

Arabidopsis thaliana culture conditions

A. thaliana ecotype Columbia 0 (Col-0) plants were grown in soil under long day conditions (16 hr light/8 hr dark, 22 °C and 60 % relative humidity) in soil (Stender, catalogue number: A210) and in growth cabinets walk-in climate chambers (photon flux density 87.90 $\mu mol\ m^{-2}\ s^{-1}$).

Genomic DNA isolation of *B. cinerea* mycelium

4-day-old mycelium was harvested and flash frozen in liquid nitrogen before being ground with a TissueLyser (QIAgen). gDNA was extracted following a CTAB-based protocol (D.-H. Chen & Ronald, 1999).

RNA extraction, reverse transcription, PCR and quantitative PCR

Total RNA from *B. cinerea* mycelium was extracted using a CTAB-based method (Bemm et al., 2016). 1 µg of total RNA was used for removing genomic DNA with DNase I treatment (Thermo Fisher, catalogue number: EN0521), followed by cDNA synthesis using SuperScript III RT (Thermo Fisher Scientific, catalogue number: 18080085). *Bc*sRNAs from *Bc*EVs were extracted with TRIzol (Invitrogen, catalogue number: 15596-026). RNA from the supernatant of the last ultracentrifugation, which pellets *Bc*EVs, was extracted following a published method (Rutter & Innes, 2017). For PCR, *B. cinerea* mRNAs were detected using GoTaq polymerase (Promega, catalogue number: M7848). *BcActin* (Bcin16g02020) was used for PCR in crude *Bc*EVs. For measuring gene expression by quantitative PCR, a Quantstudio5 cycler (Thermo Fisher Scientific) was used, with the Primaquant low ROX qPCR master mix (Steinbrenner Laborsysteme, catalogue number: SL-9902RB). *Bc*Tubulin (Bcin01g08040) was used for normalisation and differential expression was calculated following the $2^{-\Delta\Delta Ct}$ method (Livak & Schmittgen, 2001). Primers are listed in Annexe 3.

Stem-loop RT-PCR

Stem-loop reverse transcription was carried out following a published protocol (Varkonyi-Gasic et al., 2007), using the totality of *Bc*sRNAs extracted from *Bc*EVs without prior quantification. cDNA was synthesised with SuperScript III RT (Thermo Fisher Scientific, catalogue number: 18080085) and PCR reactions were performed using GoTaq polymerase (Promega, catalogue number: M7848). PCR products were visualised on 10 % on-denaturing polyacrylamide gels. Primers are listed in Annexe 3.

sRNA library, sequencing and data analysis

sRNAs were isolated from *B. cinerea* mycelium grown on solid rich media for 4 days or from *Bc*EVs samples (crude or treated with MNase). sRNAs libraries were cloned with the Next® Small RNA Prep Kit (NEB, catalogue number: E7300S) and sequenced on an Illumina HiSeq1500 platform. The sequencing data were analysed with the GALAXY Biostar server (Giardine et al., 2005). Raw data were de-multiplexed (Illumina Demultiplex, Galaxy Version 1.0.0) and the adapter sequences were removed (Clip adaptor sequence, Galaxy Version 1.0.0) (Dai et al., 2018). For the project focused on LTR retrotransposons as pathogenicity factors, the raw data are deposited at the NCBI SRA server (BioProject PRJNA730711, SRA

accessions SRR14576251 - SRR14576256 and SRR14576386 - SRR14576389). For all sRNAseq, the sequenced reads were mapped to *B. cinerea* B05.10 reference genome assembly from BioProject: PRJNA15632) or the genomes we d*e novo* sequenced of the isolated D08_H24 and D14_KF, using the BOWTIE algorithm (Galay Version 1.1.0) and allowing 0 mismatches (-v 0). Ribosomal RNAs were filtered out also with the BOWTIE algorithm and with allowing 3 mismatches (-v 3). Then, other sRNA species were filtered, transfer RNAs, small nuclear/nucleolar RNAs, messenger RNAs and transposon-derived RNAs, also using BOWTIE 2 and with the default settings (Langmead & Salzberg, 2012).

Plots and statistical analysis

Computational analyses were done with R studio (version 1.0.136 and 1.4.1717) using tydiverse (version 1.3.1) and ggplot2 (version 3.3.5).

Pathogen assay

Pathogen assay description is available in Porquier et al 2021. Briefly, aggressiveness of the different *B. cinerea* isolates was assessed on 4-to-5-week-old detached tomato leaves, as described here (Porquier et al., 2016). Briefly, leaves were inoculated with 20 µl drops of a 5.0E+04 conidia/ml suspension in 1 % malt extract, and kept in humidity boxes. After 48 hours, leaves were photographed and lesion sizes were measured using the freeware Fiji (ImageJ version 2.1.0/1.53c).

Trypan Blue staining and microscopy

Trypan Blue staining on infected tomato leaf discs, imaging and quantification descriptions are available in Porquier et al 2021. Images were taken with a DFC450 CDD-Camera (Leica) mounted on a CTR 6000 microscope (Leica Microsystems). Image analysis and quantification were performed with the software Fiji (version 2.1.0./1.53c).

Cloning and *B. cinerea* transformation

Cloning strategy and details are also available in Porquier et al 2021. The constructs were generated using the Golden Gate cloning strategy (Binder et al., 2014). Primers are listed in the Annexe 3 and construct schemes are available in Fig. 14a and 17a. Plasmids were digested with BsaI (NEB, catalogue number: R0535S), to isolate the cassette of interest,

before *B. cinerea* transformation. *B. cinerea* transformations were performed following a published protocol (Müller et al., 2018), with slight modifications. Briefly, 1.0E+08 conidia were inoculated in 100 ml of liquid nutrient-rich media (10 $g.l^{-1}$ malt extract, 4 $g.l^{-1}$ yeast extract, 4 $g.l^{-1}$ glucose) and grown for 18 hours at 20 °C and 180 rpm shaking. The mycelium was harvested by centrifugation (1,000 g-force for 8 min) and washed with KCl buffer (0.6 M KCl, 0.1 M NaPi, pH 5.8). The mycelium was harvested by centrifugation (1,000 g-force for 10 min) and incubated with 20 ml of protoplastic enzyme mix (0.6 M KCl, 0.1 M NaPi, 1 % Glucanex (Sigma) and 300 µl KOH 1M) on a 3D rocky shaker for 60 to 90 min at room temperature. The reaction can be monitored by taking aliquots and observing with a light microscope. The protoplasting reaction was filtered through a sterile Miracloth filter paper (pore size 22 to 25 µm, VWR, catalogue number: 475855-1) into an ice-cold TMS buffer (1 M sorbitol, 10 mM MOPS, pH 6.3). The protoplasts were harvested by centrifugation (2,500 g-force for 5 min at 4 °C) and resuspended into TMSC buffer (TMS + 50 mM $CaCl_2$). The protoplasts were counted with a Neubauer chamber and adjusted to 2.0E+07 protoplasts per 100 µl, per transformation. Per transformation, 10 to 15 µg of DNA was added in Tris-$CaCl_2$ buffer (10 mM Tris-HCl, 1 mM EDTA, 40 mM $CaCl_2$, pH 6.) by gently mixing, and the aliquots were kept on ice for 10 min. After, 160 µl of PEG solution was added (0.6 g ml-1 PEG3350, 1 M sorbitol, 10 mM MOPS, pH 6.3) by gently mixing and the samples incubated for 20 min at room temperature. The protoplasts were washed with TMSC by centrifugation (2,500 g-force for 5 min), and resuspended into TMSC. The protoplast were mixed with liquid (42 °C) SH agar (0.6 M sucrose, 5 mM Tris-HCl (pH 6.5), 1 mM $(NH_4)H_2PO_4$, 8 $g.l^{-1}$ bacto agar) and poured into Petri plates. After 24 hours in the dark of incubation, a layer of SH agar containing the appropriate antibiotic was layered. For mutants with target insertion into the *Bc*niaD locus, transformants were selected by plating them on Czapek Dox liquid medium (30 $g.l^{-1}$ sucrose, 3 $g.l^{-1}$ $NaNO_3$, 1 $g.l^{-1}$ K_2HPO_4, 0.5 $g.l^{-1}$ KCl, 0.5 $g.l^{-1}$ $MgSO_4$ and 0.01 $g.l^{-1}$ $FeSO_4$; pH 6.0) supplemented with 0.4 M potassium chlorate (Schumacher, 2012).

RNAseq and analysis

RNAseq sample preparation and analysis are detailed in Porquier et al., 2021. Briefly, *A. thaliana* Col-0 leaves were inoculated with 4 drops of 5 µl, containing 1.0E+06 conidia/ml of *B. cinerea* diluted in 1 % malt extract. 24 plants were infected per *B. cinerea* strain.

24 hours post-inoculation, 3 leaves from each plant were randomly harvested. The infection sites were cut out from 2 leaves and pooled to form 1 biological replicate. From these samples, total RNA was extracted following the CTAB method (Bemm et al., 2016). mRNA sequencing was performed using a version of the primer-seq method available online at https://www.protocols.io/view/prime-seq-s9veh66. Illumina paired-end sequencing was performed with an HiSeq 1500 instrument. Concerning the data processing, demultiplexing of the raw data was performed with deML (Renaud et al., 2015), trimming of the adapters and polyA tails with cudadapt (version 2.3) and further processing using the zUMIs pipeline (Parekh et al., 2018) with STAR (Dobin et al., 2013). The processed raw data are available at the NCBI server (BioProject PRJNA730711, SRA accessions SRR14577137-SRR14577147 and SRR14590656-SRR14590667). Mapping of the reads was done on *A. thaliana* (TAIR10) and *B. cinerea* (ASM83294v1) genomes with Araport11 and ASM83294v1.41 gene annotations. Concerning the data analysis, differential gene expression was performed using iDEP.91 (Ge et al., 2018) with a FDR cut-off at 0.05 using limma-voon normalisation.

Whole genome sequencing

Sequencing of *B. cinerea* D08_H24 and D14_KF genomes was performed by hybrid Oxford Nanopore (Promethion) long-read sequencing and Illumina HiSeq1500 short-read sequencing. Base calling was performed with guppy version 2.3.7) and adapters were removed with porechop (https://github.com/rrwick/Porechop), then the long reads were assembled with wtdbg2 (Ruan & Li, 2020) and polished with two rounds of racon (Vaser et al., 2017). The short reads were used to polish the assembly using pilon (Walker et al., 2014). Whole genome comparisons were visualised with the Circos plotting library (Krzywinski et al., 2009) via R circlize (Gu et al., 2014). Assembled genome sequence contigs of the two isolates D08_H24 and D14_KF are deposited at NCBI SRA server (BioProject PRJNA730711).

Transposon annotation and RIP analysis

For this study we used a previous annotation of *B. cinerea* B05.10 transposable elements (Porquier et al., 2016). Annotation of the two newly sequenced genomes of v was performed using the REPET package as described previously (Porquier et al., 2016). Concerning the sequence alignment and phylogenetic tree, we used the CLC main workbench software

(version 20.0.4, Qiagen), with the Neighbor Joining method and Jukes-Cantor nucleotide distance measure. Bootstrap analysis was run with 500 replicates. To identify truncated transposons (< 400 bp), we performed Blastn searches with the (parameters: -word_sie 20, -max_target_seqs 50000, -gapopen 5, -gapextend 2, -reward 2, penalty -3, dust no, -soft_masking false), with as a query the GC-richest copy of each LTR retrotransposon subfamilies from B05.10. The sequences from the hits longer than 1000 pb were aligned with the REPET package (tool refalign) (https://urgi.versailles.inra.fr/Tools/REPET) to then run further RIPCAL analysis (Hane & Oliver, 2008), using the GC-richest copy as reference.

We calculated all possible RIP mutation signatures (CA → TA, CT, → TT, CC → TC, CG → TG, and the reverse complements) also using RIPCAL. To identify the occurrence of RIP, we calculated the TA/AT index (Margolin et al., 1998) but solely on full-length copies identified with the REPET analysis we ran. To calculate the RIP index, the compseq tool (from EMBOSS package) was used, counting the different dinucleotide combinations.

To predict the protein domains in the different LTR retrotransposons, we used a GC-rich copy sequence from each consensus class and used the NCBI conserved domain database (Lu et al., 2020). The sizes and lengths of the LTR flanking regions were obtained from a previous study (Porquier et al., 2016). The *Bc*Gypsy1 element carries an additional ORF coding for *brtn*, which sequence was also obtained from a previous study (Zhao et al., 2011). Importantly, the annotation of the *Bc*Gypsy1 additional ORF is not present in B05.10 last genome annotation. In the P26.1 consensus, which is grouped in the *Bc*Gypsy1 subfamily, the beginning of the *brtn* ORF is absent, but a putative additional ORF is still present (dashed arrow in the Fig. 7). The other putative additional ORFs were predicted in the last annotation of B05.10 genome (http://fungi.ensembl.org/Botrytis_cinerea). The protein domains of the LTR retrotransposons were predicted using IBS (http://ibs.biocuckoo.org/).

Isolation of *Bc*EVs from *B. cinerea* liquid cultures

B. cinerea B05.10 conidia were inoculated in 700 to 1000 ml of optimised liquid minimal medium (20 $g.l^{-1}$ sucrose, 1 $g.l^{-1}$ K_2HPO_4, 4 $g.l^{-1}$ $NaNO_3$, 0.5 $g.l^{-1}$ KCl, 0.01 $g.l^{-1}$ $FeSO_4$, 0.5 $g.l^{-1}$ $MgSO_4$,pH 6.0, see Annexe 1) to reach a final concentration of 35.0E+03 conidia/ml (counted with a Neubauer chamber) and grown for 4 days, at 20 °C and permanent shaking at 100 rpm. Fungal cells were separated from the supernatant by centrifugation at 4,000 g-force

for 20 min, 4 °C. The first steps have to be done gently to avoid cell disruption and artificial production of nanoparticles. The supernatant was filtered through two layers of Miracloth filter paper (pore size 22 to 25 µm, VWR, catalogue number: 475855-1). Cellular debris were eliminated by centrifugation at 13,000 g-force for 40 min at 4 °C. The supernatant was collected and filtered through Steritop^{TM} sterile filters (pore size 0.22 µm, Merck Millipore). EVs were collected by ultracentrifugation at 100,000 g-force for 60 min, 4 °C. The pellet was resuspended in MES Buffer (20 mM MES Hydrate, 2 mM $CaCl_2$, 0.1 M NaCl, pH 6.0), and washed by ultracentrifugation. If not used directly after for downstream experiments, *Bc*EVs were flash frozen in liquid nitrogen and stored up to a few days at -80 °C.

Nanoparticle tracking analysis

*Bc*EV sizes and concentrations were determined using a ZetaView (Basic NTA Nanoparticle Tracking Video Microscope PMX-120, Particle Metrix) with the ZetaView in-built software (version 8.05.11). Samples were diluted 100 to 1000 times in MES buffer previously filtered with 0.22 µm pore size syringe filter (Chromafil®, catalogue number: 729024). Dilutions were made accordingly to track approximately 50 to 200 particles in total on the 11 positions. For all measurements, the sensitivity was 85 %, shutter 100 %, frame rate 30 and the temperature was kept at 22 to 24 °C. Raw data provided by the software were plotted using ggplot2. The graphical outputs of *Bc*EV NTA measurements represent raw data which were smoothed following the locally weighted least squares regression (loess) model using ggplot2, with a span between 0.1 and 0.4 and an n between 80 and 100.

Transmission and Scanning Electron Microscopy

For transmission electron microscopy (TEM) of crude *Bc*EVs, 5 µl of the sample was applied to 400 mesh carbon-coated copper grids and negative-stained with 1 % uranyl acetate as described previously (Kaletta et al., 2020). Transmission electron microscopy was carried out using either a Zeiss EM912 TEM (Carl Zeiss AG, Oberkochen, Germany), equipped with a 2k x 2k slow-scan CCD Camera (TRS, Tröndle Restlichtverstärkersysteme, Moorenweis, Germany) and operated at 80 kV, or a JEOL F200 cryo-(S)TEM (JEOL, Freising, Germany) with a XAROSA 20 megapixel CMOS camera (EMSIS, Münster, Germany) and operated at 200 kV.

Scanning electron microscopy (SEM) of *B. cinerea* mycelium was performed as described earlier (Beheshti et al., 2021). In more detail, samples were chemically fixed with 2.5 % glutaraldehyde in 75 mM cacodylate buffer, supplemented with 2 mM MgCl2 (pH 7.0) for 1h. Postfixation was carried out with 0.2 % osmium tetroxide for 30 min. After dehydration in a graded acetone series and critical-point drying, the samples were mounted on aluminium stubs using Tempfix and sputter-coated with platinum. Samples were pre-washed with ethanol to get rid of the extracellular glucan sugar coat of the mycelium.

Nuclease protection assays

Crude *Bc*EVs samples were divided equally into three to four aliquots. Triton X-100 (Sigma-Aldrich, catalogue number. T8787-250ML) treatment was carried out for 5 min at 70 °C with a final concentration of 1 %. Proteinase K (Thermo Scientific, catalogue number: EO0491) was added to reach 50 $\mu g.ml^{-1}$ and incubated for 15 min at 37 °C, and inhibited by the addition of phenylmethylsulfonyl fluoride (PMSF) to a concentration of 100 mM and an incubation of 10 min at room temperature. Finally, nucleic acid digestion was performed with 1000 units of MNase (NEB, catalogue number: M0247S) for 30 min at 37 °C, at this step the total volume of the reaction reached 200 µl. For the RNase A (Thermo Fisher Scientific, catalogue number: EN0521) treatment, a final concentration of 1 $\mu g.ml^{-1}$ was used. Immediately after the treatments, *Bc*EVs were analysed by NTA and/or RNA was extracted following the TRIzol (Invitrogen, catalogue number: 15596-026) method as stated before.

Cloning of *Bc*siR20 from gel and sequencing

Stem-loop RT-PCR was run on 10 % non-denaturing polyacrylamide gel and bands corresponding to *Bc*siR20 were cut out. Briefly, the bands were crushed in 0.3 M NaCl. After 12 h incubation at 4 °C under permanent shaking, the liquid fractions were collected and DNA precipitated with 3M NaOAC and 96 % EtOH, then washed with 80 % EtOH. As the GoTaq (Promega, catalogue number: M7848) used for the stem-loop RT-PCR generates fragments with 3’ overhangs, the PCR fragments were processed by klenow (NEB, catalogue number: M0212L) to generate blunt ends. PCR fragments were ligated into the BB02 plasmid from the plant Golden Gate system (Binder et al., 2014) by StuI (NEB, catalogue number: R0187s) with a cut ligation (2 min at 37 °C - 5 min at 16 °C, 50 cycles) performed in a thermocycler. Constructs were transformed into TOP 10 *E. coli* via heat shock and bacteria

were plated on Pétri dishes. Correct colonies were selected with the white/blue screening and grown over-night in liquid cultures. Plasmids were extracted by miniprep (Thermo Fisher Scientific, catalogue number: K0503). Sequencing was done at the Genomics service unit of the LMU (Planegg, Germany) with the M13F or M13R primers (Annexe 3).

EV isolation from infected *A. thaliana* plants and density gradient fractionation

125 six-week-old Col-0 plants were used for each experiment. 25 plants were mock treated by spraying 12 ml of 1 % malt extract and 100 plants were infected by spraying 3.5E+06 B05.10 conidia resuspended in 50 ml 1 % malt extract. After 4 days, the EVs were collected from apoplastic wash fluid following a published protocol (Rutter & Innes, 2017). Briefly, mock treated and infected *A. thaliana* leaves were cut out of the plant and quickly washed from the soil. The leaves were vacuum infiltrated in MES buffer (as previously) then quickly dried with paper. To harvest the apoplastic wash fluid, the leaves were placed into syringes, with the cut sites facing down, themselves placed in 50 ml Falcon Tubes and centrifuged for 20 minutes at 900 g-force and 4 °C. EVs were isolated from the apoplastic wash fluid by DUC, with a first centrifugation for 30 min at 10,000 g-force and 4 °C, followed by filtration through 0,45 µm pores (syringe filter Chromafil®, catalogue number: 729025), and a last ultracentrifugation for 60 min at 100,000 g-force and 4 °C.

To enhance the purification, EVs were fractionated on a discontinuous density gradient. 10 ml gradients were poured by hand in an ultracentrifugation tube by layering solutions of Optiprep® (non-ionic iodixanol-based medium, Sigma-Aldrich, catalogue number: D1556-250ML) diluted in MES buffer (40 %, 20 %, 10 % and 5 %). Crude EV samples obtained by the previous ultracentrifugation were loaded on the top. The gradient was ultracentrifugated in a swinging-bucket rotor (Sorvall TH-641) at 100,000 g-force for 14 hours at 4 °C. Eleven equal fractions were collected by hand from the top to the bottom and washed in MES buffer by a last ultracentrifugation for 60 min at 100,000 g-force and 4 °C.

Seedling growth inhibition

The assay was performed as previously described (Schwessinger et al., 2011), with slight modifications. *A. thaliana* Col-0 seeds were surface sterilised in 96 % ethanol supplemented with 1 % sodium hypochlorite before being stratified on ½ MS + 1 % sucrose plates (MS:

2.2 g.l^{-1} MS, 10 g.l^{-1} sucrose, supplemented with 8 g.l^{-1} agar for plates, with pH adjusted to 5.8), in the dark at 4 °C, for 4 days. The plates were then placed under long day conditions (16 h light / 8 h dark, 22 °C and 60 % relative humidity) for 4 days before transferring seedlings of similar sizes into 96 well plates containing 100 µl ½ MS + 1 % sucrose and the different treatments. 7 to 8 seedlings were used for each condition. For the vesicle treatment, crude *Bc*EVs were diluted into ½ MS + 1 % sucrose before being sterile filtered and applied to seedlings to final concentrations ranging from 2,75E+06 to 2,25E+08 particles/ml. Flg22 (EZbiolabs, custom synthesised peptides QRLSTGSRINSAKDDAAGLQIA sequence from *P. aeruginosa*) and Elf18 (EZbiolabs, custom synthesised peptides: N-acetylated SKEKFERTKPHVNVGTIG sequence from *E. coli*) were applied to final concentrations of 300 nM as positive controls. MES buffer was used as negative controls. Seedling weights were measured 8 days post-treatment.

ROS measurements

The assay was performed as previously described (Gimenez-Ibanez et al., 2009), with slight modifications. Briefly, *A. thaliana* (on 4-week-old plants) leaf discs were cut out, and washed overnight in water in order to dilute the secreted ROS in response to wounding. 2 or 12 hours before ROS measurement, the leaf discs were incubated either with *Bc*EVs or with only the buffer where *Bc*EVs are resuspended (MES buffer). The reaction buffer containing Flg22 (EZbiolabs, like previously) and the necessary chemicals for luminescence quantification (100 nM Flg22, 17 µg.ml^{-1} Luminol, 10 µg.ml^{-1} HRP) were added to the leaf discs was added to the leaf discs, and the ROS was immediately measured with a plate reader (TECAN luminometer, Infinite 200 Pro).

Annexes

Annexe 1: liquid media tested for *B. cinerea* culture prior to *Bc*EV isolation.

In general, many different culture conditions were tested: different inoculation strength, duration of culture, low to strong shaking or no shaking, 20 °C.

Tested media	**Composition**
HA	4 $g.l^{-1}$ saccharose, 10 $g.l^{-1}$ malt extract, 4 $g.l^{-1}$ yeast extract (pH 5.8)
Modified HA	10 $g.l^{-1}$ malt extract, 4 $g.l^{-1}$ yeast extract (pH 5.8)
Czapek Dox (CD)	30 $g.l^{-1}$ saccharose, 1 $g.l^{-1}$ K_2HPO_4, 3 $g.l^{-1}$ $NaNO_3$, 0.5 $g.l^{-1}$ KCl, 0.01 $g.l^{-1}$ $FeSO_4$, 0.5 $g.l^{-1}$ $MgSO_4$ (pH 6)
Preculture (1 or 2 days) with HA before 4 days culture with CD	
Supplemented CD 1	CD + 0.2 % of grinded plant tissues (pH 6)
Supplemented CD 2	CD + 0.2 % peptone (pH 6)
Supplemented CD 3	CD + 0.2 % yeast extract(pH 6)
Supplemented CD 4	CD + 0.2 % peptone + 0.2 % yeast extract (pH 6)
V8	10 % tomato juice (0.6 $g.l^{-1}$ salt, 2.9 $g.l^{-1}$ sugar), 3$g.l^{-1}$ $CaCO_3$
CD with different N source NH_4Cl	30 $g.l^{-1}$ sucrose, 1 $g.l^{-1}$ K_2HPO_4, 3 $NH_4Clg.l^{-1}$, 0.5 $g.l^{-1}$ KCl, 0.01 $g.l^{-1}$ $FeSO_4$, 0.5 $g.l^{-1}$ $MgSO_4$ (pH 6)
CD with different N source NH_4Cl and lower C/N ratio	20 $g.l^{-1}$ sucrose, 1 $g.l^{-1}$ K_2HPO_4, 3 $NH_4Clg.l^{-1}$, 0.5 $g.l^{-1}$ KCl, 0.01 $g.l^{-1}$ $FeSO_4$, 0.5 $g.l^{-1}$ $MgSO_4$ (pH 6)
Optimised (and lower C/N ratio) CD	20 $g.l^{-1}$ sucrose, 1 $g.l^{-1}$ K_2HPO_4, 4 $g.l^{-1}$ $NaNO_3$, 0.5 $g.l^{-1}$ KCl, 0.01 $g.l^{-1}$ $FeSO_4$, 0.5 $g.l^{-1}$ $MgSO_4$ (pH 6)

Annexe 2: Parameters of EV isolation from different fungal species.

Information collected from published articles, where fungal EV isolations were performed. Not all studies shared the parameters I was interested in, thus only a sub-selection is present.

Species	**Concentration of particles**	**Culture conditions**	**Reference**
Fusarium oxysporum f. sp. vasinfectum	30E+06	72 hours	(Bleackley et al., 2020)
Malassezia sympodialis	200E+09	2.0E+06 cells/ml in 300 ml	(Rayner et al., 2017)
Penicillium digitatum	3.5E+07	1.0E+06 conidia ml^{-1} on 1 plate which is scrapped in 30ml	(Costa et al., 2021)
Zymoseptoria tritici	1.5E+06	100 ml, 2.0E+05 spores/ml, 72-hours	(Hill & Solomon, 2020)
Aspergillus fumigatus	6.0E+09 to 10E+010	1E+07 conidia from A. fumigatus were inoculated in 50 ml	(Souza et al., 2019)
Aspergillus fumigatus	1.0E+07	cell-wall regenerating protoplast	(Rizzo, Chaze, et al., 2020)
Heligmosomoides bakeri	2.0E+10		(Buck et al., 2014; Chow et al., 2019)
Colletotrichum higginsianum	1.0E+11	cell-wall regenerating protoplast from 3 day-old liquid culture	(Rutter et al., 2022)

Annexe 3: all primers used in these studies.

Primer names	Purposes	Sequences
*Bc*Gypsy1 FOR	genotyping of LTR retrotransposons on wt strains	GCGAACTGTGCCATGGGTAA
*Bc*Gypsy1 REV		ACGACAAGGATGCTACTGCC
*Bc*Gypsy2 FOR		CCGATACCCCTTACCATTGA
*Bc*Gypsy2 REV		TCGAATAGACCGAAGCGAGT
*Bc*Gypsy3 FOR		TACCGCCAGACAGCGCTCTCAGA
*Bc*Gypsy3 REV		GCGTGATGGGTCACTTGGGTTTG
*Bc*Gypsy4 FOR		TCGAATAGACCGAAGCGAGT
*Bc*Gypsy4 REV		ACTTTGCACCAACAGCACAG
*Bc*Copia1 FOR		CGATACAGCATTTGGCATTG
*Bc*Copia1 REV		TGATCCATTCTCGTGCTGAG
*Bc*Copia2 FOR		TCCACTGCAATGGGTATTCA
*Bc*Copia2 REV		TTGCTATGAGAGCCATCACG
*Bc*actin FOR	genotyping of LTR retrotransposons on wt strains and RT-PCR on crude *Bc*EV samples	CATTGTTATGTCTGGTGGAACCAC
*Bc*actin REV		AGAACCACCAATCCAGACGGAGTA
*Bc*Gypsy3 RT FOR	*Bc*Gypsy3 gene expression by qRT-PCR	CGAAGGGGTCACCACAGCGA
*Bc*Gypsy3 RT REV		CTCCCATCGCTGCTTTCGCA
*Bc*tubulin RT FOR		GAGGTTGAGGACCAAATGCG
*Bc*tubulin RT REV		GGACATCTTGAGACCACGGG
*Bc*siR3.1 RT	stem-loop RT and PCR on wt strains and *Bc*EV samples	GTCGTATCCAGTGCAGGGTCCGAGGT ATTCGCACTGGATACGACGCCCAC
*Bc*siR3.1 FOR		GCGGCGGTTGTGGATCTTGTA
*Bc*siR3.2 RT		GTCGTATCCAGTGCAGGGTCCGAGGT ATTCGCACTGGATACGACACTCAC
*Bc*siR3.2 FOR		GCGGCGGTACATTGTGGATCT
sRNA universal REV		GTATCCAGTGCAGGGTCCGAGGT
*Bc*niaD FOR	genotyping *Bc*niaD locus	GCCACAGACTCCGCCAGATTCTAATG
*Bc*niaD REV		CAACCATTTCACGCTGCGACCACC
*Bc*204	genotyping mutant strains (ssGypsy3 and dsGypsy3) for 5' insertion at the *Bc*niaD locus	CTCTTAATCTTCCCCCTTTC
*Bc*86	genotyping mutant strains (EV_Δ*BcniaD*) for 5' insertion at the *Bc*niaD locus	ATGAAGACGCTACGCTGTCGAACTTT TC
*Bc*237	genotyping mutant strains (5` LTR *Bc*Gypsy3) for 5' insertion at the *Bc*niaD locus	TAGAAGACGGCAGAGGTCTCAGGTG AGTGATATCGACGGTGATTC
*Bc*372	genotyping mutant strains for 5' insertion at the *Bc*niaD locus	CGCATATCAGCATATCGAGATGTCC

*Bc*161	genotyping mutant strains for 3' insertion at the *Bc*niaD locus	TACACAAATCGCCCGCAGAA
*Bc*373		GAGTACCCATCCGATGGAGTTGTTG
*Bc*106	genotyping mutant strains (np*Bc*Gypsy3) for 5' insertion at the *Bc*niaD locus	CCTGAAGGGCGTACTAGGGT
*Bc*262	amplifying TtrpC in position 1 for LI cloning	ATGAAGACGGTACGGGTCTCAGCGGTGATTTAATAGCTCCATGTCAAC
*Bc*263		TAGAAGACGGCAGAGGTCTCACAGATCGAGTGGAGATGTGGAGTG
*Bc*264		ATGAAGACTCAAGACCTACGAGACTGAGGAATC
*Bc*265		ATGAAGACTGTCTTTTGACGACCGTTGATC
*Bc*362	amplifying *Bc*niaD 5' flank for direct LII cloning	ATGAAGACGGTACGGGTCTCAGCGGGTGAATGGGATTCATTGTTTATTTC
*Bc*363		TAGAAGACGGCAGAGGTCTCAGACATTACTCCGTGGATGCAACAG
*Bc*364	amplifying *Bc*niaD 3' flank for direct LII cloning	ATGAAGACGGTACGGGTCTCAGCGGGAGGTTTTAAGTAACTGAGAGGTG
*Bc*365		TAGAAGACGGCAGAGGTCTCAGACAGCAGTGGATTAATAATTGTTGCTAAGC
CR6	amplifying hygromycin resistance cassette for direct LII cloning	ATGGTCTCAGACACTATTCCTTTGCCCTCGGAC
*Bc*87	amplifying hygromycin resistance cassette for direct LII cloning & hygromycin resistance cassette in position 6 for LI cloning	ATGAAGACGGTA CG GGTCTC A GCGG GATATTGAAGGAGCAT
CR5	amplifying hygromycin resistance cassette in position 6 for LI cloning	ATGGTCTCGTGAGGATATTGAAGGAGCATTTTT
CR 9	amplifying TgluC (T5) for LI cloning	ATGAAGACAGTACGGGTCTCGAATCCGTATGTAGATAAGATGTAT
CR 10		ATGAAGACTACAAGACAAAAGAGGGCGGAA
CR 11		ATGAAGACTACTTGCGCTAAAACACCCCCT
CR 12		ATGAAGACTACAGAGGTCTCACTCAATCTTGTTGGGGGGAAGGGG
CR 15	amplifying TgluC (T4) for LI cloning	ATGGTCTCAAAGGCGTATGTAGATAAGATGTAT
CR 16		ATGGTCTCAGATTATCTTGTTGGGGGGAAGGGG
*Bc*110	amplifying PactA in position 1 for LI cloning & PactA-TtrpC_inv in position 1 for LI cloning	ATGGTCTCAGCGGTGTGCGTCCTCTTCTGCCTA
*Bc*111	amplifying PactA in position 1 for LI cloning	TAGGTCTCTCAGAGGGGTTGATAAATTAAGACG
*Bc*178	amplifying PoliC_inv in position 5 for LI cloning	CAGGTCTCGAATCTTGGATCGATTGTGATGTGAT

*Bc*179		CAGGTCTCGCTCATGCAGCTGTGGAG CCGCATT
*Bc*196	amplifying PactA-TtrpC_inv in position 1 for LI cloning	TAGGTCTCTCAGATCGAGTGGAGATG TGGAG
*Bc*73	amplifying *Bc*gypsy3 (G3) in position 2 for LI cloning	ATGAAGACGCTACGGGTCTCGTCTGA ACAATGGTTTCCACGAGA
*Bc*74		ATGAAGACTGCAGAGGTCTCCGGTGC CTCTGTATTGGTAATGCT
*Bc*75		ATGAAGACGCATACGACACCTTGTCG AAGT
*Bc*76		ATGAAGACGCGTATTCACTAAATTGG ACCTGCG
*Bc*77		TAGAAGACGCATTCCATTCGTCGCCTT CCCTG
*Bc*78		TAGAAGACATGAATACGGCGTTCCGC ACGCG
*Bc*79		GAGAAGACGCCGTCTTTCTGAAGCCG CAATAAAG
*Bc*80		GAGAAGACGAGACGACGATTTTATAA AGAATAAAGAGTACC
*Bc*81		CCGAAGACGACATCCGCCGGTTGGTA GCCCT
*Bc*82		CCGAAGACGAGATGACACGTGGGAA GCACCCT
*Bc*249	amplifying 5' LTR of *Bc*Gypsy3 in position 1 for LI cloning	TAGAAGACGGCAGAGGTCTCACAGA AGTGATATCGACGGTGATTCGCTG
*Bc*266		ATGAAGACGGTACGGGTCTCAGCGGT GTTACGGGACAAAACGTGAC
M13 F	sequencing of *Bc*siR20 cloned into the BB02 backbone	TGTAAAACGACGGCCAGT
M13 R	sequencing of *Bc*siR20 cloned into the BB02 backbone	GGAAACAGCTATGACCAT

List of figures and tables

Figures

Tables

References

Abels, E. R., & Breakefield, X. O. (2016). Introduction to Extracellular Vesicles: Biogenesis, RNA Cargo Selection, Content, Release, and Uptake. *Cellular and Molecular Neurobiology*, *36*(3), 301–312. https://doi.org/10.1007/s10571-016-0366-z

Albuquerque, P. C., Nakayasu, E. S., Rodrigues, M. L., Frases, S., Casadevall, A., Zancope-Oliveira, R. M., Almeida, I. C., & Nosanchuk, J. D. (2008). Vesicular transport in *Histoplasma capsulatum*: An effective mechanism for trans-cell wall transfer of proteins and lipids in ascomycetes. *Cellular Microbiology*, *10*(8), 1695–1710. https://doi.org/10.1111/j.1462-5822.2008.01160.x

Alves, C. S., & Nogueira, F. T. S. (2021). Plant Small RNA World Growing Bigger: TRNA-Derived Fragments, Longstanding Players in Regulatory Processes. *Frontiers in Molecular Biosciences*, *8*, 638911. https://doi.org/10.3389/fmolb.2021.638911

Alves, L. R., Peres da Silva, R., Sanchez, D. A., Zamith-Miranda, D., Rodrigues, M. L., Goldenberg, S., Puccia, R., & Nosanchuk, J. D. (2019). Extracellular Vesicle-Mediated RNA Release in *Histoplasma capsulatum*. *MSphere*, *4*(2). https://doi.org/10.1128/mSphere.00176-19

Amselem, J., Cuomo, C. A., van Kan, J. A. L., Viaud, M., Benito, E. P., Couloux, A., Coutinho, P. M., de Vries, R. P., Dyer, P. S., Fillinger, S., Fournier, E., Gout, L., Hahn, M., Kohn, L., Lapalu, N., Plummer, K. M., Pradier, J.-M., Quévillon, E., Sharon, A., … Dickman, M. (2011). Genomic Analysis of the Necrotrophic Fungal Pathogens Sclerotinia sclerotiorum and Botrytis cinerea. *PLoS Genetics*, *7*(8), e1002230. https://doi.org/10.1371/journal.pgen.1002230

Amselem, J., Lebrun, M.-H., & Quesneville, H. (2015). Whole genome comparative analysis of transposable elements provides new insight into mechanisms of their inactivation in fungal genomes. *BMC Genomics*, *16*(1), 141. https://doi.org/10.1186/s12864-015-1347-1

An, Q., Ehlers, K., Kogel, K., Van Bel, A. J. E., & Hückelhoven, R. (2006). Multivesicular compartments proliferate in susceptible and resistant *MLA12*‐barley leaves in response to infection by the biotrophic powdery mildew fungus. *New Phytologist*, *172*(3), 563–576. https://doi.org/10.1111/j.1469-8137.2006.01844.x

An, Q., Huckelhoven, R., Kogel, K.-H., & van Bel, A. J. E. (2006). Multivesicular bodies participate in a cell wall-associated defence response in barley leaves attacked by the pathogenic powdery mildew fungus. *Cellular Microbiology*, *8*(6), 1009–1019. https://doi.org/10.1111/j.1462-5822.2006.00683.x

Anderson, J. P., Gleason, C. A., Foley, R. C., Thrall, P. H., Burdon, J. B., & Singh, K. B. (2010). Plants versus pathogens: An evolutionary arms race. *Functional Plant Biology*, *37*(6), 499. https://doi.org/10.1071/FP09304

Antico, C. J., Colon, C., Banks, T., & Ramonell, K. M. (2012). Insights into the role of jasmonic acid-mediated defenses against necrotrophic and biotrophic fungal pathogens. *Frontiers in Biology*, *7*(1), 48–56. https://doi.org/10.1007/s11515-011-1171-1

Artuyants, A., Campos, T. L., Rai, A. K., Johnson, P. J., Dauros-Singorenko, P., Phillips, A., & Simoes-Barbosa, A. (2020). Extracellular vesicles produced by the protozoan parasite Trichomonas vaginalis contain a preferential cargo of tRNA-derived small RNAs. *International Journal for Parasitology*, *50*(14), 1145–1155. https://doi.org/10.1016/j.ijpara.2020.07.003

Asano, T., Masuda, D., Yasuda, M., Nakashita, H., Kudo, T., Kimura, M., Yamaguchi, K., & Nishiuchi, T. (2007). AtNFXL1, an Arabidopsis homologue of the human transcription factor NF-X1, functions as a negative regulator of the trichothecene phytotoxin-induced defense response: Trichothecene-inducible AtNFXL1 gene. *The Plant Journal*, *53*(3), 450–464. https://doi.org/10.1111/j.1365-313X.2007.03353.x

Asano, T., Yasuda, M., Nakashita, H., Kimura, M., Yamaguchi, K., & Nishiuchi, T. (2008). The *AtNFXL1* gene functions as a signaling component of the type A trichothecene-dependent response. *Plant Signaling & Behavior*, *3*(11), 991–992. https://doi.org/10.4161/psb.6291

Bachurski, D., Schuldner, M., Nguyen, P.-H., Malz, A., Reiners, K. S., Grenzi, P. C., Babatz, F., Schauss, A. C., Hansen, H. P., Hallek, M., & Pogge von Strandmann, E. (2019). Extracellular vesicle measurements with nanoparticle tracking analysis – An accuracy and repeatability comparison between NanoSight

NS300 and ZetaView. *Journal of Extracellular Vesicles*, *8*(1), 1596016. https://doi.org/10.1080/20013078.2019.1596016

Baldrich, P., Rutter, B. D., Karimi, H. Z., Podicheti, R., Meyers, B. C., & Innes, R. W. (2019). Plant Extracellular Vesicles Contain Diverse Small RNA Species and Are Enriched in 10- to 17-Nucleotide "Tiny" RNAs. *The Plant Cell*, *31*(2), 315–324. https://doi.org/10.1105/tpc.18.00872

Barnes, S. E., & Shaw, M. W. (2003). Infection of Commercial Hybrid Primula Seed by *Botrytis cinerea* and Latent Disease Spread Through the Plants. *Phytopathology®*, *93*(5), 573–578. https://doi.org/10.1094/PHYTO.2003.93.5.573

Beheshti, H., Strotbek, C., Arif, M. A., Klingl, A., Top, O., & Frank, W. (2021). PpGRAS12 acts as a positive regulator of meristem formation in Physcomitrium patens. *Plant Molecular Biology*, *107*(4–5), 293–305. https://doi.org/10.1007/s11103-021-01125-z

Bemm, F., Becker, D., Larisch, C., Kreuzer, I., Escalante-Perez, M., Schulze, W. X., Ankenbrand, M., Van de Weyer, A.-L., Krol, E., Al-Rasheid, K. A., Mithöfer, A., Weber, A. P., Schultz, J., & Hedrich, R. (2016). Venus flytrap carnivorous lifestyle builds on herbivore defense strategies. *Genome Research*, *26*(6), 812–825. https://doi.org/10.1101/gr.202200.115

Bielska, E., Sisquella, M. A., Aldeieg, M., Birch, C., O'Donoghue, E. J., & May, R. C. (2018). Pathogen-derived extracellular vesicles mediate virulence in the fatal human pathogen Cryptococcus gattii. *Nature Communications*, *9*(1), 1556. https://doi.org/10.1038/s41467-018-03991-6

Bigeard, J., Colcombet, J., & Hirt, H. (2015). Signaling Mechanisms in Pattern-Triggered Immunity (PTI). *Molecular Plant*, *8*(4), 521–539. https://doi.org/10.1016/j.molp.2014.12.022

Binder, A., Lambert, J., Morbitzer, R., Popp, C., Ott, T., Lahaye, T., & Parniske, M. (2014). A Modular Plasmid Assembly Kit for Multigene Expression, Gene Silencing and Silencing Rescue in Plants. *PLoS ONE*, *9*(2), e88218. https://doi.org/10.1371/journal.pone.0088218

Bleackley, M. R., Dawson, C. S., & Anderson, M. A. (2019). Fungal Extracellular Vesicles with a Focus on Proteomic Analysis. *PROTEOMICS*, *19*(8), 1800232. https://doi.org/10.1002/pmic.201800232

Bleackley, M. R., Samuel, M., Garcia-Ceron, D., McKenna, J. A., Lowe, R. G. T., Pathan, M., Zhao, K., Ang, C.-S., Mathivanan, S., & Anderson, M. A. (2020). Extracellular Vesicles From the Cotton Pathogen Fusarium oxysporum f. Sp. Vasinfectum Induce a Phytotoxic Response in Plants. *Frontiers in Plant Science*, *10*, 1610. https://doi.org/10.3389/fpls.2019.01610

Boddy, L. (2016). Pathogens of Autotrophs. In *The Fungi* (pp. 245–292). Elsevier. https://doi.org/10.1016/B978-0-12-382034-1.00008-6

Boevink, P. C. (2017). Exchanging missives and missiles: The roles of extracellular vesicles in plant–pathogen interactions. *Journal of Experimental Botany*, *68*(20), 5411–5414. https://doi.org/10.1093/jxb/erx369

Bologna, N. G., & Voinnet, O. (2014). The Diversity, Biogenesis, and Activities of Endogenous Silencing Small RNAs in *Arabidopsis*. *Annual Review of Plant Biology*, *65*(1), 473–503. https://doi.org/10.1146/annurev-arplant-050213-035728

Bolukbasi, M. F., Mizrak, A., Ozdener, G. B., Madlener, S., Ströbel, T., Erkan, E. P., Fan, J.-B., Breakefield, X. O., & Saydam, O. (2012). MiR-1289 and "Zipcode"-like Sequence Enrich mRNAs in Microvesicles. *Molecular Therapy - Nucleic Acids*, *1*, e10. https://doi.org/10.1038/mtna.2011.2

Bozkurt, T. O., & Kamoun, S. (2020). The plant–pathogen haustorial interface at a glance. *Journal of Cell Science*, *133*(5), jcs237958. https://doi.org/10.1242/jcs.237958

Brown, L., Wolf, J. M., Prados-Rosales, R., & Casadevall, A. (2015). Through the wall: Extracellular vesicles in Gram-positive bacteria, mycobacteria and fungi. *Nature Reviews Microbiology*, *13*(10), 620–630. https://doi.org/10.1038/nrmicro3480

Buck, A. H., Coakley, G., Simbari, F., McSorley, H. J., Quintana, J. F., Le Bihan, T., Kumar, S., Abreu-Goodger, C., Lear, M., Harcus, Y., Ceroni, A., Babayan, S. A., Blaxter, M., Ivens, A., & Maizels, R. M. (2014). Exosomes secreted by nematode parasites transfer small RNAs to mammalian cells and modulate innate immunity. *Nature Communications*, *5*(1), 5488. https://doi.org/10.1038/ncomms6488

Cai, Q., Qiao, L., Wang, M., He, B., Lin, F.-M., Palmquist, J., Huang, S.-D., & Jin, H. (2018). Plants send small RNAs in extracellular vesicles to fungal pathogen to silence virulence genes. *Science*, *360*(6393), 1126–1129. https://doi.org/10.1126/science.aar4142

Carthew, R. W., & Sontheimer, E. J. (2009). Origins and Mechanisms of miRNAs and siRNAs. *Cell*, *136*(4), 642–655. https://doi.org/10.1016/j.cell.2009.01.035

Chang, Y. C., Penoyer, L. A., & Kwon-Chung, K. J. (1996). The second capsule gene of cryptococcus neoformans, CAP64, is essential for virulence. *Infection and Immunity*, *64*(6), 1977–1983. https://doi.org/10.1128/iai.64.6.1977-1983.1996

Chen, D.-H., & Ronald, P. C. (1999). A rapid DNA minipreparation method suitable for AFLP and other PCR applications. *Plant Molecular Biology Reporter*, *17*(1), 53–57. https://doi.org/10.1023/A:1007585532036

Chen, H.-M., Chen, L.-T., Patel, K., Li, Y.-H., Baulcombe, D. C., & Wu, S.-H. (2010). 22-nucleotide RNAs trigger secondary siRNA biogenesis in plants. *Proceedings of the National Academy of Sciences*, *107*(34), 15269–15274. https://doi.org/10.1073/pnas.1001738107

Chen, Y., Li, G., & Liu, M.-L. (2018). Microvesicles as Emerging Biomarkers and Therapeutic Targets in Cardiometabolic Diseases. *Genomics, Proteomics & Bioinformatics*, *16*(1), 50–62. https://doi.org/10.1016/j.gpb.2017.03.006

Chiou, N.-T., Kageyama, R., & Ansel, K. M. (2018). Selective Export into Extracellular Vesicles and Function of tRNA Fragments during T Cell Activation. *Cell Reports*, *25*(12), 3356-3370.e4. https://doi.org/10.1016/j.celrep.2018.11.073

Choi, D.-S., Kim, D.-K., Kim, Y.-K., & Gho, Y. S. (2013). Proteomics, transcriptomics and lipidomics of exosomes and ectosomes. *PROTEOMICS*, *13*(10–11), 1554–1571. https://doi.org/10.1002/pmic.201200329

Chow, F. W.-N., Koutsovoulos, G., Ovando-Vázquez, C., Neophytou, K., Bermúdez-Barrientos, J. R., Laetsch, D. R., Robertson, E., Kumar, S., Claycomb, J. M., Blaxter, M., Abreu-Goodger, C., & Buck, A. H. (2019). Secretion of an Argonaute protein by a parasitic nematode and the evolution of its siRNA guides. *Nucleic Acids Research*, *47*(7), 3594–3606. https://doi.org/10.1093/nar/gkz142

Cleare, L. G., Zamith, D., Heyman, H. M., Couvillion, S. P., Nimrichter, L., Rodrigues, M. L., Nakayasu, E. S., & Nosanchuk, J. D. (2020). Media matters! Alterations in the loading and release of *Histoplasma capsulatum* extracellular vesicles in response to different nutritional milieus. *Cellular Microbiology*, *22*(9). https://doi.org/10.1111/cmi.13217

Cocucci, E., Racchetti, G., & Meldolesi, J. (2009). Shedding microvesicles: Artefacts no more. *Trends in Cell Biology*, *19*(2), 43–51. https://doi.org/10.1016/j.tcb.2008.11.003

Cohrs, K. C., Simon, A., Viaud, M., & Schumacher, J. (2016). Light governs asexual differentiation in the grey mould fungus *Botrytis cinerea* via the putative transcription factor BcLTF2: BcLTF2 regulates conidiation in *Botrytis cinerea*. *Environmental Microbiology*, *18*(11), 4068–4086. https://doi.org/10.1111/1462-2920.13431

Colombo, M., Raposo, G., & Théry, C. (2014). Biogenesis, Secretion, and Intercellular Interactions of Exosomes and Other Extracellular Vesicles. *Annual Review of Cell and Developmental Biology*, *30*(1), 255–289. https://doi.org/10.1146/annurev-cellbio-101512-122326

Costa, J. H., Bazioli, J. M., Barbosa, L. D., dos Santos Júnior, P. L. T., Reis, F. C. G., Klimeck, T., Crnkovic, C. M., Berlinck, R. G. S., Sussulini, A., Rodrigues, M. L., & Fill, T. P. (2021). Phytotoxic Tryptoquialanines Produced *In Vivo* by *Penicillium digitatum* Are Exported in Extracellular Vesicles. *MBio*, *12*(1), e03393-20. https://doi.org/10.1128/mBio.03393-20

Cui, C., Wang, Y., Liu, J., Zhao, J., Sun, P., & Wang, S. (2019). A fungal pathogen deploys a small silencing RNA that attenuates mosquito immunity and facilitates infection. *Nature Communications*, *10*(1), 4298. https://doi.org/10.1038/s41467-019-12323-1

Cui, H., Tsuda, K., & Parker, J. E. (2015). Effector-Triggered Immunity: From Pathogen Perception to Robust Defense. *Annual Review of Plant Biology*, *66*(1), 487–511. https://doi.org/10.1146/annurev-arplant-050213-040012

Cuomo, C. A., Güldener, U., Xu, J.-R., Trail, F., Turgeon, B. G., Di Pietro, A., Walton, J. D., Ma, L.-J., Baker, S. E., Rep, M., Adam, G., Antoniw, J., Baldwin, T., Calvo, S., Chang, Y.-L., DeCaprio, D., Gale, L. R., Gnerre, S., Goswami, R. S., … Kistler, H. C. (2007). The *Fusarium graminearum* Genome Reveals a Link Between Localized Polymorphism and Pathogen Specialization. *Science*, *317*(5843), 1400–1402.

https://doi.org/10.1126/science.1143708

Daboussi, M.-J., & Capy, P. (2003). Transposable Elements in Filamentous Fungi. *Annual Review of Microbiology*, *57*(1), 275–299. https://doi.org/10.1146/annurev.micro.57.030502.091029

Dai, X., Zhuang, Z., & Zhao, P. X. (2018). psRNATarget: A plant small RNA target analysis server (2017 release). *Nucleic Acids Research*, *46*(W1), W49–W54. https://doi.org/10.1093/nar/gky316

Dangl, J. L., & Jones, J. D. G. (2001). Plant pathogens and integrated defence responses to infection. *Nature*, *411*(6839), 826–833. https://doi.org/10.1038/35081161

De Wit, P. J. G. M., Mehrabi, R., Van Den Burg, H. A., & Stergiopoulos, I. (2009). Fungal effector proteins: Past, present and future. *Molecular Plant Pathology*, *10*(6), 735–747. https://doi.org/10.1111/j.1364-3703.2009.00591.x

Dean, R., Van Kan, J. A. L., Pretorius, Z. A., Hammond-Kosack, K. E., Di Pietro, A., Spanu, P. D., Rudd, J. J., Dickman, M., Kahmann, R., Ellis, J., & Foster, G. D. (2012). The Top 10 fungal pathogens in molecular plant pathology: Top 10 fungal pathogens. *Molecular Plant Pathology*, *13*(4), 414–430. https://doi.org/10.1111/j.1364-3703.2011.00783.x

Deatherage, B. L., & Cookson, B. T. (2012). Membrane Vesicle Release in Bacteria, Eukaryotes, and Archaea: A Conserved yet Underappreciated Aspect of Microbial Life. *Infection and Immunity*, *80*(6), 1948–1957. https://doi.org/10.1128/IAI.06014-11

Dobin, A., Davis, C. A., Schlesinger, F., Drenkow, J., Zaleski, C., Jha, S., Batut, P., Chaisson, M., & Gingeras, T. R. (2013). STAR: Ultrafast universal RNA-seq aligner. *Bioinformatics*, *29*(1), 15–21. https://doi.org/10.1093/bioinformatics/bts635

Dong, S., Raffaele, S., & Kamoun, S. (2015). The two-speed genomes of filamentous pathogens: Waltz with plants. *Current Opinion in Genetics & Development*, *35*, 57–65. https://doi.org/10.1016/j.gde.2015.09.001

Dragovic, R. A., Gardiner, C., Brooks, A. S., Tannetta, D. S., Ferguson, D. J. P., Hole, P., Carr, B., Redman, C. W. G., Harris, A. L., Dobson, P. J., Harrison, P., & Sargent, I. L. (2011). Sizing and phenotyping of cellular vesicles using Nanoparticle Tracking Analysis. *Nanomedicine: Nanotechnology, Biology and Medicine*, *7*(6), 780–788. https://doi.org/10.1016/j.nano.2011.04.003

Dubin, M. J., Mittelsten Scheid, O., & Becker, C. (2018). Transposons: A blessing curse. *Current Opinion in Plant Biology*, *42*, 23–29. https://doi.org/10.1016/j.pbi.2018.01.003

Dunker, F., Trutzenberg, A., Rothenpieler, J. S., Kuhn, S., Pröls, R., Schreiber, T., Tissier, A., Kemen, A., Kemen, E., Hückelhoven, R., & Weiberg, A. (2020). Oomycete small RNAs bind to the plant RNA-induced silencing complex for virulence. *ELife*, *9*, e56096. https://doi.org/10.7554/eLife.56096

Elsharkasy, O. M., Nordin, J. Z., Hagey, D. W., de Jong, O. G., Schiffelers, R. M., Andaloussi, S. E., & Vader, P. (2020). Extracellular vesicles as drug delivery systems: Why and how? *Advanced Drug Delivery Reviews*, *159*, 332–343. https://doi.org/10.1016/j.addr.2020.04.004

Feldmesser, M., Kress, Y., Novikoff, P., & Casadevall, A. (2000). *Cryptococcus neoformans* Is a Facultative Intracellular Pathogen in Murine Pulmonary Infection. *Infection and Immunity*, *68*(7), 4225–4237. https://doi.org/10.1128/IAI.68.7.4225-4237.2000

Finkemeier, I., Goodman, M., Lamkemeyer, P., Kandlbinder, A., Sweetlove, L. J., & Dietz, K.-J. (2005). The Mitochondrial Type II Peroxiredoxin F Is Essential for Redox Homeostasis and Root Growth of Arabidopsis thaliana under Stress. *Journal of Biological Chemistry*, *280*(13), 12168–12180. https://doi.org/10.1074/jbc.M413189200

Fire, A., Xu, S., Montgomery, M. K., Kostas, S. A., Driver, S. E., & Mello, C. C. (1998). Potent and specific genetic interference by double-stranded RNA in Caenorhabditis elegans. *Nature*, *391*(6669), 806–811. https://doi.org/10.1038/35888

Flutre, T., Duprat, E., Feuillet, C., & Quesneville, H. (2011). Considering Transposable Element Diversification in De Novo Annotation Approaches. *PLoS ONE*, *6*(1), e16526. https://doi.org/10.1371/journal.pone.0016526

Fouché, S., Badet, T., Oggenfuss, U., Plissonneau, C., Francisco, C. S., & Croll, D. (2020). Stress-Driven Transposable Element De-repression Dynamics and Virulence Evolution in a Fungal Pathogen. *Molecular Biology and Evolution*, *37*(1), 221–239. https://doi.org/10.1093/molbev/msz216

Fournier, E., & Giraud, T. (2008). Sympatric genetic differentiation of a generalist pathogenic fungus, *Botrytis cinerea* , on two different host plants, grapevine and bramble: Sympatric genetic differentiation. *Journal of Evolutionary Biology*, *21*(1), 122–132. https://doi.org/10.1111/j.1420-9101.2007.01462.x

Frankel, E. B., & Audhya, A. (2018). ESCRT-dependent cargo sorting at multivesicular endosomes. *Seminars in Cell & Developmental Biology*, *74*, 4–10. https://doi.org/10.1016/j.semcdb.2017.08.020

Frantzeskakis, L., Kracher, B., Kusch, S., Yoshikawa-Maekawa, M., Bauer, S., Pedersen, C., Spanu, P. D., Maekawa, T., Schulze-Lefert, P., & Panstruga, R. (2018). Signatures of host specialization and a recent transposable element burst in the dynamic one-speed genome of the fungal barley powdery mildew pathogen. *BMC Genomics*, *19*(1), 381. https://doi.org/10.1186/s12864-018-4750-6

Galagan, J. E., & Selker, E. U. (2004). RIP: The evolutionary cost of genome defense. *Trends in Genetics*, *20*(9), 417–423. https://doi.org/10.1016/j.tig.2004.07.007

Galiana, E., Bonnet, P., Conrod, S., Keller, H., Panabieres, F., Ponchet, M., Poupet, A., & Ricci, P. (1997). RNase Activity Prevents the Growth of a Fungal Pathogen in Tobacco Leaves and Increases upon Induction of Systemic Acquired Resistance with Elicitin. *Plant Physiology*, *115*(4), 1557–1567. https://doi.org/10.1104/pp.115.4.1557

Gámbaro, F., Li Calzi, M., Fagúndez, P., Costa, B., Greif, G., Mallick, E., Lyons, S., Ivanov, P., Witwer, K., Cayota, A., & Tosar, J. P. (2020). Stable tRNA halves can be sorted into extracellular vesicles and delivered to recipient cells in a concentration-dependent manner. *RNA Biology*, *17*(8), 1168–1182. https://doi.org/10.1080/15476286.2019.1708548

Garcia-Ceron, D., Lowe, R. G. T., McKenna, J. A., Brain, L. M., Dawson, C. S., Clark, B., Berkowitz, O., Faou, P., Whelan, J., Bleackley, M. R., & Anderson, M. A. (2021). Extracellular Vesicles from Fusarium graminearum Contain Protein Effectors Expressed during Infection of Corn. *Journal of Fungi*, *7*(11), 977. https://doi.org/10.3390/jof7110977

Ge, S. X., Son, E. W., & Yao, R. (2018). iDEP: An integrated web application for differential expression and pathway analysis of RNA-Seq data. *BMC Bioinformatics*, *19*(1), 534. https://doi.org/10.1186/s12859-018-2486-6

Gehrmann, U., Qazi, K. R., Johansson, C., Hultenby, K., Karlsson, M., Lundeberg, L., Gabrielsson, S., & Scheynius, A. (2011). Nanovesicles from Malassezia sympodialis and Host Exosomes Induce Cytokine Responses – Novel Mechanisms for Host-Microbe Interactions in Atopic Eczema. *PLoS ONE*, *6*(7), e21480. https://doi.org/10.1371/journal.pone.0021480

Gellert, M. (2002). V(D)J Recombination: RAG Proteins, Repair Factors, and Regulation. *Annual Review of Biochemistry*, *71*(1), 101–132. https://doi.org/10.1146/annurev.biochem.71.090501.150203

Giardine, B., Riemer, C., Hardison, R. C., Burhans, R., Elnitski, L., Shah, P., Zhang, Y., Blankenberg, D., Albert, I., Taylor, J., Miller, W., Kent, W. J., & Nekrutenko, A. (2005). Galaxy: A platform for interactive large-scale genome analysis. *Genome Research*, *15*(10), 1451–1455. https://doi.org/10.1101/gr.4086505

Gimenez-Ibanez, S., Hann, D. R., Ntoukakis, V., Petutschnig, E., Lipka, V., & Rathjen, J. P. (2009). AvrPtoB Targets the LysM Receptor Kinase CERK1 to Promote Bacterial Virulence on Plants. *Current Biology*, *19*(5), 423–429. https://doi.org/10.1016/j.cub.2009.01.054

Giraud, T., Fortini, D., Levis, C., Leroux, P., & Brygoo, Y. (1997). RFLP markers show genetic recombination in Botryotinia fuckeliana (Botrytis cinerea) and transposable elements reveal two sympatric species. *Molecular Biology and Evolution*, *14*(11), 1177–1185. https://doi.org/10.1093/oxfordjournals.molbev.a025727

Gladyshev, E. (2017). Repeat-Induced Point Mutation and Other Genome Defense Mechanisms in Fungi. *Microbiology Spectrum*, *5*(4). https://doi.org/10.1128/microbiolspec.FUNK-0042-2017

Glazebrook, J. (2005). Contrasting Mechanisms of Defense Against Biotrophic and Necrotrophic Pathogens. *Annual Review of Phytopathology*, *43*(1), 205–227. https://doi.org/10.1146/annurev.phyto.43.040204.135923

Gourgues, M., Brunet-Simon, A., Lebrun, M.-H., & Levis, C. (2003). The tetraspanin BcPls1 is required for appressorium-mediated penetration of Botrytis cinerea into host plant leaves: Botrytis tetraspanin. *Molecular Microbiology*, *51*(3), 619–629. https://doi.org/10.1046/j.1365-2958.2003.03866.x

Gu, Z., Gu, L., Eils, R., Schlesner, M., & Brors, B. (2014). Circlize implements and enhances circular visualization in R. *Bioinformatics*, *30*(19), 2811–2812. https://doi.org/10.1093/bioinformatics/btu393

Hane, J. K., & Oliver, R. P. (2008). RIPCAL: A tool for alignment-based analysis of repeat-induced point mutations in fungal genomic sequences. *BMC Bioinformatics*, *9*(1), 478. https://doi.org/10.1186/1471-2105-9-478

Havecker, E. R., Gao, X., & Voytas, D. F. (2004). The diversity of LTR retrotransposons. *Genome Biology*, *5*(6), 225. https://doi.org/10.1186/gb-2004-5-6-225

He, B., Cai, Q., Qiao, L., Huang, C.-Y., Wang, S., Miao, W., Ha, T., Wang, Y., & Jin, H. (2021). RNA-binding proteins contribute to small RNA loading in plant extracellular vesicles. *Nature Plants*, *7*(3), 342–352. https://doi.org/10.1038/s41477-021-00863-8

Hevia, M. A., Canessa, P., Müller-Esparza, H., & Larrondo, L. F. (2015). A circadian oscillator in the fungus *Botrytis cinerea* regulates virulence when infecting *Arabidopsis thaliana*. *Proceedings of the National Academy of Sciences*, *112*(28), 8744–8749. https://doi.org/10.1073/pnas.1508432112

Hill, E. H., & Solomon, P. S. (2020). Extracellular vesicles from the apoplastic fungal wheat pathogen Zymoseptoria tritici. *Fungal Biology and Biotechnology*, *7*(1), 13. https://doi.org/10.1186/s40694-020-00103-2

Hou, Y., Zhai, Y., Feng, L., Karimi, H. Z., Rutter, B. D., Zeng, L., Choi, D. S., Zhang, B., Gu, W., Chen, X., Ye, W., Innes, R. W., Zhai, J., & Ma, W. (2019). A Phytophthora Effector Suppresses Trans-Kingdom RNAi to Promote Disease Susceptibility. *Cell Host & Microbe*, *25*(1), 153-165.e5. https://doi.org/10.1016/j.chom.2018.11.007

Huang, J., Si, W., Deng, Q., Li, P., & Yang, S. (2014). Rapid evolution of avirulence genes in rice blast fungus Magnaporthe oryzae. *BMC Genetics*, *15*(1), 45. https://doi.org/10.1186/1471-2156-15-45

Hugot, K., Ponchet, M., Marais, A., Ricci, P., & Galiana, E. (2002). A Tobacco S-like RNase Inhibits Hyphal Elongation of Plant Pathogens. *Molecular Plant-Microbe Interactions®*, *15*(3), 243–250. https://doi.org/10.1094/MPMI.2002.15.3.243

Hurley, J. H. (2015). ESCRT s are everywhere. *The EMBO Journal*, *34*(19), 2398–2407. https://doi.org/10.15252/embj.201592484

Ikeda, M. A. K., de Almeida, J. R. F., Jannuzzi, G. P., Cronemberger-Andrade, A., Torrecilhas, A. C. T., Moretti, N. S., da Cunha, J. P. C., de Almeida, S. R., & Ferreira, K. S. (2018). Extracellular Vesicles From Sporothrix brasiliensis Are an Important Virulence Factor That Induce an Increase in Fungal Burden in Experimental Sporotrichosis. *Frontiers in Microbiology*, *9*, 2286. https://doi.org/10.3389/fmicb.2018.02286

Janas, T., Janas, M. M., Sapoń, K., & Janas, T. (2015). Mechanisms of RNA loading into exosomes. *FEBS Letters*, *589*(13), 1391–1398. https://doi.org/10.1016/j.febslet.2015.04.036

Jangam, D., Feschotte, C., & Betrán, E. (2017). Transposable Element Domestication As an Adaptation to Evolutionary Conflicts. *Trends in Genetics*, *33*(11), 817–831. https://doi.org/10.1016/j.tig.2017.07.011

Jedlicka, P., Lexa, M., & Kejnovsky, E. (2020). What Can Long Terminal Repeats Tell Us About the Age of LTR Retrotransposons, Gene Conversion and Ectopic Recombination? *Frontiers in Plant Science*, *11*, 644. https://doi.org/10.3389/fpls.2020.00644

Jian, J., & Liang, X. (2019). One Small RNA of Fusarium graminearum Targets and Silences CEBiP Gene in Common Wheat. *Microorganisms*, *7*(10), 425. https://doi.org/10.3390/microorganisms7100425

Jiang, Y., & Yu, D. (2016). The WRKY57 Transcription Factor Affects the Expression of Jasmonate ZIM-Domain Genes Transcriptionally to Compromise *Botrytis cinerea* Resistance. *Plant Physiology*, *171*(4), 2771–2782. https://doi.org/10.1104/pp.16.00747

Jones, J. D. G., & Dangl, J. L. (2006). The plant immune system. *Nature*, *444*(7117), 323–329. https://doi.org/10.1038/nature05286

Kakarla, R., Hur, J., Kim, Y. J., Kim, J., & Chwae, Y.-J. (2020). Apoptotic cell-derived exosomes: Messages from dying cells. *Experimental & Molecular Medicine*, *52*(1), 1–6. https://doi.org/10.1038/s12276-019-0362-8

Kaletta, J., Pickl, C., Griebler, C., Klingl, A., Kurmayer, R., & Deng, L. (2020). A rigorous assessment and comparison of enumeration methods for environmental viruses. *Scientific Reports*, *10*(1), 18625.

https://doi.org/10.1038/s41598-020-75490-y

Kars, I., & van Kan, J. A. L. (2007). Extracellular Enzymes and Metabolites Involved in Pathogenesis of Botrytis. In Y. Elad, B. Williamson, P. Tudzynski, & N. Delen (Eds.), *Botrytis: Biology, Pathology and Control* (pp. 99–118). Springer Netherlands. https://doi.org/10.1007/978-1-4020-2626-3_7

Krupovic, M., Makarova, K. S., Forterre, P., Prangishvili, D., & Koonin, E. V. (2014). Casposons: A new superfamily of self-synthesizing DNA transposons at the origin of prokaryotic CRISPR-Cas immunity. *BMC Biology*, *12*(1), 36. https://doi.org/10.1186/1741-7007-12-36

Krzywinski, M., Schein, J., Birol, İ., Connors, J., Gascoyne, R., Horsman, D., Jones, S. J., & Marra, M. A. (2009). Circos: An information aesthetic for comparative genomics. *Genome Research*, *19*(9), 1639–1645. https://doi.org/10.1101/gr.092759.109

Kwon, S., Rupp, O., Brachmann, A., Blum, C. F., Kraege, A., Goesmann, A., & Feldbrügge, M. (2021). MRNA Inventory of Extracellular Vesicles from Ustilago maydis. *Journal of Fungi*, *7*(7), 562. https://doi.org/10.3390/jof7070562

Kwon, S., Tisserant, C., Tulinski, M., Weiberg, A., & Feldbrügge, M. (2020). Inside-out: From endosomes to extracellular vesicles in fungal RNA transport. *Fungal Biology Reviews*, *34*(2), 89–99. https://doi.org/10.1016/j.fbr.2020.01.001

Lambou, K., Tharreau, D., Kohler, A., Sirven, C., Marguerettaz, M., Barbisan, C., Sexton, A. C., Kellner, E. M., Martin, F., Howlett, B. J., Orbach, M. J., & Lebrun, M.-H. (2008). Fungi have three tetraspanin families with distinct functions. *BMC Genomics*, *9*(1), 63. https://doi.org/10.1186/1471-2164-9-63

Langmead, B., & Salzberg, S. L. (2012). Fast gapped-read alignment with Bowtie 2. *Nature Methods*, *9*(4), 357–359. https://doi.org/10.1038/nmeth.1923

Leal, J. A., Rupérez, P., & Gomez-Miranda, B. (1979). Extracellular glucan production by Botrytis cinerea. *Transactions of the British Mycological Society*, *72*(1), 172–176. https://doi.org/10.1016/S0007-1536(79)80026-1

Lefebvre, F. A., & Lécuyer, E. (2017). Small Luggage for a Long Journey: Transfer of Vesicle-Enclosed Small RNA in Interspecies Communication. *Frontiers in Microbiology*, *8*. https://doi.org/10.3389/fmicb.2017.00377

Li, L., Chang, S., & Liu, Y. (2010). RNA interference pathways in filamentous fungi. *Cellular and Molecular Life Sciences*, *67*(22), 3849–3863. https://doi.org/10.1007/s00018-010-0471-y

Li, P., Kaslan, M., Lee, S. H., Yao, J., & Gao, Z. (2017). Progress in Exosome Isolation Techniques. *Theranostics*, *7*(3), 789–804. https://doi.org/10.7150/thno.18133

Li, Z., & Stanton, B. A. (2021). Transfer RNA-Derived Fragments, the Underappreciated Regulatory Small RNAs in Microbial Pathogenesis. *Frontiers in Microbiology*, *12*, 687632. https://doi.org/10.3389/fmicb.2021.687632

Livak, K. J., & Schmittgen, T. D. (2001). Analysis of Relative Gene Expression Data Using Real-Time Quantitative PCR and the 2−ΔΔCT Method. *Methods*, *25*(4), 402–408. https://doi.org/10.1006/meth.2001.1262

Llorens, C., Muñoz-Pomer, A., Bernad, L., Botella, H., & Moya, A. (2009). Network dynamics of eukaryotic LTR retroelements beyond phylogenetic trees. *Biology Direct*, *4*(1), 41. https://doi.org/10.1186/1745-6150-4-41

Llorente, F., Muskett, P., Sánchez-Vallet, A., López, G., Ramos, B., Sánchez-Rodríguez, C., Jordá, L., Parker, J., & Molina, A. (2008). Repression of the Auxin Response Pathway Increases Arabidopsis Susceptibility to Necrotrophic Fungi. *Molecular Plant*, *1*(3), 496–509. https://doi.org/10.1093/mp/ssn025

Lorrain, C., Feurtey, A., Möller, M., Haueisen, J., & Stukenbrock, E. (2021). Dynamics of transposable elements in recently diverged fungal pathogens: Lineage-specific transposable element content and efficiency of genome defenses. *G3 Genes|Genomes|Genetics*, *11*(4), jkab068. https://doi.org/10.1093/g3journal/jkab068

Lötvall, J., Hill, A. F., Hochberg, F., Buzás, E. I., Di Vizio, D., Gardiner, C., Gho, Y. S., Kurochkin, I. V., Mathivanan, S., Quesenberry, P., Sahoo, S., Tahara, H., Wauben, M. H., Witwer, K. W., & Théry, C. (2014). Minimal experimental requirements for definition of extracellular vesicles and their functions: A position statement from the International Society for Extracellular Vesicles. *Journal of Extracellular*

Vesicles, *3*(1), 26913. https://doi.org/10.3402/jev.v3.26913

Lu, S., Wang, J., Chitsaz, F., Derbyshire, M. K., Geer, R. C., Gonzales, N. R., Gwadz, M., Hurwitz, D. I., Marchler, G. H., Song, J. S., Thanki, N., Yamashita, R. A., Yang, M., Zhang, D., Zheng, C., Lanczycki, C. J., & Marchler-Bauer, A. (2020). CDD/SPARCLE: The conserved domain database in 2020. *Nucleic Acids Research*, *48*(D1), D265–D268. https://doi.org/10.1093/nar/gkz991

Ma, L.-J., & Fedorova, N. D. (2010). A practical guide to fungal genome projects: Strategy, technology, cost and completion. *Mycology*, *1*(1), 9–24. https://doi.org/10.1080/21501201003680943

Maas, J. L., & Powelson, R. L. (1972). Growth and Sporulation of Botrytis Convoluta with Various Carbon and Nitrogen Sources. *Mycologia*, *64*(4), 897. https://doi.org/10.2307/3757944

Maas, S. L. N., Breakefield, X. O., & Weaver, A. M. (2017). Extracellular Vesicles: Unique Intercellular Delivery Vehicles. *Trends in Cell Biology*, *27*(3), 172–188. https://doi.org/10.1016/j.tcb.2016.11.003

Magee, R., & Rigoutsos, I. (2020). On the expanding roles of tRNA fragments in modulating cell behavior. *Nucleic Acids Research*, *48*(17), 9433–9448. https://doi.org/10.1093/nar/gkaa657

Makałowski, W., Gotea, V., Pande, A., & Makałowska, I. (2019). Transposable Elements: Classification, Identification, and Their Use As a Tool For Comparative Genomics. In M. Anisimova (Ed.), *Evolutionary Genomics* (Vol. 1910, pp. 177–207). Springer New York. https://doi.org/10.1007/978-1-4939-9074-0_6

Manavella, P. A., Koenig, D., & Weigel, D. (2012). Plant secondary siRNA production determined by microRNA-duplex structure. *Proceedings of the National Academy of Sciences*, *109*(7), 2461–2466. https://doi.org/10.1073/pnas.1200169109

Maori, E., Navarro, I. C., Boncristiani, H., Seilly, D. J., Rudolph, K. L. M., Sapetschnig, A., Lin, C.-C., Ladbury, J. E., Evans, J. D., Heeney, J. L., & Miska, E. A. (2019). A Secreted RNA Binding Protein Forms RNA-Stabilizing Granules in the Honeybee Royal Jelly. *Molecular Cell*, *74*(3), 598-608.e6. https://doi.org/10.1016/j.molcel.2019.03.010

Margolin, B. S., Garrett-Engele, P. W., Stevens, J. N., Fritz, D. Y., Garrett-Engele, C., Metzenberg, R. L., & Selker, E. U. (1998). A Methylated Neurospora 5S rRNA Pseudogene Contains a Transposable Element Inactivated by Repeat-Induced Point Mutation. *Genetics*, *149*(4), 1787–1797. https://doi.org/10.1093/genetics/149.4.1787

Marí-Ordóñez, A., Marchais, A., Etcheverry, M., Martin, A., Colot, V., & Voinnet, O. (2013). Reconstructing de novo silencing of an active plant retrotransposon. *Nature Genetics*, *45*(9), 1029–1039. https://doi.org/10.1038/ng.2703

Martinez, F., Blancard, D., Lecomte, P., Levis, C., Dubos, B., & Fermaud, M. (2003). Phenotypic differences between vacuma and transposa subpopulations of Botrytis cinerea. *European Journal of Plant Pathology*, *109*(5), 479–488. https://doi.org/10.1023/A:1024222206991

Martinez, F., Dubos, B., & Fermaud, M. (2005). The Role of Saprotrophy and Virulence in the Population Dynamics of *Botrytis cinerea* in Vineyards. *Phytopathology®*, *95*(6), 692–700. https://doi.org/10.1094/PHYTO-95-0692

Mat Razali, N., Cheah, B. H., & Nadarajah, K. (2019). Transposable Elements Adaptive Role in Genome Plasticity, Pathogenicity and Evolution in Fungal Phytopathogens. *International Journal of Molecular Sciences*, *20*(14), E3597. https://doi.org/10.3390/ijms20143597

Mattei, B., França, A. D. C., & Riske, K. A. (2015). Solubilization of Binary Lipid Mixtures by the Detergent Triton X-100: The Role of Cholesterol. *Langmuir*, *31*(1), 378–386. https://doi.org/10.1021/la504004r

McClintock, B. (1950). The origin and behavior of mutable loci in maize. *Proceedings of the National Academy of Sciences*, *36*(6), 344–355. https://doi.org/10.1073/pnas.36.6.344

McDowell, J. M., & Dangl, J. L. (2000). Signal transduction in the plant immune response. *Trends in Biochemical Sciences*, *25*(2), 79–82. https://doi.org/10.1016/S0968-0004(99)01532-7

Meldolesi, J. (2018). Exosomes and Ectosomes in Intercellular Communication. *Current Biology*, *28*(8), R435–R444. https://doi.org/10.1016/j.cub.2018.01.059

Mi, S., Cai, T., Hu, Y., Chen, Y., Hodges, E., Ni, F., Wu, L., Li, S., Zhou, H., Long, C., Chen, S., Hannon, G. J., & Qi, Y. (2008). Sorting of Small RNAs into Arabidopsis Argonaute Complexes Is Directed by the 5′ Terminal Nucleotide. *Cell*, *133*(1), 116–127. https://doi.org/10.1016/j.cell.2008.02.034

Micali, C. O., Neumann, U., Grunewald, D., Panstruga, R., & O'Connell, R. (2011). Biogenesis of a specialized plant-fungal interface during host cell internalization of Golovinomyces orontii haustoria: Plant-fungal interface around powdery mildew haustoria. *Cellular Microbiology*, *13*(2), 210–226. https://doi.org/10.1111/j.1462-5822.2010.01530.x

Mims, C. W., & Richardson, E. A. (2004). Ultrastructure of Haustoria of Plant Pathogenic Fungi. *Microscopy and Microanalysis*, *10*(S02), 1442–1443. https://doi.org/10.1017/S1431927604880747

Minciacchi, V. R., Freeman, M. R., & Di Vizio, D. (2015). Extracellular Vesicles in Cancer: Exosomes, Microvesicles and the Emerging Role of Large Oncosomes. *Seminars in Cell & Developmental Biology*, *40*, 41–51. https://doi.org/10.1016/j.semcdb.2015.02.010

Mir, B., & Goettsch, C. (2020). Extracellular Vesicles as Delivery Vehicles of Specific Cellular Cargo. *Cells*, *9*(7), 1601. https://doi.org/10.3390/cells9071601

Monguió-Tortajada, M., Gálvez-Montón, C., Bayes-Genis, A., Roura, S., & Borràs, F. E. (2019). Extracellular vesicle isolation methods: Rising impact of size-exclusion chromatography. *Cellular and Molecular Life Sciences*, *76*(12), 2369–2382. https://doi.org/10.1007/s00018-019-03071-y

Müller, N., Leroch, M., Schumacher, J., Zimmer, D., Könnel, A., Klug, K., Leisen, T., Scheuring, D., Sommer, F., Mühlhaus, T., Schroda, M., & Hahn, M. (2018). Investigations on VELVET regulatory mutants confirm the role of host tissue acidification and secretion of proteins in the pathogenesis of *Botrytis cinerea*. *New Phytologist*, *219*(3), 1062–1074. https://doi.org/10.1111/nph.15221

Murata, T., Kadotani, N., Yamaguchi, M., Tosa, Y., Mayama, S., & Nakayashiki, H. (2007). SiRNA-dependent and -independent post-transcriptional cosuppression of the LTR-retrotransposon MAGGY in the phytopathogenic fungus Magnaporthe oryzae. *Nucleic Acids Research*, *35*(18), 5987–5994. https://doi.org/10.1093/nar/gkm646

Nakajima, M., & Akutsu, K. (2014). Virulence factors of Botrytis cinerea. *Journal of General Plant Pathology*, *80*(1), 15–23. https://doi.org/10.1007/s10327-013-0492-0

Nefedova, L., & Kim, A. (2017). Mechanisms of LTR‐Retroelement Transposition: Lessons from Drosophila melanogaster. *Viruses*, *9*(4), 81. https://doi.org/10.3390/v9040081

Ngou, B. P. M., Ahn, H.-K., Ding, P., & Jones, J. D. G. (2021). Mutual potentiation of plant immunity by cell-surface and intracellular receptors. *Nature*. https://doi.org/10.1038/s41586-021-03315-7

Nimrichter, L., de Souza, M. M., Del Poeta, M., Nosanchuk, J. D., Joffe, L., Tavares, P. de M., & Rodrigues, M. L. (2016). Extracellular Vesicle-Associated Transitory Cell Wall Components and Their Impact on the Interaction of Fungi with Host Cells. *Frontiers in Microbiology*, *7*. https://doi.org/10.3389/fmicb.2016.01034

Nowara, D., Gay, A., Lacomme, C., Shaw, J., Ridout, C., Douchkov, D., Hensel, G., Kumlehn, J., & Schweizer, P. (2010). HIGS: Host-Induced Gene Silencing in the Obligate Biotrophic Fungal Pathogen *Blumeria graminis*. *The Plant Cell*, *22*(9), 3130–3141. https://doi.org/10.1105/tpc.110.077040

Oliveira, D. L., Nakayasu, E. S., Joffe, L. S., Guimarães, A. J., Sobreira, T. J. P., Nosanchuk, J. D., Cordero, R. J. B., Frases, S., Casadevall, A., Almeida, I. C., Nimrichter, L., & Rodrigues, M. L. (2010). Characterization of Yeast Extracellular Vesicles: Evidence for the Participation of Different Pathways of Cellular Traffic in Vesicle Biogenesis. *PLoS ONE*, *5*(6), e11113. https://doi.org/10.1371/journal.pone.0011113

Oliveira, D., Rizzo, J., Joffe, L., Godinho, R., & Rodrigues, M. (2013). Where Do They Come from and Where Do They Go: Candidates for Regulating Extracellular Vesicle Formation in Fungi. *International Journal of Molecular Sciences*, *14*(5), 9581–9603. https://doi.org/10.3390/ijms14059581

Osteikoetxea, X., Sódar, B., Németh, A., Szabó-Taylor, K., Pálóczi, K., Vukman, K. V., Tamási, V., Balogh, A., Kittel, Á., Pállinger, É., & Buzás, E. I. (2015). Differential detergent sensitivity of extracellular vesicle subpopulations. *Organic & Biomolecular Chemistry*, *13*(38), 9775–9782. https://doi.org/10.1039/C5OB01451D

Pachulska-Wieczorek, K., Le Grice, S., & Purzycka, K. (2016). Determinants of Genomic RNA Encapsidation in the Saccharomyces cerevisiae Long Terminal Repeat Retrotransposons Ty1 and Ty3. *Viruses*, *8*(7), 193. https://doi.org/10.3390/v8070193

Pandey, K. K., Madhry, D., Ravi Kumar, Y. S., Malvankar, S., Sapra, L., Srivastava, R. K., Bhattacharyya, S., &

Verma, B. (2021). Regulatory roles of tRNA-derived RNA fragments in human pathophysiology. *Molecular Therapy - Nucleic Acids*, *26*, 161–173. https://doi.org/10.1016/j.omtn.2021.06.023

Panepinto, J., Komperda, K., Frases, S., Park, Y.-D., Djordjevic, J. T., Casadevall, A., & Williamson, P. R. (2009). Sec6-dependent sorting of fungal extracellular exosomes and laccase of *Cryptococcus neoformans*. *Molecular Microbiology*, *71*(5), 1165–1176. https://doi.org/10.1111/j.1365-2958.2008.06588.x

Pardo, F., Villalobos-Labra, R., Sobrevia, B., Toledo, F., & Sobrevia, L. (2018). Extracellular vesicles in obesity and diabetes mellitus. *Molecular Aspects of Medicine*, *60*, 81–91. https://doi.org/10.1016/j.mam.2017.11.010

Parekh, S., Ziegenhain, C., Vieth, B., Enard, W., & Hellmann, I. (2018). zUMIs—A fast and flexible pipeline to process RNA sequencing data with UMIs. *GigaScience*, *7*(6). https://doi.org/10.1093/gigascience/giy059

Patel, G. K., Khan, M. A., Zubair, H., Srivastava, S. K., Khushman, M., Singh, S., & Singh, A. P. (2019). Comparative analysis of exosome isolation methods using culture supernatant for optimum yield, purity and downstream applications. *Scientific Reports*, *9*(1), 5335. https://doi.org/10.1038/s41598-019-41800-2

Peres da Silva, R., Longo, L. G. V., Cunha, J. P. C. da, Sobreira, T. J. P., Rodrigues, M. L., Faoro, H., Goldenberg, S., Alves, L. R., & Puccia, R. (2019). Comparison of the RNA Content of Extracellular Vesicles Derived from Paracoccidioides brasiliensis and Paracoccidioides lutzii. *Cells*, *8*(7), 765. https://doi.org/10.3390/cells8070765

Peres da Silva, R., Puccia, R., Rodrigues, M. L., Oliveira, D. L., Joffe, L. S., César, G. V., Nimrichter, L., Goldenberg, S., & Alves, L. R. (2015). Extracellular vesicle-mediated export of fungal RNA. *Scientific Reports*, *5*(1), 7763. https://doi.org/10.1038/srep07763

Pielken, P., Stahmann, P., & Sahm, H. (1990). Increase in glucan formation by Botrytis cinerea and analysis of the adherent glucan. *Applied Microbiology and Biotechnology*, *33*(1). https://doi.org/10.1007/BF00170559

Pinedo, M., Regente, M., Elizalde, M., Y. Quiroga, I., A. Pagnussat, L., Jorrin-Novo, J., Maldonado, A., & de la Canal, L. (2012). Extracellular Sunflower Proteins: Evidence on Non-classical Secretion of a Jacalin-Related Lectin. *Protein & Peptide Letters*, *19*(3), 270–276. https://doi.org/10.2174/092986612799363163

Plissonneau, C., Benevenuto, J., Mohd-Assaad, N., Fouché, S., Hartmann, F. E., & Croll, D. (2017). Using Population and Comparative Genomics to Understand the Genetic Basis of Effector-Driven Fungal Pathogen Evolution. *Frontiers in Plant Science*, *8*. https://doi.org/10.3389/fpls.2017.00119

Porquier, A., Morgant, G., Moraga, J., Dalmais, B., Luyten, I., Simon, A., Pradier, J.-M., Amselem, J., Collado, I. G., & Viaud, M. (2016). The botrydial biosynthetic gene cluster of Botrytis cinerea displays a bipartite genomic structure and is positively regulated by the putative Zn(II)2Cys6 transcription factor BcBot6. *Fungal Genetics and Biology*, *96*, 33–46. https://doi.org/10.1016/j.fgb.2016.10.003

Porquier, A., Tisserant, C., Salinas, F., Glassl, C., Wange, L., Enard, W., Hauser, A., Hahn, M., & Weiberg, A. (2021). Retrotransposons as pathogenicity factors of the plant pathogenic fungus Botrytis cinerea. *Genome Biology*, *22*(1), 225. https://doi.org/10.1186/s13059-021-02446-4

Qiao, L., Lan, C., Capriotti, L., Ah‐Fong, A., Nino Sanchez, J., Hamby, R., Heller, J., Zhao, H., Glass, N. L., Judelson, H. S., Mezzetti, B., Niu, D., & Jin, H. (2021). Spray‐induced gene silencing for disease control is dependent on the efficiency of pathogen RNA uptake. *Plant Biotechnology Journal*, *19*(9), 1756–1768. https://doi.org/10.1111/pbi.13589

Raffaele, S., & Kamoun, S. (2012). Genome evolution in filamentous plant pathogens: Why bigger can be better. *Nature Reviews Microbiology*, *10*(6), 417–430. https://doi.org/10.1038/nrmicro2790

Raman, V., Simon, S. A., Romag, A., Demirci, F., Mathioni, S. M., Zhai, J., Meyers, B. C., & Donofrio, N. M. (2013). Physiological stressors and invasive plant infections alter the small RNA transcriptome of the rice blast fungus, Magnaporthe oryzae. *BMC Genomics*, *14*(1), 326. https://doi.org/10.1186/1471-2164-14-326

Raposo, G., & Stahl, P. D. (2019). Extracellular vesicles: A new communication paradigm? *Nature Reviews*

Molecular Cell Biology, *20*(9), 509–510. https://doi.org/10.1038/s41580-019-0158-7

Rayner, S., Bruhn, S., Vallhov, H., Andersson, A., Billmyre, R. B., & Scheynius, A. (2017). Identification of small RNAs in extracellular vesicles from the commensal yeast Malassezia sympodialis. *Scientific Reports*, *7*(1), 39742. https://doi.org/10.1038/srep39742

Regente, M., Corti-Monzón, G., Maldonado, A. M., Pinedo, M., Jorrín, J., & de la Canal, L. (2009). Vesicular fractions of sunflower apoplastic fluids are associated with potential exosome marker proteins. *FEBS Letters*, *583*(20), 3363–3366. https://doi.org/10.1016/j.febslet.2009.09.041

Regente, M., Pinedo, M., San Clemente, H., Balliau, T., Jamet, E., & de la Canal, L. (2017). Plant extracellular vesicles are incorporated by a fungal pathogen and inhibit its growth. *Journal of Experimental Botany*, *68*(20), 5485–5495. https://doi.org/10.1093/jxb/erx355

Ren, B., Wang, X., Duan, J., & Ma, J. (2019). Rhizobial tRNA-derived small RNAs are signal molecules regulating plant nodulation. *Science*, *365*(6456), 919–922. https://doi.org/10.1126/science.aav8907

Renaud, G., Stenzel, U., Maricic, T., Wiebe, V., & Kelso, J. (2015). deML: Robust demultiplexing of Illumina sequences using a likelihood-based approach. *Bioinformatics*, *31*(5), 770–772. https://doi.org/10.1093/bioinformatics/btu719

Rishishwar, L., Wang, L., Wang, J., Yi, S. V., Lachance, J., & Jordan, I. K. (2018). Evidence for positive selection on recent human transposable element insertions. *Gene*, *675*, 69–79. https://doi.org/10.1016/j.gene.2018.06.077

Rizzo, J., Chaze, T., Miranda, K., Roberson, R. W., Gorgette, O., Nimrichter, L., Matondo, M., Latgé, J.-P., Beauvais, A., & Rodrigues, M. L. (2020). Characterization of Extracellular Vesicles Produced by Aspergillus fumigatus Protoplasts. *MSphere*, *5*(4). https://doi.org/10.1128/mSphere.00476-20

Rizzo, J., Rodrigues, M. L., & Janbon, G. (2020). Extracellular Vesicles in Fungi: Past, Present, and Future Perspectives. *Frontiers in Cellular and Infection Microbiology*, *10*, 346. https://doi.org/10.3389/fcimb.2020.00346

Rizzo, J., Wong, S. S. W., Gazi, A. D., Moyrand, F., Chaze, T., Commere, P., Novault, S., Matondo, M., Péhau‐Arnaudet, G., Reis, F. C. G., Vos, M., Alves, L. R., May, R. C., Nimrichter, L., Rodrigues, M. L., Aimanianda, V., & Janbon, G. (2021). *Cryptococcus* extracellular vesicles properties and their use as vaccine platforms. *Journal of Extracellular Vesicles*, *10*(10). https://doi.org/10.1002/jev2.12129

Rodenburg, S. Y. A., Terhem, R. B., Veloso, J., Stassen, J. H. M., & van Kan, J. A. L. (2018). Functional Analysis of Mating Type Genes and Transcriptome Analysis during Fruiting Body Development of *Botrytis cinerea*. *MBio*, *9*(1). https://doi.org/10.1128/mBio.01939-17

Rodrigues, M. L., Nakayasu, E. S., Oliveira, D. L., Nimrichter, L., Nosanchuk, J. D., Almeida, I. C., & Casadevall, A. (2008). Extracellular Vesicles Produced by *Cryptococcus neoformans* Contain Protein Components Associated with Virulence. *Eukaryotic Cell*, *7*(1), 58–67. https://doi.org/10.1128/EC.00370-07

Rodrigues, M. L., Nimrichter, L., Oliveira, D. L., Frases, S., Miranda, K., Zaragoza, O., Alvarez, M., Nakouzi, A., Feldmesser, M., & Casadevall, A. (2007). Vesicular Polysaccharide Export in *Cryptococcus neoformans* Is a Eukaryotic Solution to the Problem of Fungal Trans-Cell Wall Transport. *Eukaryotic Cell*, *6*(1), 48–59. https://doi.org/10.1128/EC.00318-06

Romanazzi, G., & Feliziani, E. (2014). Botrytis cinerea (Gray Mold). In *Postharvest Decay* (pp. 131–146). Elsevier. https://doi.org/10.1016/B978-0-12-411552-1.00004-1

Ruan, J., & Li, H. (2020). Fast and accurate long-read assembly with wtdbg2. *Nature Methods*, *17*(2), 155–158. https://doi.org/10.1038/s41592-019-0669-3

Rutter, B. D., Chu, T.-T.-H., Zajt, K. K., Dallery, J.-F., O'Connell, R. J., & Innes, R. W. (2022). *Isolation and Characterization of Extracellular Vesicles from the Fungal Phytopathogen* Colletotrichum higginsianum [Preprint]. Cell Biology. https://doi.org/10.1101/2022.01.07.475419

Rutter, B. D., & Innes, R. W. (2017). Extracellular Vesicles Isolated from the Leaf Apoplast Carry Stress-Response Proteins. *Plant Physiology*, *173*(1), 728–741. https://doi.org/10.1104/pp.16.01253

Rutter, B. D., & Innes, R. W. (2018). Extracellular vesicles as key mediators of plant–microbe interactions. *Current Opinion in Plant Biology*, *44*, 16–22. https://doi.org/10.1016/j.pbi.2018.01.008

Rutter, B. D., & Innes, R. W. (2020). Growing pains: Addressing the pitfalls of plant extracellular vesicle

research. *New Phytologist*, *228*(5), 1505–1510. https://doi.org/10.1111/nph.16725

Rybak, K., & Robatzek, S. (2019). Functions of Extracellular Vesicles in Immunity and Virulence. *Plant Physiology*, *179*(4), 1236–1247. https://doi.org/10.1104/pp.18.01557

Samuel, M., Bleackley, M., Anderson, M., & Mathivanan, S. (2015). Extracellular vesicles including exosomes in cross kingdom regulation: A viewpoint from plant-fungal interactions. *Frontiers in Plant Science*, *6*. https://doi.org/10.3389/fpls.2015.00766

Samuel, S., Veloukas, T., Papavasileiou, A., & Karaoglanidis, G. S. (2012). Differences in Frequency of Transposable Elements Presence in *Botrytis cinerea* Populations from Several Hosts in Greece. *Plant Disease*, *96*(9), 1286–1290. https://doi.org/10.1094/PDIS-01-12-0103-RE

Sarkies, P., & Miska, E. A. (2014). Small RNAs break out: The molecular cell biology of mobile small RNAs. *Nature Reviews Molecular Cell Biology*, *15*(8), 525–535. https://doi.org/10.1038/nrm3840

Schmidt, O., & Teis, D. (2012). The ESCRT machinery. *Current Biology*, *22*(4), R116–R120. https://doi.org/10.1016/j.cub.2012.01.028

Schuh, A. L., & Audhya, A. (2014). The ESCRT machinery: From the plasma membrane to endosomes and back again. *Critical Reviews in Biochemistry and Molecular Biology*, *49*(3), 242–261. https://doi.org/10.3109/10409238.2014.881777

Schumacher, J. (2012). Tools for Botrytis cinerea: New expression vectors make the gray mold fungus more accessible to cell biology approaches. *Fungal Genetics and Biology*, *49*(6), 483–497. https://doi.org/10.1016/j.fgb.2012.03.005

Schumacher, J. (2017). How light affects the life of Botrytis. *Fungal Genetics and Biology*, *106*, 26–41. https://doi.org/10.1016/j.fgb.2017.06.002

Schwessinger, B., Roux, M., Kadota, Y., Ntoukakis, V., Sklenar, J., Jones, A., & Zipfel, C. (2011). Phosphorylation-Dependent Differential Regulation of Plant Growth, Cell Death, and Innate Immunity by the Regulatory Receptor-Like Kinase BAK1. *PLoS Genetics*, *7*(4), e1002046. https://doi.org/10.1371/journal.pgen.1002046

Seidl, M. F., & Thomma, B. P. H. J. (2017). Transposable Elements Direct The Coevolution between Plants and Microbes. *Trends in Genetics*, *33*(11), 842–851. https://doi.org/10.1016/j.tig.2017.07.003

Shahid, S., Kim, G., Johnson, N. R., Wafula, E., Wang, F., Coruh, C., Bernal-Galeano, V., Phifer, T., dePamphilis, C. W., Westwood, J. H., & Axtell, M. J. (2018). MicroRNAs from the parasitic plant Cuscuta campestris target host messenger RNAs. *Nature*, *553*(7686), 82–85. https://doi.org/10.1038/nature25027

Shindo, T., Misas-Villamil, J. C., Hörger, A. C., Song, J., & van der Hoorn, R. A. L. (2012). A Role in Immunity for Arabidopsis Cysteine Protease RD21, the Ortholog of the Tomato Immune Protease C14. *PLoS ONE*, *7*(1), e29317. https://doi.org/10.1371/journal.pone.0029317

Silva, B. M. A., Prados-Rosales, R., Espadas-Moreno, J., Wolf, J. M., Luque-Garcia, J. L., Goncalves, T., & Casadevall, A. (2014). Characterization of Alternaria infectoria extracellular vesicles. *Medical Mycology*, *52*(2), 202–210. https://doi.org/10.1093/mmy/myt003

Slotkin, R. K., & Martienssen, R. (2007). Transposable elements and the epigenetic regulation of the genome. *Nature Reviews Genetics*, *8*(4), 272–285. https://doi.org/10.1038/nrg2072

Sork, H., Conceicao, M., Corso, G., Nordin, J., Lee, Y. X. F., Krjutskov, K., Orzechowski Westholm, J., Vader, P., Pauwels, M., Vandenbroucke, R. E., Wood, M. J., EL Andaloussi, S., & Mäger, I. (2021). Profiling of Extracellular Small RNAs Highlights a Strong Bias towards Non-Vesicular Secretion. *Cells*, *10*(6), 1543. https://doi.org/10.3390/cells10061543

Sot, J., Collado, M. I., Arrondo, J. L. R., Alonso, A., & Goñi, F. M. (2002). Triton X-100-Resistant Bilayers: Effect of Lipid Composition and Relevance to the Raft Phenomenon. *Langmuir*, *18*(7), 2828–2835. https://doi.org/10.1021/la011381c

Souza, J. A. M., Baltazar, L. de M., Carregal, V. M., Gouveia-Eufrasio, L., de Oliveira, A. G., Dias, W. G., Campos Rocha, M., Rocha de Miranda, K., Malavazi, I., Santos, D. de A., Frézard, F. J. G., de Souza, D. da G., Teixeira, M. M., & Soriani, F. M. (2019). Characterization of Aspergillus fumigatus Extracellular Vesicles and Their Effects on Macrophages and Neutrophils Functions. *Frontiers in Microbiology*, *10*, 2008. https://doi.org/10.3389/fmicb.2019.02008

Sowley, E. N. K., Dewey, F. M., & Shaw, M. W. (2010). Persistent, symptomless, systemic, and seed-borne infection of lettuce by Botrytis cinerea. *European Journal of Plant Pathology*, *126*(1), 61–71. https://doi.org/10.1007/s10658-009-9524-1

Staats, M. (2004). Molecular Phylogeny of the Plant Pathogenic Genus Botrytis and the Evolution of Host Specificity. *Molecular Biology and Evolution*, *22*(2), 333–346. https://doi.org/10.1093/molbev/msi020

Statello, L., Maugeri, M., Garre, E., Nawaz, M., Wahlgren, J., Papadimitriou, A., Lundqvist, C., Lindfors, L., Collén, A., Sunnerhagen, P., Ragusa, M., Purrello, M., Di Pietro, C., Tigue, N., & Valadi, H. (2018). Identification of RNA-binding proteins in exosomes capable of interacting with different types of RNA: RBP-facilitated transport of RNAs into exosomes. *PLOS ONE*, *13*(4), e0195969. https://doi.org/10.1371/journal.pone.0195969

Streit, R. S. A., Ferrareze, P. A. G., Vainstein, M. H., & Staats, C. C. (2021). Analysis of tRNA-derived RNA fragments (tRFs) in Cryptococcus spp.: RNAi-independent generation and possible compensatory effects in a RNAi-deficient genotype. *Fungal Biology*, *125*(5), 389–399. https://doi.org/10.1016/j.funbio.2020.12.003

Stukenbrock, E. H., & McDonald, B. A. (2009). Population Genetics of Fungal and Oomycete Effectors Involved in Gene-for-Gene Interactions. *Molecular Plant-Microbe Interactions®*, *22*(4), 371–380. https://doi.org/10.1094/MPMI-22-4-0371

Szatanek, R., Baj-Krzyworzeka, M., Zimoch, J., Lekka, M., Siedlar, M., & Baran, J. (2017). The Methods of Choice for Extracellular Vesicles (EVs) Characterization. *International Journal of Molecular Sciences*, *18*(6), 1153. https://doi.org/10.3390/ijms18061153

Théry, C., Witwer, K. W., Aikawa, E., Alcaraz, M. J., Anderson, J. D., Andriantsitohaina, R., Antoniou, A., Arab, T., Archer, F., Atkin-Smith, G. K., Ayre, D. C., Bach, J.-M., Bachurski, D., Baharvand, H., Balaj, L., Baldacchino, S., Bauer, N. N., Baxter, A. A., Bebawy, M., … Zuba-Surma, E. K. (2018). Minimal information for studies of extracellular vesicles 2018 (MISEV2018): A position statement of the International Society for Extracellular Vesicles and update of the MISEV2014 guidelines. *Journal of Extracellular Vesicles*, *7*(1), 1535750. https://doi.org/10.1080/20013078.2018.1535750

Théry, C., Zitvogel, L., & Amigorena, S. (2002). Exosomes: Composition, biogenesis and function. *Nature Reviews Immunology*, *2*(8), 569–579. https://doi.org/10.1038/nri855

Thompson, P. J., Macfarlan, T. S., & Lorincz, M. C. (2016). Long Terminal Repeats: From Parasitic Elements to Building Blocks of the Transcriptional Regulatory Repertoire. *Molecular Cell*, *62*(5), 766–776. https://doi.org/10.1016/j.molcel.2016.03.029

Thulasi Devendrakumar, K., Li, X., & Zhang, Y. (2018). MAP kinase signalling: Interplays between plant PAMP- and effector-triggered immunity. *Cellular and Molecular Life Sciences*, *75*(16), 2981–2989. https://doi.org/10.1007/s00018-018-2839-3

Timmons, L., & Fire, A. (1998). Specific interference by ingested dsRNA. *Nature*, *395*(6705), 854–854. https://doi.org/10.1038/27579

Torres, D. E., Oggenfuss, U., Croll, D., & Seidl, M. F. (2020). Genome evolution in fungal plant pathogens: Looking beyond the two-speed genome model. *Fungal Biology Reviews*, *34*(3), 136–143. https://doi.org/10.1016/j.fbr.2020.07.001

Torres, D. E., Thomma, B. P. H. J., & Seidl, M. F. (2021). Transposable Elements Contribute to Genome Dynamics and Gene Expression Variation in the Fungal Plant Pathogen *Verticillium dahliae*. *Genome Biology and Evolution*, *13*(7), evab135. https://doi.org/10.1093/gbe/evab135

Torres-Martínez, S., & Ruiz-Vázquez, R. M. (2017). The RNAi Universe in Fungi: A Varied Landscape of Small RNAs and Biological Functions. *Annual Review of Microbiology*, *71*(1), 371–391. https://doi.org/10.1146/annurev-micro-090816-093352

Tricarico, C., Clancy, J., & D'Souza-Schorey, C. (2017). Biology and biogenesis of shed microvesicles. *Small GTPases*, *8*(4), 220–232. https://doi.org/10.1080/21541248.2016.1215283

U. Stotz, H., Brotherton, D., & Inal, J. (2022). Communication is key: Extracellular vesicles as mediators of infection and defence during host–microbe interactions in animals and plants. *FEMS Microbiology Reviews*, *46*(1), fuab044. https://doi.org/10.1093/femsre/fuab044

Váczy, K. Z., Sándor, E., Karaffa, L., Fekete, E., Fekete, É., Árnyasi, M., Czeglédi, L., Kövics, G. J.,

Druzhinina, I. S., & Kubicek, C. P. (2008). Sexual Recombination in the *Botrytis cinerea* Populations in Hungarian Vineyards. *Phytopathology®*, *98*(12), 1312–1319. https://doi.org/10.1094/PHYTO-98-12-1312

Valadi, H., Ekström, K., Bossios, A., Sjöstrand, M., Lee, J. J., & Lötvall, J. O. (2007). Exosome-mediated transfer of mRNAs and microRNAs is a novel mechanism of genetic exchange between cells. *Nature Cell Biology*, *9*(6), 654–659. https://doi.org/10.1038/ncb1596

Valero-Jiménez, C. A., Veloso, J., Staats, M., & van Kan, J. A. L. (2019). Comparative genomics of plant pathogenic Botrytis species with distinct host specificity. *BMC Genomics*, *20*(1), 203. https://doi.org/10.1186/s12864-019-5580-x

Vallejo, M. C., Matsuo, A. L., Ganiko, L., Medeiros, L. C. S., Miranda, K., Silva, L. S., Freymüller-Haapalainen, E., Sinigaglia-Coimbra, R., Almeida, I. C., & Puccia, R. (2011). The Pathogenic Fungus Paracoccidioides brasiliensis Exports Extracellular Vesicles Containing Highly Immunogenic α-Galactosyl Epitopes. *Eukaryotic Cell*, *10*(3), 343–351. https://doi.org/10.1128/EC.00227-10

Vallejo, M. C., Nakayasu, E. S., Longo, L. V. G., Ganiko, L., Lopes, F. G., Matsuo, A. L., Almeida, I. C., & Puccia, R. (2012). Lipidomic Analysis of Extracellular Vesicles from the Pathogenic Phase of Paracoccidioides brasiliensis. *PLoS ONE*, *7*(6), e39463. https://doi.org/10.1371/journal.pone.0039463

van den Berg, M. A., & Maruthachalam, K. (Eds.). (2015). *Genetic Transformation Systems in Fungi, Volume 2*. Springer International Publishing. https://doi.org/10.1007/978-3-319-10503-1

van Kan, J. A. L. (2005). INFECTION STRATEGIES OF BOTRYTIS CINEREA. *Acta Horticulturae*, *669*, 77–90. https://doi.org/10.17660/ActaHortic.2005.669.9

van Kan, J. A. L., Shaw, M. W., & Grant‐Downton, R. T. (2014). *Botrytis* species: Relentless necrotrophic thugs or endophytes gone rogue? *Molecular Plant Pathology*, *15*(9), 957–961. https://doi.org/10.1111/mpp.12148

Van Kan, J. A. L., Stassen, J. H. M., Mosbach, A., Van Der Lee, T. A. J., Faino, L., Farmer, A. D., Papasotiriou, D. G., Zhou, S., Seidl, M. F., Cottam, E., Edel, D., Hahn, M., Schwartz, D. C., Dietrich, R. A., Widdison, S., & Scalliet, G. (2017). A gapless genome sequence of the fungus *Botrytis cinerea*: Gapless Genome Sequence of *B. Cinerea*. *Molecular Plant Pathology*, *18*(1), 75–89. https://doi.org/10.1111/mpp.12384

van Niel, G., D'Angelo, G., & Raposo, G. (2018). Shedding light on the cell biology of extracellular vesicles. *Nature Reviews Molecular Cell Biology*, *19*(4), 213–228. https://doi.org/10.1038/nrm.2017.125

van Wyk, S., Harrison, C. H., Wingfield, B. D., De Vos, L., van der Merwe, N. A., & Steenkamp, E. T. (2019). The RIPper, a web-based tool for genome-wide quantification of Repeat-Induced Point (RIP) mutations. *PeerJ*, *7*, e7447. https://doi.org/10.7717/peerj.7447

van Wyk, S., Wingfield, B. D., De Vos, L., van der Merwe, N. A., & Steenkamp, E. T. (2021). Genome-Wide Analyses of Repeat-Induced Point Mutations in the Ascomycota. *Frontiers in Microbiology*, *11*, 622368. https://doi.org/10.3389/fmicb.2020.622368

Vargas, G., Rocha, J. D. B., Oliveira, D. L., Albuquerque, P. C., Frases, S., Santos, S. S., Nosanchuk, J. D., Gomes, A. M. O., Medeiros, L. C. A. S., Miranda, K., Sobreira, T. J. P., Nakayasu, E. S., Arigi, E. A., Casadevall, A., Guimaraes, A. J., Rodrigues, M. L., Freire-de-Lima, C. G., Almeida, I. C., & Nimrichter, L. (2015). Compositional and immunobiological analyses of extracellular vesicles released by *C andida albicans*: Extracellular vesicles from *Candida albicans*. *Cellular Microbiology*, *17*(3), 389–407. https://doi.org/10.1111/cmi.12374

Varkonyi-Gasic, E., Wu, R., Wood, M., Walton, E. F., & Hellens, R. P. (2007). Protocol: A highly sensitive RT-PCR method for detection and quantification of microRNAs. *Plant Methods*, *3*(1), 12. https://doi.org/10.1186/1746-4811-3-12

Vaser, R., Sović, I., Nagarajan, N., & Šikić, M. (2017). Fast and accurate de novo genome assembly from long uncorrected reads. *Genome Research*, *27*(5), 737–746. https://doi.org/10.1101/gr.214270.116

Veloso, J., & van Kan, J. A. L. (2018). Many Shades of Grey in Botrytis–Host Plant Interactions. *Trends in Plant Science*, *23*(7), 613–622. https://doi.org/10.1016/j.tplants.2018.03.016

Vicient, C. M., & Casacuberta, J. M. (2020). Additional ORFs in Plant LTR-Retrotransposons. *Frontiers in*

Plant Science, *11*, 555. https://doi.org/10.3389/fpls.2020.00555

Viotti, C. (2016). ER to Golgi-Dependent Protein Secretion: The Conventional Pathway. In A. Pompa & F. De Marchis (Eds.), *Unconventional Protein Secretion* (Vol. 1459, pp. 3–29). Springer New York. https://doi.org/10.1007/978-1-4939-3804-9_1

Walker, B. J., Abeel, T., Shea, T., Priest, M., Abouelliel, A., Sakthikumar, S., Cuomo, C. A., Zeng, Q., Wortman, J., Young, S. K., & Earl, A. M. (2014). Pilon: An Integrated Tool for Comprehensive Microbial Variant Detection and Genome Assembly Improvement. *PLoS ONE*, *9*(11), e112963. https://doi.org/10.1371/journal.pone.0112963

Walker, L., Sood, P., Lenardon, M. D., Milne, G., Olson, J., Jensen, G., Wolf, J., Casadevall, A., Adler-Moore, J., & Gow, N. A. R. (2018). The Viscoelastic Properties of the Fungal Cell Wall Allow Traffic of AmBisome as Intact Liposome Vesicles. *MBio*, *9*(1). https://doi.org/10.1128/mBio.02383-17

Wang, B., Sun, Y., Song, N., Zhao, M., Liu, R., Feng, H., Wang, X., & Kang, Z. (2017). *Puccinia striiformis* f. Sp. *Tritici* mi croRNA -like RNA 1 (*Pst* -milR1), an important pathogenicity factor of *Pst* , impairs wheat resistance to *Pst* by suppressing the wheat pathogenesis-related 2 gene. *New Phytologist*, *215*(1), 338–350. https://doi.org/10.1111/nph.14577

Wang, M., & Jin, H. (2017). Spray-Induced Gene Silencing: A Powerful Innovative Strategy for Crop Protection. *Trends in Microbiology*, *25*(1), 4–6. https://doi.org/10.1016/j.tim.2016.11.011

Wang, M., Weiberg, A., Dellota, E., Yamane, D., & Jin, H. (2017). Botrytis small RNA *Bc* -siR37 suppresses plant defense genes by cross-kingdom RNAi. *RNA Biology*, *14*(4), 421–428. https://doi.org/10.1080/15476286.2017.1291112

Wang, M., Weiberg, A., Lin, F.-M., Thomma, B. P. H. J., Huang, H.-D., & Jin, H. (2016). Bidirectional cross-kingdom RNAi and fungal uptake of external RNAs confer plant protection. *Nature Plants*, *2*(10), 16151. https://doi.org/10.1038/nplants.2016.151

Weiberg, A., & Jin, H. (2015). Small RNAs—The secret agents in the plant–pathogen interactions. *Current Opinion in Plant Biology*, *26*, 87–94. https://doi.org/10.1016/j.pbi.2015.05.033

Weiberg, A., Wang, M., Lin, F.-M., Zhao, H., Zhang, Z., Kaloshian, I., Huang, H.-D., & Jin, H. (2013). Fungal Small RNAs Suppress Plant Immunity by Hijacking Host RNA Interference Pathways. *Science*, *342*(6154), 118–123. https://doi.org/10.1126/science.1239705

White, R., Kumar, S., Chow, F. W.-N., Robertson, E., Hayes, K. S., Grencis, R. K., Duque-Correa, M. A., & Buck, A. H. (2020). Extracellular vesicles from Heligmosomoides bakeri and Trichuris muris contain distinct microRNA families and small RNAs that could underpin different functions in the host. *International Journal for Parasitology*, *50*(9), 719–729. https://doi.org/10.1016/j.ijpara.2020.06.002

Wicker, T., Sabot, F., Hua-Van, A., Bennetzen, J. L., Capy, P., Chalhoub, B., Flavell, A., Leroy, P., Morgante, M., Panaud, O., Paux, E., SanMiguel, P., & Schulman, A. H. (2007). A unified classification system for eukaryotic transposable elements. *Nature Reviews Genetics*, *8*(12), 973–982. https://doi.org/10.1038/nrg2165

Williamson, B., Tudzynski, B., Tudzynski, P., & Van Kan, J. A. L. (2007). Botrytis cinerea: The cause of grey mould disease. *Molecular Plant Pathology*, *8*(5), 561–580. https://doi.org/10.1111/j.1364-3703.2007.00417.x

Wilson, R. C., & Doudna, J. A. (2013). Molecular Mechanisms of RNA Interference. *Annual Review of Biophysics*, *42*(1), 217–239. https://doi.org/10.1146/annurev-biophys-083012-130404

Witwer, K. W., Goberdhan, D. C., O'Driscoll, L., Théry, C., Welsh, J. A., Blenkiron, C., Buzás, E. I., Di Vizio, D., Erdbrügger, U., Falcón-Pérez, J. M., Fu, Q., Hill, A. F., Lenassi, M., Lötvall, J., Nieuwland, R., Ochiya, T., Rome, S., Sahoo, S., & Zheng, L. (2021). Updating MISEV: Evolving the minimal requirements for studies of extracellular vesicles. *Journal of Extracellular Vesicles*, *10*(14). https://doi.org/10.1002/jev2.12182

Wolf, P. (1967). The Nature and Significance of Platelet Products in Human Plasma. *British Journal of Haematology*, *13*(3), 269–288. https://doi.org/10.1111/j.1365-2141.1967.tb08741.x

Wong-Bajracharya, J., Singan, V. R., Monti, R., Plett, K. L., Ng, V., Grigoriev, I. V., Martin, F. M., Anderson, I. C., & Plett, J. M. (2022). The ectomycorrhizal fungus *Pisolithus microcarpus* encodes a microRNA involved in cross-kingdom gene silencing during symbiosis. *Proceedings of the National Academy of*

Sciences, *119*(3), e2103527119. https://doi.org/10.1073/pnas.2103527119

Yáñez-Mó, M., Siljander, P. R.-M., Andreu, Z., Bedina Zavec, A., Borràs, F. E., Buzas, E. I., Buzas, K., Casal, E., Cappello, F., Carvalho, J., Colás, E., Cordeiro-da Silva, A., Fais, S., Falcon-Perez, J. M., Ghobrial, I. M., Giebel, B., Gimona, M., Graner, M., Gursel, I., … De Wever, O. (2015). Biological properties of extracellular vesicles and their physiological functions. *Journal of Extracellular Vesicles*, *4*(1), 27066. https://doi.org/10.3402/jev.v4.27066

Yoshida, K., Saunders, D. G. O., Mitsuoka, C., Natsume, S., Kosugi, S., Saitoh, H., Inoue, Y., Chuma, I., Tosa, Y., Cano, L. M., Kamoun, S., & Terauchi, R. (2016). Host specialization of the blast fungus Magnaporthe oryzae is associated with dynamic gain and loss of genes linked to transposable elements. *BMC Genomics*, *17*(1), 370. https://doi.org/10.1186/s12864-016-2690-6

Yuan, H.-M., Liu, W.-C., & Lu, Y.-T. (2017). CATALASE2 Coordinates SA-Mediated Repression of Both Auxin Accumulation and JA Biosynthesis in Plant Defenses. *Cell Host & Microbe*, *21*(2), 143–155. https://doi.org/10.1016/j.chom.2017.01.007

Yuan, M., Jiang, Z., Bi, G., Nomura, K., Liu, M., Wang, Y., Cai, B., Zhou, J.-M., He, S. Y., & Xin, X.-F. (2021). Pattern-recognition receptors are required for NLR-mediated plant immunity. *Nature*. https://doi.org/10.1038/s41586-021-03316-6

Yuan, M., Ngou, B. P. M., Ding, P., & Xin, X.-F. (2021). PTI-ETI crosstalk: An integrative view of plant immunity. *Current Opinion in Plant Biology*, *62*, 102030. https://doi.org/10.1016/j.pbi.2021.102030

Zand Karimi, H., Baldrich, P., Rutter, B. D., Borniego, L., Zajt, K. K., Meyers, B. C., & Innes, R. W. (2021). *Arabidopsis Apoplastic Fluid Contains sRNA- and Circular RNA-Protein Complexes that Are Located Outside Extracellular Vesicles* [Preprint]. Plant Biology. https://doi.org/10.1101/2021.10.02.462881

Zeng, Gupta, Jiang, Yang, Gong, & Zhu. (2019). Cross-Kingdom Small RNAs Among Animals, Plants and Microbes. *Cells*, *8*(4), 371. https://doi.org/10.3390/cells8040371

Zhang, T., Zhao, Y.-L., Zhao, J.-H., Wang, S., Jin, Y., Chen, Z.-Q., Fang, Y.-Y., Hua, C.-L., Ding, S.-W., & Guo, H.-S. (2016). Cotton plants export microRNAs to inhibit virulence gene expression in a fungal pathogen. *Nature Plants*, *2*(10), 16153. https://doi.org/10.1038/nplants.2016.153

Zhang, Y., Liu, Y., Liu, H., & Tang, W. H. (2019). Exosomes: Biogenesis, biologic function and clinical potential. *Cell & Bioscience*, *9*(1), 19. https://doi.org/10.1186/s13578-019-0282-2

Zhao, K., Bleackley, M., Chisanga, D., Gangoda, L., Fonseka, P., Liem, M., Kalra, H., Al Saffar, H., Keerthikumar, S., Ang, C.-S., Adda, C. G., Jiang, L., Yap, K., Poon, I. K., Lock, P., Bulone, V., Anderson, M., & Mathivanan, S. (2019). Extracellular vesicles secreted by Saccharomyces cerevisiae are involved in cell wall remodelling. *Communications Biology*, *2*(1), 305. https://doi.org/10.1038/s42003-019-0538-8

Zhao, M., Zhou, J. Y., Li, Z. D., Song, W. W., Gong, T., & Tan, H. (2011). Boty-like retrotransposons in the filamentous fungus Botrytis cinerea contain the additional antisense gene brtn. *Virology*, *417*(2), 248–252. https://doi.org/10.1016/j.virol.2011.06.020

Zhou, M., Weber, S. R., Zhao, Y., Chen, H., & Sundstrom, J. M. (2020). Methods for exosome isolation and characterization. In *Exosomes* (pp. 23–38). Elsevier. https://doi.org/10.1016/B978-0-12-816053-4.00002-X

Zipfel, C. (2014). Plant pattern-recognition receptors. *Trends in Immunology*, *35*(7), 345–351. https://doi.org/10.1016/j.it.2014.05.004

Zipfel, C., & Felix, G. (2005). Plants and animals: A different taste for microbes? *Current Opinion in Plant Biology*, *8*(4), 353–360. https://doi.org/10.1016/j.pbi.2005.05.004

Copyright permissions

SPRINGER NATURE LICENSE
TERMS AND CONDITIONS

Apr 07, 2022

This Agreement between Ludwig Maximilian University of Munich -- Constance Tisserant ("You") and Springer Nature ("Springer Nature") consists of your license details and the terms and conditions provided by Springer Nature and Copyright Clearance Center.

License Number	5283761261795
License date	Apr 07, 2022
Licensed Content Publisher	Springer Nature
Licensed Content Publication	Genome Biology
Licensed Content Title	The diversity of LTR retrotransposons
Licensed Content Author	Ericka R Havecker et al
Licensed Content Date	May 18, 2004
Type of Use	Thesis/Dissertation
Requestor type	academic/university or research institute
Format	print and electronic
Portion	figures/tables/illustrations
Number of figures/tables/illustrations	1
Will you be translating?	no

Circulation/distribution	1 - 29
Author of this Springer Nature content	no
Title	Botrytis cinerea communicating across kingdoms: from LTR retrotransposons to extracellular vesicles.
Institution name	Ludwig Maximilian University of Munich
Expected presentation date	Jul 2022
Portions	I will redraw the figure 1, but keeping the same type of design and the same message.
Requestor Location	Ludwig Maximilian University of Munich Grosshaderner Str. 2-4 LMU München Biozentrum Martinsried Martinsried, 82152 Germany Attn: Ludwig Maximilian University of Munich
Total	0.00 EUR

Terms and Conditions

Springer Nature Customer Service Centre GmbH
Terms and Conditions

This agreement sets out the terms and conditions of the licence (the **Licence**) between you and **Springer Nature Customer Service Centre GmbH** (the **Licensor**). By clicking 'accept' and completing the transaction for the material (**Licensed Material**), you also confirm your acceptance of these terms and conditions.

1. Grant of License

1. 1. The Licensor grants you a personal, non-exclusive, non-transferable, world-wide licence to reproduce the Licensed Material for the purpose specified in your order only. Licences are granted for the specific use requested in the order and for no other use, subject to the conditions below.

1. 2. The Licensor warrants that it has, to the best of its knowledge, the rights to license reuse of the Licensed Material. However, you should ensure that the material you are requesting is original to the Licensor and does not carry the copyright of another entity (as credited in the published version).

1. 3. If the credit line on any part of the material you have requested indicates that it was reprinted or adapted with permission from another source, then you should also seek permission from that source to reuse the material.

2. Scope of Licence

2. 1. You may only use the Licensed Content in the manner and to the extent permitted by these Ts&Cs and any applicable laws.

2. 2. A separate licence may be required for any additional use of the Licensed Material, e.g. where a licence has been purchased for print only use, separate permission must be obtained for electronic re-use. Similarly, a licence is only valid in the language selected and does not apply for editions in other languages unless additional translation rights have been granted separately in the licence. Any content owned by third parties are expressly excluded from the licence.

2. 3. Similarly, rights for additional components such as custom editions and derivatives require additional permission and may be subject to an additional fee. Please apply to Journalpermissions@springernature.com/bookpermissions@springernature.com for these rights.

2. 4. Where permission has been granted **free of charge** for material in print, permission may also be granted for any electronic version of that work, provided that the material is incidental to your work as a whole and that the electronic version is essentially equivalent to, or substitutes for, the print version.

2. 5. An alternative scope of licence may apply to signatories of the STM Permissions Guidelines, as amended from time to time.

3. Duration of Licence

3. 1. A licence for is valid from the date of purchase ('Licence Date') at the end of the relevant period in the below table:

Scope of Licence	Duration of Licence
Post on a website	12 months
Presentations	12 months
Books and journals	Lifetime of the edition in the language purchased

4. Acknowledgement

4. 1. The Licensor's permission must be acknowledged next to the Licenced Material in print. In electronic form, this acknowledgement must be visible at the same time as the figures/tables/illustrations or abstract, and must be hyperlinked to the journal/book's homepage. Our required acknowledgement format is in the Appendix below.

5. Restrictions on use

5. 1. Use of the Licensed Material may be permitted for incidental promotional use and minor editing privileges e.g. minor adaptations of single figures, changes of format, colour and/or style where the adaptation is credited as set out in Appendix 1 below. Any

other changes including but not limited to, cropping, adapting, omitting material that affect the meaning, intention or moral rights of the author are strictly prohibited.

5. 2. You must not use any Licensed Material as part of any design or trademark.

5. 3. Licensed Material may be used in Open Access Publications (OAP) before publication by Springer Nature, but any Licensed Material must be removed from OAP sites prior to final publication.

6. Ownership of Rights

6. 1. Licensed Material remains the property of either Licensor or the relevant third party and any rights not explicitly granted herein are expressly reserved.

7. Warranty

IN NO EVENT SHALL LICENSOR BE LIABLE TO YOU OR ANY OTHER PARTY OR ANY OTHER PERSON OR FOR ANY SPECIAL, CONSEQUENTIAL, INCIDENTAL OR INDIRECT DAMAGES, HOWEVER CAUSED, ARISING OUT OF OR IN CONNECTION WITH THE DOWNLOADING, VIEWING OR USE OF THE MATERIALS REGARDLESS OF THE FORM OF ACTION, WHETHER FOR BREACH OF CONTRACT, BREACH OF WARRANTY, TORT, NEGLIGENCE, INFRINGEMENT OR OTHERWISE (INCLUDING, WITHOUT LIMITATION, DAMAGES BASED ON LOSS OF PROFITS, DATA, FILES, USE, BUSINESS OPPORTUNITY OR CLAIMS OF THIRD PARTIES), AND
WHETHER OR NOT THE PARTY HAS BEEN ADVISED OF THE POSSIBILITY OF SUCH DAMAGES. THIS LIMITATION SHALL APPLY NOTWITHSTANDING ANY FAILURE OF ESSENTIAL PURPOSE OF ANY LIMITED REMEDY PROVIDED HEREIN.

8. Limitations

8. 1. ***BOOKS ONLY:***Where **'reuse in a dissertation/thesis'** has been selected the following terms apply: Print rights of the final author's accepted manuscript (for clarity, NOT the published version) for up to 100 copies, electronic rights for use only on a personal website or institutional repository as defined by the Sherpa guideline (www.sherpa.ac.uk/romeo/).

8. 2. For content reuse requests that qualify for permission under the STM Permissions Guidelines, which may be updated from time to time, the STM Permissions Guidelines supersede the terms and conditions contained in this licence.

9. Termination and Cancellation

9. 1. Licences will expire after the period shown in Clause 3 (above).

9. 2. Licensee reserves the right to terminate the Licence in the event that payment is not received in full or if there has been a breach of this agreement by you.

Appendix 1 — Acknowledgements:

For Journal Content:
Reprinted by permission from [**the Licensor**]: [**Journal Publisher** (e.g. Nature/Springer/Palgrave)] [**JOURNAL NAME**] [**REFERENCE CITATION** (Article name, Author(s) Name), [**COPYRIGHT**] (year of publication)

For **Advance Online Publication papers:**
Reprinted by permission from [**the Licensor**]: [**Journal Publisher** (e.g. Nature/Springer/Palgrave)] [**JOURNAL NAME**] [**REFERENCE CITATION** (Article name, Author(s) Name), [**COPYRIGHT**] (year of publication), advance online publication, day month year (doi: 10.1038/sj.[JOURNAL ACRONYM].)

For Adaptations/Translations:
Adapted/Translated by permission from [**the Licensor**]: [**Journal Publisher** (e.g. Nature/Springer/Palgrave)] [**JOURNAL NAME**] [**REFERENCE CITATION** (Article name, Author(s) Name), [**COPYRIGHT**] (year of publication)

Note: For any republication from the British Journal of Cancer, the following credit line style applies:

Reprinted/adapted/translated by permission from [**the Licensor**]: on behalf of Cancer Research UK: : [**Journal Publisher** (e.g. Nature/Springer/Palgrave)] [**JOURNAL NAME**] [**REFERENCE CITATION** (Article name, Author(s) Name), [**COPYRIGHT**] (year of publication)

For **Advance Online Publication** papers:
Reprinted by permission from The [**the Licensor**]: on behalf of Cancer Research UK: [**Journal Publisher** (e.g. Nature/Springer/Palgrave)] [**JOURNAL NAME**] [**REFERENCE CITATION** (Article name, Author(s) Name), [**COPYRIGHT**] (year of publication), advance online publication, day month year (doi: 10.1038/sj.[JOURNAL ACRONYM])

For Book content:
Reprinted/adapted by permission from [**the Licensor**]: [**Book Publisher** (e.g. Palgrave Macmillan, Springer etc) [**Book Title**] by [**Book author**(s)] [**COPYRIGHT**] (year of publication)

Other Conditions:

Version 1.3

Questions? customercare@copyright.com or +1-855-239-3415 (toll free in the US) or +1-978-646-2777.

Acknowledgements

First of all, I want to thank Arne for giving me the opportunity to accomplish this work with him, for his precious guidance through all these years and for always pushing me to go further. You taught me so much and inspired me a lot. When I was facing difficult times, especially at the beginning of my PhD, I was coming to see you in your office for a short mini-meeting. The sparkles in your eyes when speaking about science made your passion communicative. I don't only appreciate you as a scientist but also for the person you are.

I also want to thank Prof. Dr. Martin Parniske for hosting me in the Genetics department and for guidance during my TAC meetings. He makes this department special and I know how lucky we all are to work here. But this great atmosphere was also brought by all the awesome PhD students, post-docs and technicians so I would like to thank all the members of the department, past and present.

Thank you to Dr. Silke Robatzek for correcting this manuscript in depth and being part of the thesis committee. Thank you to Prof. Andreas Klingl for guidance during my TAC meetings and being part of the thesis committee. Thank you to Prof. Dr. Wolfgang Enard, Prof. Dr. Wolfgang Frank and Prof. Dr. Martin Heß for being part of the thesis committee.

Thank you to all the collaborators: Andreas Klingl (LMU), Wolfgang Enard (LMU), Andreas Brachman and the sequencing service (LMU), Julia Mergner (TUM) and Matthias Hahn (TU Kaiserslautern).

Thank you to the SFB924 for funding this project, for organising conferences and soft skills courses and for the Stammtisch events where we could meet other students.

Thank you to David R. and Flo who fully proof-read this manuscript, to Lucie, Amit, Vanda and David D. who read some paragraphs here or there. And thanks a lot to my brother for hunting typos and grammar mistakes!
Thank you to my students Carlotta and Alexandra, by teaching you I learnt a lot.

There are so many people towards whom I feel grateful, and without whom I could not have been able to finish this doctoral thesis. Thus, the following part is going to be quite (veeery…) long.

Morgane, you are the person I saw the least during these years yet one of the most important. It is crazy how physical distance does not split us apart and I keep thinking about you everyday. Without you every piece of my life in Munich would have been different. You listened to me (so much), advised me, made me laugh, and supported me in each possible way. Sounds cliché, but best friends for ever!

Amit and Vanda, there are no words to tell you how I feel about you and how sad I am when I think of us three not living in the same city anymore. You brought me everything I was needing and even more. Since we became friends, I had the feeling of having a family in Munich and this is priceless.

David, what a crazy story we got both of us! I don't know if the most difficult during these last years was the PhD or being far away from you. We made the best from what we had and your everyday love and presence by my side helped me a lot during this adventure in Munich.

My parents, Pady and Antoine, we say we don't choose our family but if I had the choice, I would have chosen you. Thank you for all the love and support you gave me, far away in distance but always in my heart. I also have a special thought for the grand-parents who couldn't see me graduate but who are in my heart.

Berni, who could dream about something better than going to work every day and meeting a dear friend there! I am so glad we were office-mates and bench-mates, you made coming to the lab easier in the difficult moments. With you I felt completely myself and was never afraid of showing my craziest side. I keep many memories to cherish (mainly laughing a lot and doing stupid stuff) and I hope you come to visit me (and my baby goats) wherever I'll be later. And thanks in advance for the moustache group picture you will organise for me (now you have to do it).

Lolo my dear Lolo, we did not work long together in 2017 when we met but from this was born one of my favourite friendships in Munich. I wish we were from the same family so we could never lose contact but anyway I know we won't. I wish you all the best with this EV project and I'll always be here if you want to talk (complain) about it!

Flo, I was always so amazed by your knowledge, wisdom, generosity and am so grateful you made us all profit from it. You were the best colleague we could have and on top of that you became my friend. I will always have very funny memories from the time we spent together, you are the guy who made butter from cream in my garden, who presented a Tuesday Seminar in trachten, who always had great stories to tell. But I especially know how important you were for me at the beginning of my thesis, I felt like you were our second PI!

Jessica, my partner in crime in the lab! Somehow the first time we really spoke to each other something clicked and we instantly became friends. I loved how we could have the most serious conversation followed by the stupidest things afterwards. Thank you for making me feel loved and for taking care of me when I needed it.

Antoine P., I wish I had only used lyrics from K-Maro or Tribal King in your paragraph, sadly I don't have enough time to make this up, and no I don't know them by heart. Thank you for being my friend and supporting me during these years; you are in many great memories from your terrace, to you crashing my couch or to my grandpa's swimming pool. I hope we stay in touch, and even more, I hope we work together again!

Thanks to Lucie for staying my friend even though we met only twice in 5 years. I am impatient to be in a situation where we can see each other more regularly, rediscover each other (the new us after doing a PhD!) and keep on being good friends for a long long time.

My two favourite chippies Béren & Mama, you allowed me to have bubbles of life outside of science. You made me push my limits while hiking (and also drinking red wine) and brought me a lot of joy, even more you made me discover a side of me I didn't know. Of course I extend these comments to the two missing baleines, Lulu and Xabi.

David Roquis, my mentor and dear friend for several years (soon ten!). From my Bachelor's thesis supervisor, to my friend, and then the person who shared with me the job offer for this PhD. So nothing of these last years would have happened if it wasn't for you. Thank you for all the time you spent reading my thesis, for your constructive comments.

Benj Salar Michi Andy Aline Chloé Isa Janet Duncan AnPo Reshi Santi Dani Liza Alessa Eliana Simon Mirj Chiara Chris Phil… Am I forgetting anyone? I hope not…
Thanks to *Botrytis*, my bike, music, the snow, red wine, France Culture & FIP radios, the food, the Alps, and many more things that all together made my life how it was.